KWAME NKRUMAH UNIVERSITY OF SCIENCE AND TECHNOLOGY
KUMASI GHANA

Assessing Urban Flood Risks under Changing Climate and Land Use in Abidjan District, South Cote d'Ivoire

By

Jean Homian DANUMAH

Msc. Hydrogeology

A Thesis submitted to the Department of Civil Engineering, College of Engineering

In partial fulfilment of the requirements for the degree of

DOCTOR OF PHILOSOPHY

In

Climate Change and Land-use

APRIL, 2016

DECLARATION

I hereby declare that this submission is my own work towards the PhD in Climate Change and Land Use and that, to the best of my knowledge, it contains no material previously published by another person, nor material which has been accepted for the award of any other degree of the University, except where due acknowledgment has been made in the text.

KNUST

Jean Homian DANUMAH (PG8392512)	..... Signature	03/05/2016 Date

Certified By:

Prof. Samuel Nii Odai (Supervisor 1)	..... Signature	3-5-2016 Date
Prof. Bachir M. Saley (Supervisor 2)	Signature	02/05/2016 Date
Prof. Y. A. Tuffour (Head of Department)	..... Signature	..... Date

W J SANE NO

ABSTRACT

Climate change has become one of the global environmental issues more visible in recent decades. Flooding is one of the natural disasters that combine with climate change to create effects and cause some of the most destructive damages in Cote d'Ivoire. The District of Abidjan located in the south of Cote d'Ivoire which is subjected to heavy rainfall, rapid population growth and uncontrolled urbanisation is not an exception to the problem of flood risk. The aim of this study was to identify, map and model areas of flood risk to facilitate decision making for better land use planning under changing climate in this District. The maximum likelihood classification algorithm and post-classification change detection procedures were used in this study. The spatio-temporal land use/ land cover change in relation to urbanisation sprawl was assessed based on a series of Landsat images for 1990, 2002 and 2014. Statistical methods were also used to characterise and determine hydro-climatic drivers of flood. LARS-WG model was used to generate future scenario based on HadCM3 model and SRA1B emissions and in rclimdex model, ten (10) rainfall indices were calculated. LARS-WG and rclimdex were used to determine and analyse trends of rainfall and temperature under present and future climatic conditions. Analytic Hierarchy Process (AHP) method as a multi-criteria analysis allows the integration of several elements under two criteria: hazard and vulnerability for flood risk assessment and mapping. Flood Hazard Index (FHI) model was carried out to determine flood prone areas by combining rational and statistical methods. The results revealed urban area expansion (15%) as a major land use change for the period 1990-2014. However, there was an important increase in urban area between 2002 and 2014, compared to 1990-2002. Regarding future weather, LARS-WG statistical results showed that, temperature will increase from 0.32°C to 2.54°C for the period 2011-2100. Also, rainfall in the same period will increase from 4 %, to 10 %. Results of rclimdex through ten (10) rainfall indices and comparison between observed and future indices indicated an increased trend of some rainfall indices:

Consecutive wet Days (*CWD)* and number of heavy rainfall days above 10mm (*R10)* from 2011 to 2100. AHP flood risk map showed that areas under high and very high flood risk covers 34% of the study area while Flood Hazard Index (FHI) model revealed that about 25.09 % of the study area were within the high FHI areas. Both results showed that eight out of thirteen (8/13) municipalities of Abidjan District are within high and very high flood risk areas. Therefore, there is a need for decision makers to call for optimal design of technical solutions and an effective preparedness strategy to be developed for future flood occurrence within Abidjan District (South of Cote d'Ivoire).

KNUST

DEDICATION

To Almighty God, for supporting, assisting and above all, filling me with His graces all my life.

To my mother Ema Fodjo, May God bless you with his infinite grace for all the sacrifices you have made to my success and good education received from you.

To my late father Daniel Danumah who before dying told me, my share of the inheritance was that he put me in school and my destiny was now in my hands.

To my fiancee Mireille Kouassi for the love and support, Only God knows your contribution to this work and to my life. May He bless you.

To my son, Yedidiah Yanis-Mael Nathan Danumah.

Thank you all.

KNUST

ACKNOWLEDGMENTS

Before the presentation of this thesis, I would like to thank the Almighty God for his abundant grace, support, source of strength and assistance from the beginning to the end of this work. I also wish to express my thanks to all those who have contributed in one way or another to the realisation of this thesis.

I express my sincere gratitude to my principal supervisor Prof. Samuel Nii Odai. His guidance, suggestions, comments and constructive criticisms formed this thesis in the right direction. I am grateful to him for his confidence in me.

I am also extremely grateful to my second supervisor, Prof. Bachir Mahaman Saley for his unfailing and constant guidance, encouragement, love of work well done, constructive criticism associated with scientific advice and wealth of experience in natural disaster research at any stage of the research. More especially, for his availability and ease of access always.

I would also like to thank Dr. Jorg Szarzynski, my third supervisor and Dr Kwaku Adjei for their comments and suggestions which improved the overall quality of this study. Special thanks also goes to Dr. Michael Thiel who assisted me as my advisor and mentor during my scientific visit in Germany especially in Wurzburg and Bonn.

I am grateful to the German Federal Ministry of Education and Research (BMBF) for offering me a scholarship and providing financial assistance for this study through the West African Science Service Center for Climate Change and Adapted Land Use (WASCAL) PhD program. I am thankful and grateful to the Director of WASCAL-CCLU, Prof. Samuel Nii Odai and the Coordinator of WASCAL-CCLU, Dr. Wilson Agyare all of the Kwame Nkrumah University of

Science and Technology (KNUST), for their unconditional support, encouragement. Also, I would like to express a special thank you to members of the local Advisory board for their support, suggestions, comment and time during the different presentations that helped me to the final stage. I wish to thank all Professors and Lecturers who travelled from far and near distance to offer courses during the program and for sharing their knowledge and experiences as well. I thank the administrative staffs of logistical support.

Sincere thanks go to the Director of Centre Universitaire de Recherche et d'Application en Teledetection (CURAT), Prof. Fernand Koffi Kouame and all lecturers of the "UFR STRM" of Felix Houphouet Boigny University for their encouragement and support. I also thank Dje Kouakou Bernard, Director of Climatology Department at SODEXAM for data acquisition facilities.

I would like to say a big thank you to all WASCAL CCLU mates: Jean-Bosco Zougrana, Koutcha Mariama, Raymond Abeyi, Divine Appiah, Manu Wireku, Chabi Adeyemi, Laurice Faye, Mahmoud Ibrahim, Amadou Dicko and Badabate Diwediga for the great friendship you extended to me and the academic and social assistance you provided me during these three years. My thanks also go to my classmates "Promotion Affian Kouadio" in Cote d'Ivoire for encouragement and support.

I' am also grateful to those who have always been with me from the beginning special mention to Carine, Derving, Lucette, Jean-baptiste, Anthony, Alexis, Brice, Laetitia for your friendship and your unwavering support. My whole hearted acknowledgement goes to these special people: my spiritual father Abraham Marie and my community "Sacerdoce Royal" who supported me in prayers.

Finally, deep in my heart, I express my infinite gratitude to my fiancee Mireille Kouassi and my son Yanis-mael Nathan Danumah, my mother, my brothers and sisters. May God grant you long life and bless you for all you do and continue to do for me.

KNUST



TABLE OF CONTENTS

ABSTRACT iii

DEDICATION v

ACKNOWLEDGMENTS vi

LIST OF FIGURES xiv

LIST OF TABLES xvii

LIST OF PLATES xviii

ACRONYMS xix

CHAPTER 1: GENERAL INTRODUCTION 1

1.1. Background 1

1.2. Problem Statement and Justification 3

1.3. Research Objectives 5

1.4. Scope of the thesis 6

1.5. Overview of Thesis 6

CHAPTER 2: LITERATURE REVIEW 7

2.1. Overview 7

2.2. Urban Land use/land cover dynamic 7

2.2.1. Classic classification (unsupervised and supervised) method. 9

2.2.2. Oriented based Image analysis (OBIA) method 10

2.3. Weather variability 11

2.4. Historical Rainfall variability in Cote d'Ivoire 13

2.5. Flood Risk Assessment 14

2.6. Flood risk in Cote d'Ivoire 16

2.7. Definition of Concepts 17

2.7.1. Climate Change....17
2.7.2-Land use/Land cover 17
2.7.3-Hazard.... 18
2.7.4. Vulnerability 18
2.7.5. Flood risk Assessment 19
CHAPTER 3: MATERIALS AND METHODS 20
3.1. Study area 20
3.1.1. Climatic context 21
3.1.2. Topography 26
3.1.3. Vegetation 28
3.1.4. Hydrogeological and geological context 29
3.1.5. Socio-economics and human environment 33
3.2. Dynamic of Land use / land cover 35
3.2.1. Data acquisition and Pre-treatment 35
3.2.2. Data collection and processing 36
3.2.3. Image classification and Validation 37
3.2.4. Post-classification 37
3.2.5. Land Use Change Detection 38
3.3. Normalized Difference Build-up Index (NDBI) 39
3.4. Urban Structure Types classification 40
3.4.1. Estimation of scale parameter 41
3.4.2. Image segmentation 41
3.4.3. Oriented object classification.... 43
3.5. Climatic variability methodology approaches. 44
3.5.1. Standardised precipitation index (SPI) 44
3.5.2. Detection of changes within rainfall series 46

3.5.3. Gumbel distribution method 47
3.6. LARS-WG and rclimdex models 50
3.6.1. LARS-WG model processing 50
3.6.2. Rclimdex model processing 51
3.7. Analytic Hierarchic Process (AHP) approach for flood risk assessment 55
3.7.1. Hazard 56
3.7.2. Vulnerability to flooding 59
3.7.3. Spatial mapping of multi-combination 61
3.8. Flood hazard index model 74
3.8.1. Rational model 74
3.8.2. Categorisation of maps 76
3.8.3. Flood hazard index (FHI) map 77
CHAPTER 4: RESULTS 78
4.1. Land Use/ Land Cover dynamic of Abidjan District 78
4.1.1. Land use/ land cover classification between 1990, 2002 and 2014 78
4.1.2. Validation of land use /land cover classification 80
4.1.3. Land Use/ Land Cover dynamic 81
4.1.4 Land use/ land cover change detection 84
4.2. Normalized Difference Build-up Index (NDBI) 86
4.3. Urban Structure Types Classification 88
4.4. Rainfall Variability Analysis 89
4.4.1 Standardised Precipitation Index (SPI) 89
4.4.2. Change detection tests 91
4.5. Gumbel Approach 93
4.6. Temperature, Precipitation, Solar Radiation and PET Predictions in LARS-WG model ..95
4.7. Rclimdex Rainfall Indices 100

4.7.1. Consecutive wet days (*CWD*) 101
4.7.2. Annual total wet-day precipitation (*PRCPTOT*) 102
4.7.3. Number of heavy precipitation days (*R10*) 104
4.7.4. Number of very heavy precipitation days (*R20*) 105
4.7.5. Number of days above 25 mm (*Rnn*) 107
4.7.6. Very wet days (*R95p*) 108
4.7.7. Extremely wet days (*R99p*)..... 109
4.7.8. Maximum 1-day precipitation amount (*RX1day*) 111
4.7.9. Maximum 5-day precipitation amount (*RX5day*) 112
4.7.10. Simple daily intensity index (*SDII*) 114
4.8. Analytic Hierarchic Process (AHP) Flood Risk 115
4.8.1. AHP Hazard map 115
4.8.2. AHP vulnerability map 125
4.8.3. AHP flood risk map of Abidjan 131
4.8.4. Validation of AHP flood risk map of Abidjan 132
4.9. Flood Hazard Index (FHI) model 133
4.9.1. Peak of runoff estimation 133
4.9.2. Digital Elevation Model (DEM) 137
4.9.3. Flood hazard index map 138
CHAPTER 5: DISCUSSIONS 140
5.1. Land use/land cover dynamics of Abidjan 140
5.2. LARS-WG model 141
5.3. rclimdex processing 142
5.4. AHP flood risk map 143
5.5. Flood hazard index model 145
CHAPTER 6: CONCLUSIONS AND RECOMMENDATIONS 146

6.1. CONCLUSIONS 146

6.2. RECOMMENDATIONS 148

REFERENCES 150

APPENDICES 178

Appendix 1: Rational Method Runoff Coefficient Table from U.S. Soil Conservation Service (SCS) 178

KNUST



LIST OF FIGURES

Figure 3.1: Location of the study area 21
Figure 3.2: Annual rainfall trend from 1961-2012..... 22
Figure 3.3: Variability of average monthly rainfall of Abidjan from 1961-2012 23
Figure 3.4: Average monthly relative humidity of Abidjan from 1961-2000..... 24
Figure 3.5: Average monthly temperature from 1961-2012 25
Figure 3.6: Ombrothermic diagram of Abidjan from 1961-2012 25
Figure 3.7: Plot of annual rainfall for two rainiest months (May and June) from 1960-2012 26
Figure 3.8: Digital Terrain Model (DTM) map of Abidjan 27
Figure 3.9: Vegetation map of Abidjan..... 29
Figure 3.10: Hydrography of Abidjan District 31
Figure 3.11: Geological Map of the District of Abidjan 33
Figure 3.12: Population growth of Abidjan from 1998-2014 (INS, 2014) 34
Figure 3.13: Flow chart for spatio-temporal dynamic of land use/land cover in Abidjan 39
Figure 3.14: Image object information..... 42
Figure 3.15: Process tree development for segmentation and classification 43
Figure 3.16: AHP model use in the process flood risk map 65
Figure 3.17: Flood risk flowchart for development of flood risk map..... 73
Figure 3.18: Flood hazard index (FHI) framework 77
Figure 4.1: Land use/Land cover dynamic of Abidjan District in 1990 79
Figure 4.2: Land use/Land cover dynamic of Abidjan District in 2002 79
Figure 4.3: Land use/Land cover dynamic of Abidjan District in 2014 80
Figure 4.4: Land use/land cover change for the years of 1990, 2002 and 2014 in Abidjan 84
Figure 4.5: Normalized Difference Build-up Index (NDBI) of 1990, 2002 and 2014 87
Figure 4.6: Urban structure types of Abidjan from spot image 89
Figure 4.7: Standardised Precipitation Index of Abidjan station from 1960 - 2012 90
Figure 4.8: Curve weighted indices of Abidjan station from 1960-2012 91
Figure 4.9: Buishand's test of Abidjan from 1960-2012 92
Figure 4.10: Pettit test of Abidjan from 1960-2012 93
Figure 4.11: Gumbel test of measure (a) and estimate (b) precipitation at Abidjan 94

Figure 4.12a: Minimum temperature variability from 1960 to horizon 2100 97
Figure 4.12b: Maximun temperature variability from 1960 to horizon 2100 97
Figure 4.12c: Rainfall variability from 1960 to horizon 2100 98
Figure 4.12d: Solar radiation variability from 1960 to horizon 2100 98
Figure 4.12e: Potential evapotranspiration variability from 1960 to horizon 2100 99
Figure 4.13a: Consecutive wet days (CWD) from 1960 to 2010 101
Figure 4.13b: Consecutive wet days (CWD) from 2011 to 2100 101
Figure 4.14a: Annual total wet-day precipitation (PRCPTOT) from 1960 to 2010 102
Figure 4.14b: Annual total wet-day precipitation (PRCPTOT) from 2011 to 2100 103
Figure 4.15a: Number of heavy precipitation days (R10) from 1960 to 2010 104
Figure 4.15b: Number of heavy precipitation days (R10) from 2011 to 2100 104
Figure 4.16a: Number of very heavy precipitation days (R20) from 1960 to 2010..... 105
Figure 4.16b: Number of very heavy precipitation days (R20) from 2011 to 2100 106
Figure 4.17a: Number of days above 25 mm (Rnn) from 1960 to 2010 107
Figure 4.17b: Number of days above 25 mm (Rnn) from 2011 to 2100 107
Figure 4.18a: Very wet days (R95p) from 1960 to 2010 108
Figure 4.18b: Very wet days (R95p) from 2011 to 2100 109
Figure 4.19a: Extremely wet days (R99p) from 1960 to 2010 109
Figure 4.19b: Extremely wet days (R99p) from 2011 to 2100 110
Figure 4.20a: Maximum 1-day precipitation amount (RX1day) from 1960 to 2010..... 111
Figure 4.20b: Maximum 1-day precipitation amount (RX1day) from 2011 to 2100 111
Figure 4.21a: Maximum 5-day precipitation amount (RX5day) from 1960 to 2010..... 113
Figure 4.21b: Maximum 5-day precipitation amount (RX5day) from 2011 to 2100 113
Figure 4.22a: Simple daily intensity index (SDII) from 1960 to 2010 114
Figure 4.22b: Simple daily intensity index (SDII) from 2011 to 2100 114
Figure 4.23: Drainage density map 116
Figure 4.24: Slope map of Abidjan 117
Figure 4.25: Soil type map of Abidjan 118
Figure 4.26a: Rainfall variability in Abidjan from 1961-1970 120
Figure 4.26b: Rainfall variability in Abidjan from 1971-1980 121
Figure 4.26c: Rainfall variability in Abidjan from 1981-1990 121

Figure 4.26d: Rainfall variability in Abidjan from 1991-2000 122
Figure 4.26e: Rainfall variability in Abidjan from 2001-2012 122
Figure 4.27: Isohyet map of Abidjan 123
Figure 4.28: Hazard map of Abidjan 124
Figure 4.29: Population density of Abidjan 126
Figure 4.30: Drainage system density of Abidjan 127
Figure 4.31: Urban structure types of Abidjan..... 128
Figure 4.32: Vulnerability map of Abidjan 130
Figure 4.33: AHP flood risk map of Abidjan 131
Figure 4.34: Validation of AHP flood risk map with flooded areas records 133
Figure 4.35: Runoff coefficient map of Abidjan 134
Figure 4.36: LULC based on SCS table 135
Figure 4.37: Rainfall intensity map of Abidjan 136
Figure 4.38: Peak runoff map of Abidjan 137
Figure 4.39: Digital Elevation Model (DEM) map of Abidjan 138
Figure 4.40: Flood hazard index map of Abidjan 139

KNUST

LIST OF TABLES

Table 3. 1: Landsat satellite data acquired for the years 1990, 2002 and 2014 35
Table 3. 2: Daily extreme precipitation indices 55
Table 3. 3: Reports the scale of the various elements of comparison (Saaty, 1980). 66
Table 3. 4: Random Index matrix of the same dimension (Saaty, 1980) 67
Table 3. 5: Hazard matrix [A] 68
Table 3. 6: Normalized Matrix [A] 69
Table 3. 7: Weight of Hazard indicators 70
Table 3. 8: Vulnerability Matrix 70
Table 3. 9: Weight of the vulnerability indicators 71
Table 3. 10: General objective matrix 71
Table 3. 11: Weight of flood criteria 71
Table 4. 1: Confusion matrix (percentages) for classified land use land cover map of the years 1990, 2002 and 2014 81
Table 4. 2: Change in areas of each land use/ land cover class between 1990 and 2002 82
Table 4. 3: Change in areas of each land use/ land cover class between 2002 and 2014 83
Table 4. 4: Change in areas of each land use/ land cover class between 1990 and 2014 83
Table 4. 5: Land use / land cover change detection in Abidjan 85
Table 4. 6: NDBI for 1990, 2002, 2014 years in Abidjan 86
Table 4. 7: Correlation between measured and estimated annual daily maximum rainfall 95
Table 4. 8: Precipitation returns period for 100, 50, 20, 5, 2 years 95
Table 4. 9: Minimum/maximum temperature, precipitation, solar radiation and evapotranspiration change prevision at Abidjan. 96
Table 4. 10: Weight assigned to “drainage density” classes 116
Table 4. 11: Weight assigned to "Slope" classes 117
Table 4. 12: Weight assigned to "Soil type" classes 119
Table 4. 13: Weight assigned to "Isohyet" classes 124
Table 4. 14: Weight assigned to "population density" classes 126
Table 4. 15: Weight assigned to "Drainage system density" classes 127
Table 4. 16: Weight assigned to parameter "UST" classes 129

LIST OF PLATES

Plate 3.1:……...……58

Plate 3.2:……...……61

Plate 4.1:……..…129

Plate 4.2:…….129

Plate 4.3:……..…129

Plate 4.4:……..…129

KNUST

ACRONYMS

AHP: **A**nalytical **H**ierarchy **P**rocess

CCI: Climate **C**hange **I**niatiative

CCT: **C**entre de **C**artographie et de **T**élédétection

DEM: **D**igital **Elevation M**odel

DTM: **D**igital **Terrain M**odel

GCM: Global **C**limate **M**odel

GIS: **G**eographic **I**nformation **S**ystem

HADCM3: Hadley **C**entre **C**oupled **M**odel, version **3 INS:**

Institution **N**ational de **S**tatistique:

ISCSU: International **C**ouncil for **S**cience **U**nions

LARS-WG: Long **A**shton **R**esearch **S**tation - **W**eather **G**enerator

MATE: Ministère de l'**A**ménagement du **T**erritoire et de l'**E**nvironnement

MCA: Multi-**Cr**iteria **A**nalysis

MEDD: **M**inistère de l'**E**nvironnement et du **D**éveloppement **D**urable

OBIA: Oriented **B**ased **I**mage **A**nalysis

OCHA: Office for the **C**oordination of **H**umanitarian **A**ffair

SRTM: **S**huttle **R**adar **T**opography **M**ission

TM: **T**hematic **M**apper

UST: **U**rban **S**tructure **T**ypes

WCP: World **C**limate **P**rogram

WCRP: World **C**limate **R**esearch **P**rogram

WMO: World **M**eteorological **O**rganization

CHAPTER 1: GENERAL INTRODUCTION

Background

Climate change has become one of the most visible global environmental problems in the last decade and hence needs to be examined on the global, regional and local scale. Climate change is considered to be the biggest challenge facing mankind in the twenty first century (Osman *et al*., 2014). In addition, population growth with its demand and development has become a world issue this last century (Txomin *et al*., 2013). Urbanisation, which results in the conversion of natural vegetation, forest, agricultural land, wetlands and natural drainages to built-up environments and construction impacts on climate. Changes in climate patterns alter the spatial and temporal distribution of hydrological characteristics with inevitable consequences that are very significant. The impact of climate change which includes, erosion, drought, landslides and floods have very serious consequences on the environment, human beings and their socio-economic activities. Climate change may also increase the frequency, magnitude and the seasonality of extreme events, especially floods.

Flood risk occurrence is a combination of natural and anthropogenic factors, hence the need to examine the spatial extent of floods. Floods are among the most devastating natural hazards in the world, claiming more lives and causing more property damage than any other natural phenomena (Kebede, 2012; Yalcin *et al*., 2004; Yahaya *et al*., 2010 and Ouma *et al*., 2014). It has been acknowledged that flood risks will not decrease in the future, and may rather occur more frequently in the future with the onset of climate change (Huong and Pathirana, 2013; Pederson *et al*., 2012). Flood intensity and frequency will threaten many regions of the world and as a result, floods are one of the greatest challenges to weather prediction (Jeyaseelan, 2003). Urban floods, caused by extreme rainfall events, is an increasing problem for cities due to land-use change. For

natural disaster planners, rapid urbanisation is one the cause of increasing flood risk in urban areas. Urban flooding often occur as a result of crowding urban developments, insufficient storm drainage capacity, river overflows, storm surge or a combination of these phenomena which means, concurrent flood hazard is of importance to urban flood risk management. However, in developing countries, inadequate maintenance of drainage channels, disposal of debris and solid waste into the drainage channels, are stress factors which accentuate urban floods.

In Africa, the situation is very likely to worsen as Intergovernmental Panel on Climate Change (IPCC) projects higher frequencies and intensities of floods and droughts (IPCC, 2007) for the continent as a consequence of climate change. Floods and flash floods cause loss of life and damage to property (Musungu *et al.*, 2012). From 1900 to 2006, floods in Africa killed nearly 20,000 people, and also affected nearly 40 million more, causing an estimated damage of US$4 billion according to the International Council for Science Unions (ICSU) Regional Office for Africa, (2007).

Urban areas have high risk of flash flooding due to the presence of large impervious areas and sometimes inefficient drainage system (Huong and Pathirana, 2013). Several additional phenomena commonly contribute to urban flooding, such as limited conveyance capacity of urban channels and rivers as well as drains and sewers because of blockages and infiltration–inflow, and decades of urban development without upgrading of the drainage infrastructure (Pederson *et al*., 2012).

While the primary cause of flooding is normally heavy rainfall, many other causes are also due to human activities such as: land degradation; deforestation of catchment areas; Sprawl and increased population density along riverbanks (Mbow *et al.*, 2008), poor land use planning, zoning, and control

of flood plain development; inadequate drainage particularly in cities, and inadequate management of discharges from river reservoirs.

Urbanisation is also an important driver of increased flood risk in cities by increasing runoff, which affects communities' downstream (Cloke *et al*., 2013). Flood hazard also increases as a result of hydrological and hydro-climatological changes brought about by land use and microclimatic changes driven by urbanisation (WMO/GWP, 2008 cited by Huong and Pathirana, 2013). Assessing extreme rainfall, predicting risk mapping and flood modelling has become essential to offer appropriate solutions for flood mitigation and sustainable environmental management of the risks they generate.

Problem Statement and Justification

More recently in Cote d'Ivoire, communities have experienced increasingly important phenomena of floods, with its effects such as environmental pollution and coastal erosion. Flooding is the main natural risk, which annually cause loss of lives and damage to property including displacement during the rainy season in Abidjan. Abidjan is the economic capital of Cote d'Ivoire, centre of business in West Africa and where many institutions have their main offices with rapid population growth (5 million). Statistical analysis in 2013 showed that 26 % of the District of Abidjan is at the risk of flooding and 21 people in 2009, 13 in 2010, and 15 in 2011 died in the District of Abidjan because of floods (OCHA, 2014). Besides, a total of 80,000 people are threatened by flooding in the District of Abidjan with 40,000 people at risk in Cocody, 12,500 people in Abobo, 10,000 in Adjame, 9,500 in Yopougon and 8,000 in Attecoube Municipalities (OCHA, 2014). These statistics indicate the gravity of the issue of flooding in the District and the fact that many lives and property are at risk.

The frequent floods and the increasing destruction that come with them in Abidjan are largely attributed to climate change and human activities such as increasing impervious surface area. Other significant factors resulting in the frequent occurrence of floods in the area are changes in land use patterns, inefficient urban drainage system and uncontrolled urbanisation. These are increasing the percentage of flood and flash flood vulnerability in Abidjan. It is estimated that urbanisation (uncontrolled and controlled) alone has contributed to a significant increase in runoff in the city due to the increase in impervious area and this is likely to continue as population increases. Scientific research has a key role to play in understanding which areas are at risk of flooding. This will enable decision makers take adequate and coordinated measures in order to prevent or reduce flood risks.

Climate change assessment often requires integrated modelling in assessing the risk of flooding. Urban flood risks assessment and modelling are complex issues that require an integrated approach to spatial planning, ecological consideration in development, political decision making and socio-economic development. This makes Remote Sensing, Geographic Information Systems (GIS) tools, hydrological modelling and multi-criteria analysis powerful techniques for the understanding of floods; creating flood risk maps to provide a basic information, plans and communicate to various target groups (including decision makers and the public) for the effective management of these risks. The advantage of using Remote Sensing and GIS for flood risk assessment and modelling is not only to generate a visualize map of flooding, but also to create the potential to further analyse and understand the process which results in this event. The multicriteria analysis methods provides a framework which can handle different views on the identification of the elements of a complex decision problem, organise the elements into a hierarchical structure, and study the relationships among components of the problem. The use of this method in the

context of flood risk assessment is still rare and Analytic Hierarchy Process (AHP) developed by Saaty (1980) is one of the best known and most widely used MCA approaches.

However, recent scientific work undertaken in the District of Abidjan concentrated on certain factors controlling flood risk such as the rainfall risks and uncontrolled urban growth in two municipalities of Abidjan: Attecoube and Abobo (Celestin, 2008 and Savane *et al*., 2003). This is a piecemeal approach and will not provide solution to the problem of flooding in the District. Other studies (Kouame *et al*., 2013; Jourda *et al*., 2003 and Ahoussi *et al*., 2013) in the District did not directly focus on flooding but pointed out the inefficiency of the drainage network and impervious area which are part of the main drivers of floods. These studies are fragmented and did not consider the entire District, and did not link climate change and land use effects. Thus, few studies have been undertaken to understand the natural causes and associated anthropogenic implications of urban flood risks. There is a clear lack of knowledge in this area and a need for identifying, mapping and modelling areas of flood risk in the District of Abidjan. Therefore, the motivation of this research is to fill this gap by assessing flood risk using an integrated multicriteria evaluation and modelling approach of the entire District. This will facilitate decision making for better land use planning and flood risk reduction under changing climate in Abidjan.

Research Objectives

The goal of this study is to identify, map and model areas of flood risk under changing climate in Abidjan. The specific objectives are to:

i) Assess urban land use/land cover dynamics on flood risk, ii) Characterise significant hydro-climatic drivers of urban flood risk, iii) Determine and analyse weather trends under observed and future climatic

conditions, iv) Create urban flood risk map using multi-criteria analysis approach, and

v) Develop flood hazard index map.

KNUST

Scope of the thesis

The scope of this thesis was to establish the extent of urbanisation as major land use change and areas in the Abidjan District which are at risk of flooding. The study also demonstrated the efficiency of multi-criteria analysis as a method (Analytic Hierarchic Approach) in the assessment of floods.

Overview of Thesis

The thesis is organised into 6 main chapters as presented below:

- Chapter 1 presents a general background to the research as well as the current problem necessitating this research. It also spells out the aim objectives and scope of the research.
- Chapter 2 presents the review of relevant literature in remote sensing (RS) based on urban land use/land cover dynamic, weather variability and flood risk assessment.
- Chapter 3 describes the materials and methods used to achieve the objectives of this study
- Chapter 4 presents the results obtained from the study.
- Chapter 5 discusses the results obtained for each specific objective of the study.
- Chapter 6 presents the conclusions drawn from the study and some recommendations.

CHAPTER 2: LITERATURE REVIEW

2.1. Overview

Climate change itself and its effect on land use has become the main interest in these last decades by most of the multi and interdisciplinary research worldwide. Many books, articles and reviews have been published on climate change impacts connected to land use patterns including agriculture, urbanisation, population growth, water resources and natural disasters.

Although, numerous of these researches have been more relevant in our study and these review is mainly concerned land use/land cover dynamic related to urbanisation, flood risk assessment, prediction and modelling under climate change. This chapter presents a review of relevant literature, including definitions of concepts and terms. It has been divided into three sections. The first section review urban land use classification and mapping. Section two reviews weather variability under present and future conditions. Section three reviews urban flood assessment and modelling. Finally, definitions and explanation of concepts like land use/ land cover, climate change, hazard, vulnerability, flood risk is provide in the last section.

2.2. Urban Land use/land cover dynamic

Many factors natural and anthropogenic including urbanisation, goods, population growth and industrialisation affect land and climate. Thus both have been recognized as a driver of the long-term change in land which automatically disturb climate. Thus, the land use/land cover (LULC) dynamics is an important component to better understand the land patterns induced by human activities and therefore to understand its implications in climate change (Lambin, 2001). Also, the understanding of the interactions between land cover and land-use in their spatial and temporal appearances is fundamental to comprehension of land-use and land cover change (Jansen *et al*., 2002). Land use/land cover changes through different process such as urbanisation,

deforestation, intensive and extensive agriculture have contributed to the climate disturbance. Population growth too has become a world issue on this century with its consequence urban sprawl due to human demand and development (Txomin *et al*., 2013). Urban sprawl one of the core LULC change process is more crucial in the developing countries. In West Africa, there is a rapid increase in the urban area in order to satisfy people's needs, but, there is a dilemma in the urban planning about how to obtain urban sustainable development. Land use/ Land cover (LULC) disappearance and dynamics in urban areas are characterised by a process of rapid urbanisation with changes in land use and urban morphology. These changes are caused by an expansion of planned areas, and informal housing settlements which reduce the number of open spaces and green space, degradation of vegetation and environment.

Cote d'Ivoire in recent times, registered increasingly more important changes in land use in several urban areas due to various causes including population exodus and demand and urbanisation. Many researchers have published on LULC change in several parts of Cote d'Ivoire (Savane *et al.*, 2001; Goula *et al*., 2006; Kouassi *et al.*, 2008; N'go *et al*., 2013; and Yao *et al*., 2015).

The results shows that, most of the land use change were due to urban sprawl. Rapid population growth, which is the result of natural population increase and migration of population from rural to urban areas, is identified as having an impact on the land. The use of remote sensing tools becomes the most appropriate and common approach to classify land use and detect the change. Recently, remote sensing data has increasingly been used in order to generate LULC (Gerl *et al*., 2014). Several methods have widely been developed in previous studies on land use/land cover classification and change using remote sensing tools and moderate or high resolution satellite image (Landsat, Spot, Ikonos, Rapideye, quickbird and so on..) in various study areas and those

specific in urban areas can be summarized into three groups: Classic method of classification, index calculation and Oriented based images analysis method in urban areas.

2.2.1. Classic classification (unsupervised and supervised) method.

Image classification is to (semi)-automatically label all pixels in an image into different classes (Lillesand *et al*., 2004). This may be done by analysing the spectral or temporal pattern of the pixels. Image classification can be done through two approaches unsupervised and supervised methods.

In an unsupervised classification, statistical approaches are only applied to image pixels without any user-defined training classes to automatically identify distinct spectral classes (clusters) in an image data. K-means and Iterative Self Organizing Data Analysis (ISODATA) are the two unsupervised classification algorithm. The approach requires the user to specify the number of clusters to be generated, and then the classifier automatically aggregates the image pixels into the required clusters by minimizing some predefined error function. The final LULC type of each cluster can then be determined by the analyst by comparing the classified image with ground reference data.

In a supervised classification, the analyst guides the classification procedure by clustering pixels in a dataset into classes corresponding to user-predefined training classes also known as regions of interest (ROIs). This classification type requires that you select training areas for use as the basis for classification and testing data (ground control truth) for assessing the accuracy of the classification results. Various classification methods are used including Parallelepiped, Minimum Distance, Mahalanobis Distance, Maximum Likelihood, Spectral Angle Mapper, Binary

Encoding, Neural Network and support vector machine. In this study, the Maximum Likelihood method which assumes that the statistics for each class in each band are normally distributed and calculates the probability that a given pixel belongs to a specific class, was used.

KNUST

2.2.2. Oriented based Image analysis (OBIA) method

To analyse the dynamics of urbanisation and their processes, it is important to get a deeper understanding of urban morphological processes and the physical patterns of a city (Huck *et al*., 2011). Therefore, it is essential to assess the dynamic of LULC within urban area by having a particular interest in assessing the relationship between land use dynamics and built-up expansion. Then, bring out the urban structure types because these are a key factor to comprehend change in urban zone. Traditional, visual mapping and updating of urban structure information of cities is a very laborious and cost-intensive task, especially for large urban areas (Wurm *et al*., 2009). Nowadays, remote sensing has become an efficient tool for providing land use information and is abound for the acquisition and mapping of the urban spatial dynamic and structure (Gerl *et al*., 2014). Object-based image analysis (OBIA) is gaining rapid popularity in remote sensing science because of the capability to link very high resolution (VHR) imagery and GIS (Dragut *et al*., 2014). OBIA approach incorporates spectral, textural and contextual information in identifying thematic classes in an image. Many ideas concerning image segmentation approaches and tools (Wurm *et al*., 2009) and object-oriented classification in urban areas have been presented (Txomin *et al*., 2013). OBIA is based on two main steps: segmentation and classification. Multi-scale image segmentation is a major step in OBIA, however, most important step in OBIA until now is the estimation of the optimal scale parameter of each class which is yet the highest challenges in several previous study (Wurm *et al*., 2009; Dragut *et al*., 2014; Txomin *et al*., 2013; Huck *et al*.,

2013; Dronova *et al*., 2015). Consequently, recent studies have developed tools and methods to estimate scale parameter for multiresolution image segmentation (Dragut *et al*., 2010 and 2014).

Many researchers have worked on high resolution satellite images for urban structure type (UST) classification by applying OBIA techniques which have been summarized in several reviews (Bremner *et al*., 2010; Huck *et al*., 2013; Dragut *et al*., 2014; Dronova *et al*., 2015 and Singh *et al*., 2014).

2.3. Weather variability

Climate change is considered to be the biggest challenge facing mankind in the twenty first century (Osman *et al*., 2014). Climate change is a global issue and needs to be examined at global, regional and local scale. Population demand, green gas emission from industrialisation and land use change lead to severe climate variability and change such as increasing temperature and rainfall across the world and more specifically in West Africa.

However, the use of future scenario and indices calculation of weather data for understanding present condition and managing future hydrologic events in Cote d'Ivoire is practically non- existent. Weather data analysis for many years were based on determining break on the times series using some statistical methods such as Pettit and Buishand test, application of standardised precipitation index (SPI) to bring out the wet and dry period in case of rainfall variability and shows general trend, and inter-annual behaviour (Brou 1997; Brou, 2005; Savane *et al.*, 2001; Goula *et al.*, 2006; Kouassi *et al.*, 2008 and Fossou *et al.*, 2014).

Climate change impact is very often related to heavy precipitation or/and increase of temperature, which leads to extremes events including drought, earthquakes, floods and Tsunami.
Therefore, knowledge about weather variability or change is crucial for natural disaster mitigation. Also, the availability of future weather data becomes a potential source for short term and long

term extreme rainfall and temperature predictions. For all that, general circulation models (GCM) has become an important tool to generate future scenarios and helpful to predict extreme rainfall under climate change. However, the output from Global Climate Models (GCMs) cannot be used directly at a site because of their very coarse spatial resolution (Semenov *et al*., 1998). Thus, weather generator can serve as a good computationally tool to produce at local scale specific climate change scenarios at the daily time-step with better resolution and fit reality. Of late, numerous climate models have been developed through Global or regional climate model to analyse climate variability for extreme event detection.

Long Ashton Research Station-Weather Generator (LARS-WG) model which is a stochastic weather generator specially designed for climate change impact studies is one of the important general circulation models for future climate change. LARS-WG is a numerical model which produces synthetic daily time series of a suite of climate variables, such as precipitation and temperature, with certain statistical properties (Semenov *et al.*, 1998).□ LARS-WG has been tested for different sites worldwide and shown its ability to model rainfall extremes with reasonable skill (Semenov, 2008). LARS-WG too has been used in various studies, including assessment of the impact of climate change (Goodarzi *et al*., 2014; Molanejad *et al*., 2014; Osman *et al*., 2014; Noori *et al*., 2013; Semenov 2008; Semenov and Doblas-Reyes 2007; Semenov and brooks 1999; Semenov *et al.*, 1998). According to Sobhany and Fateminiya, (2014); high accuracy of climate data modelling in different climatic stations has been confirmed by many researchers using LARS-WG.

Rclimdex model which is a statistical package developed by WMO CCI/CLIVAR Expert Team and ETCCDMI team for Climate Change Detection Monitoring Indices provides 27 indices based on daily weather data including rainfall and temperature (minimum and maximum). This model before all indices calculation test data homogeneity and quality. These indices gives more

comprehension in analysis of variations and trends in extreme climate events (drought and floods) which are more sensitive to climate change than are the mean values, and so have received much attention (IPCC, 2007). Several studies have used Rclimdex for temperature and precipitation extremes change detection (Cinco *et al*., 2014; Haylock *et al*., 2006; Yan *et al*., 2014; Stephenson *et al*., 2014; Keggenhoff *et al*., 2014; Yu and li, 2014; New *et al*., 2006; Revadekar *et al*., 2011; Gbode *et al*., 2015). In West Africa, Rclimdex model has been used to detect extreme events mainly drought in sahelian zone (Ly *et al*., 2013,) in addition to others weather and extremes indices models (Sarr, 2011; Ali, 2011; L'hote *et al*., 2002).

2.4. Historical Rainfall variability in Cote d'Ivoire

Mechanisms of rainfall distribution in Cote d'Ivoire are the same to those that explain general rainfall distribution in West Africa and especially in humid tropical zone. Cote d'Ivoire has experienced four big drought periods during the 20th century: 1943, 1968-1970, 1982-1983 and 1993 years (Brou *et al*., 1998 and Brou, 2005). These years of drought were due to the general decline and reduction of rainfall amount observed since 1970 in West Africa. There are significant differences between the thermal anomalies of the tropical Atlantic and some inter-regional developments Ivorian precipitation (Bigot *et al*., 2005) Ocean correlations. The beginning of the long period of drought since 1970 is identified by a break in the series of quasi-stationary general rainfall observations between 1968 and 1970 (Brou, 2005). The decrease in rainfall is remarkable, even in areas with high rainfall (1800 mm), especially in the mountainous West (Savane *et al*., 2001; Saley, 2003). Beyond this general decline trend, the inter-annual variability of precipitation in coastal areas differs from the rest of national areas. Rainfall anomalies in the coastal zones are often less intense (Brou, 1997). This climate variability is also manifested in the seasonal scale. It

was also accompanied by a decrease in the number of rainy days from the 1970s. Cote d'Ivoire is one of the countries bordering the Gulf of Guinea and affected by this phenomenon (Amani, 2007).

2.5. Flood Risk Assessment

Natural disaster is considered to be the biggest challenge that needs to be examined at global, regional and local scale. Climate changes may increase the frequency, magnitude and the seasonality of extreme events such as flood, which means that concurrent flood hazard of importance to urban flood risk management, may occur more frequently in the future (Huong and Pathirana**,** 2013; Pederson *et al.,* 2012). Urbanisation is also an important driver of increased flood risk in the city by increasing runoff which affects communities' downstream (Cloke *et al*., 2013). Floods are among the most devastating natural hazards in the world, claiming more lives and causing more property damage than any other natural phenomena (Kebede, 2012; Wang *et al*., 2011; Forkuo, 2011; Yahaya *et al*., 2010; Yalcin *et al*., 2004). As a result, floods are one of the greatest challenges to weather prediction (Jeyaseelan, 2003).

In Africa, the situation is very likely to worsen as Intergovernmental Panel on Climate Change (IPCC) projects higher frequencies and intensities of floods and droughts (IPCC, 2007) for the continent as a consequence of climate change. Floods and flash floods cause loss of life and property damage (Musungu *et al.,* 2012**)**. The demand of population growth and related urbanisation lead to severe land use change and increasing flood occurrence in West Africa.

Urban floods result from blocked or inadequate storm sewers and are due to increased urbanisation (Ajin *et al*., 2013). Urban areas have high risks of flash flooding due to the presence of large impervious areas and sometimes inefficient drainage system (Huong and Pathirana**,** 2013; Sowmya *et al*., 2015). Several additional indicators contribute to urban flooding, such as limited

conveyance capacity of urban channels and rivers, as well as drains and sewers and infiltration–inflow, and decades of urban development without upgrading of the drainage infrastructure (Pederson *et al.*, 2012). Other causes due to human activities such as: land degradation; deforestation of catchment areas; Sprawl and increased population density along riverbanks (Billi *et al*., 2015; Mbow *et al.*, 2008), poor land use planning, zoning, and control of flood plain development; inadequate drainage particularly in cities, and inadequate management. Flood hazard mapping is a vital component for appropriate land use planning in flood areas and mitigation measures (Bhatt *et al*., 2014). It provides accessible charts and maps, which can easily be read and therefore, facilitates the identification of risk areas by planners who then prioritize their mitigation efforts (Bapalu and Sinha, 2005; Forkuo, 2011; Wang *et al*., 2011; Ajin *et al*., 2013). Flood management is necessary not only because flood imposes urge damage on the society, but the optimal exploitation of the land and proper management. This cannot become technically feasible without effective use of flood hazard and risk maps (Bhatt *et al*., 2014).

Flood risk assessment and extent need spatial knowledge which means multisource data as drivers becomes a potential source for more reliable flood mitigation. Multi-criteria analysis (MCA) approach has become therefore widely used (Wang *et al*., 2011; Sowmya *et al*., 2015) to solve complex problem and to assess flood risk. Many methods (AHP, MCE, Fuzzy and AHP-fuzzy) have been proposed for multi-criteria decision making. Analytic Hierarchy Process (AHP) is one of the best known and most widely used MCA approaches (Orencio, and Fujii, 2013; Yahaya *et al*., 2010; Cozannet *et al.*, 2013; Pourghasemi *et al.*, 2014). AHP assumes complete aggregation among several criteria and develops a linear additive model. The uniqueness of applying AHP in different studies helps in modelling situations of uncertainty without losing subjectivity and objectivity of any evaluation measure. Of late, considerable attention has been given to the use of AHP in natural disasters (earthquake, landslide and flood) assessment especially flood

management in various studies: (Savane *et al*., 2003; Yahaya *et al*., 2010; Cozannet *et al*., 2013; Orencio, and Fujii, 2013; Saley *et al.*, 2013; Chakraborty and Joshi, 2014; Pourghasemi *et al*., 2014; Papaioannou *et al*., 2015; Nejad *et al*., 2015). It has been shown from these series of papers that AHP has the ability to assess and map flood risk with good accuracy. However, it is based on expert opinions and thus may be subjected to cognitive limitations with uncertainty and subjectivity (Pourghasemi *et al*., 2014).

2.6. Flood risk in Cote d'Ivoire

Climate change is causing many disasters around the world and particularly in developing countries (Brou, 2005; Goula *et al.*, 2006; Kouassi *et al.*, 2008). Cote d'Ivoire has recorded more significant natural disaster including flood, droughts and coastal erosion during this last decade. Various factors are attributed to climate change and human activities such as, changes in land use patterns, uncontrolled urbanisation, deforestation and an increase in the frequency of heavy rainfall. Other significant factors: inefficient urban drainage system, population growth, increasing of impervious surface area, inadequate maintenance of the drainage channels, and debris and solid waste disposed into drainage systems contribute and increased the risk of flooding in many parts of Cote d'Ivoire such as Abidjan, Sassandra, Grand-lahou, Grand-Bassam, Man, Facobly, Bangolo, Gagnoa, etc. Flood and coastal erosion are the most feared events for which action should be taken now to limit their consequences when they occur and develop mitigation strategies for future extremes events. The growing and uncontrolled urbanisation makes many populated areas vulnerable to flooding. Flooding causes damage to people with huge socio-economic cost such as property damage, population displacement and loss of lives in the southern part of the country especially in Abidjan. Most of the loss of lives recorded were people who lives in informal settlements, valleys around drainage channels and shantytowns. The origins of floods caused by

torrential rains are usually accentuated by inefficient drainage channels. Indeed, through ignorance and poverty, some people dump garbage in the sewers system and thus obstruct the flow of rainwater. However, the enormous flow of water cannot be channelled into ground and beds of rivers or artificial facilities for their control. Also, knowledge about flooding and its assessment and mapping remains modest because few research have been done in the country (Savane *et al*., 2003; Saley *et al.,* 2005 and Saley *et al.,* 2013), even though the variability and unpredictability of occurrence are great.

2.7. Definition of Concepts

This section explains the most important terminologies and concepts that are used frequently throughout this research. It is intended to assist all readers to better understand and be familiar with concepts described in this document and how I defined them.

2.7.1. Climate Change

Several definitions exist to understand the concept of climate change and the definition of climate change differs from one author to another. According to IPCC, 2007, climate change refers to any change in the climate over time, whether due to natural variability or as a result of human activities. Another definition from the UNFCC describes climate change as a change in the climate which is attributed directly or indirectly to human activity that alters the composition of the global atmosphere and which include natural climate variability observed over comparable time periods (IPCC, 2001). Considering both definitions, climate change refers to a significant statistical change of some parameters of the climate systems persisting for long periods.

2.7.2-Land use/Land cover

Land cover is the biophysical attributes of the earth's surface, i.e. the ecological state and physical appearance of the land surface (which includes vegetation, snow, ice field, water bodies and structure). On the other hand land use is the human use of land. Land use involves the land transformation or modification of natural environment which is a result of man-made process of changing the land use from one type to another e.g. transformation of forest area to an agricultural crop or transformation from pasture land to a residential area (Doka *et al*., 2002). Thus changes in land use and land cover is said to have a major impact on the global earth system with mostly negative consequences for both ecosystems and social systems (Lambin, 2001).

2.7.3-Hazard

Hazard is considered a physical phenomenon, natural and non- manageable, occurrence data and intensity that can cause damage by overflow stream and the extension of the field in the water flood. According to MEDD, (2000), hazard refers to hydro climatic phenomena and their impact on the flow of water. In technical settings, hazards are described quantitatively by the likely frequency of occurrence of different intensities for different areas, as determined from historical data or scientific analysis.

2.7.4. Vulnerability

Vulnerability expresses the level of foreseeable consequences of a natural phenomenon on issues (Mate, 2001) and in relation to hazards and disasters, vulnerability is a concept that links the relationship that people have with their environment. Vulnerability is conditional on a hazard and changes continuously over time. It is driven by physical, social, economic and environmental factors (Thywissen, 2006)

Flood vulnerability mapping is the process of determining the degree of susceptibility and exposure leading to flooding. These issues includes people, goods and socio-economic activities likely to be affected both quantitatively and qualitatively by a natural phenomenon. On the other hand, it is the most crucial component of risk in that it determines whether or not exposure to a hazard constitutes a risk (Ouma and Tateishi, 2014).

2.7.5. Flood risk Assessment

A flood is generally defined as an excess of the amount of discharged water compared to the drainage capacity (UNISDR, Global risk data platform). Risk can be considered as a function of the hazard event and the vulnerability of the elements exposed (Birkmann, 2007). The risk associated with the exposure of large concentrations of people and economic activities to intense hazard events, which can lead to potentially catastrophic disaster impacts involving high mortality and asset loss.

A flood risk is a result of the combination of two components: Hazard and vulnerability (Ouma and Tateishi, 2014) and also a product of three major elements: exposure to hazards, the frequency or severity of the hazard and the vulnerability (Birkmann, 2007)

CHAPTER 3: MATERIALS AND METHODS

3.1. Study area

The District of Abidjan is located in the south of Cote d'Ivoire between latitudes 5° 10’ and 5° 38’ North and longitudes 3°4’ and 5°21’ West. It is composed of thirteen (13) municipalities since 2001, ten (10) municipalities in Abidjan and three (3) others namely Bingerville, Songon and Anyama and covers an area of approximately 2,119 km^2. According to the National Statistical Institute (INS, 2013), Abidjan District has about 4,739,752 inhabitants in the metropolis, and

4,460,355 inhabitants in the main city, which represents 20.3% of the national population. In addition, this population is constant growth process mainly as a result of high industrialisation and urbanisation as well as high internal migration due to the later political crisis in the country.

Abidjan (Figure 3.1) is bounded:

- In the south by the Atlantic Ocean;
- In the southwest by the Prefecture of Dabou;
- In the west by the Prefecture of Grand Lahou;
- In the north by Agboville Prefecture;
- In the south-east by the Prefecture of Grand-Bassam;
- In the east by the Prefecture of Alepe.

KNUST

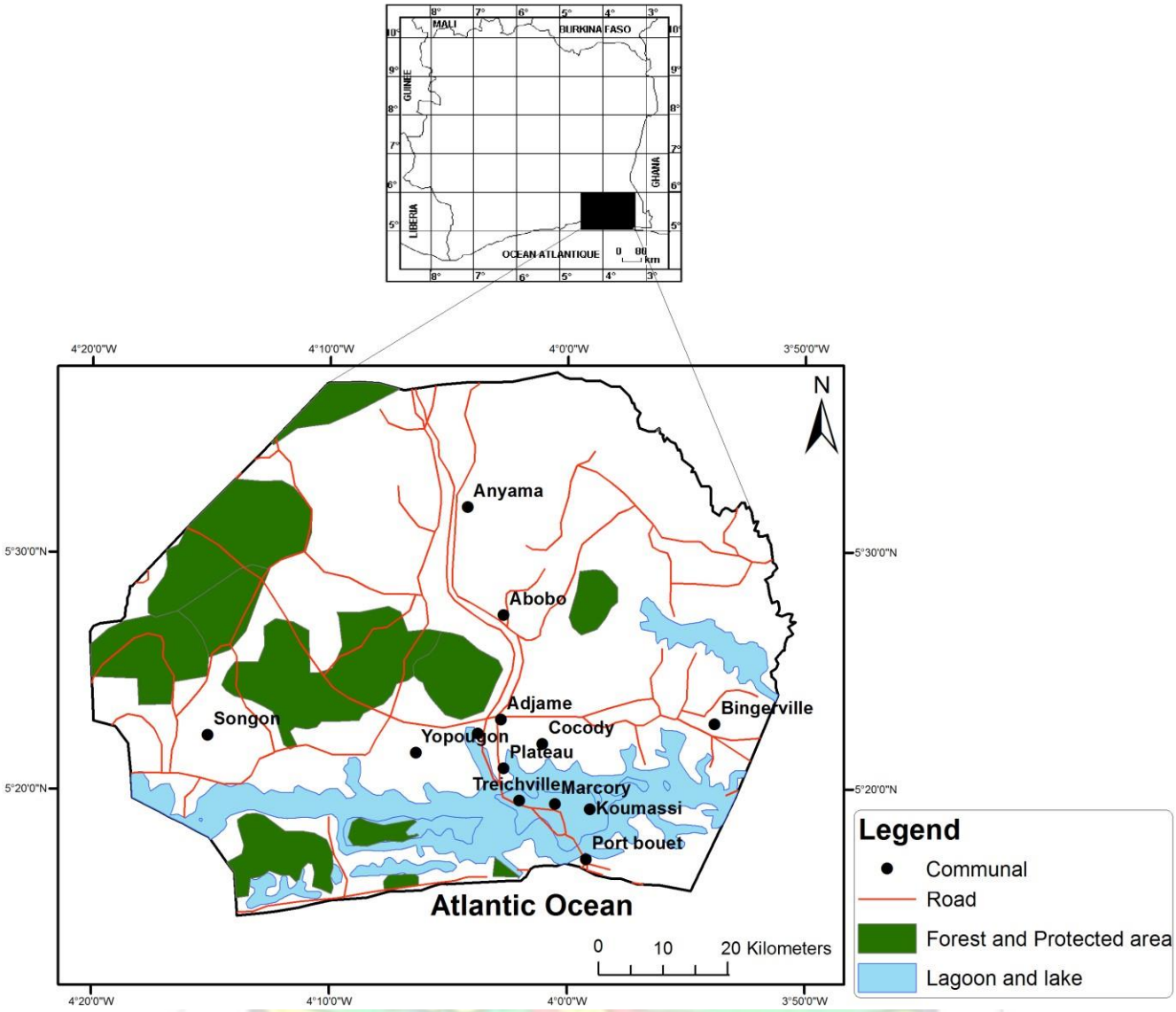


Figure 3.1: Location of the study area

3.1.1. Climatic context

The movement of the Inter Tropical Convergent Zone (ITCZ) determines the climate in Cote d'Ivoire (Saley, 2003). The study area has an equatorial transition climate (Attieen Climat) characterised by four seasons in the annual cycle: two dry seasons and two rainy seasons.

•Long dry season from December to March;

• Long rainy season from April to July;

•Short dry season from August to September;

•Short rainy season from October to November.

In recent times, the distinction between the seasons is not well pronounced. This was be attributed to climate variability/change.

The Abidjan District has three (3) rainfall stations located at Bingerville, Adiopodoumé and Abidjan airport. These stations measure and make available monthly data except Abidjan airport station which measures and makes available both monthly and daily data. Hence, daily temperature (minimum and maximum), rainfall and solar radiation data was only available for the Abidjan airport station.

3.1.1.1. Precipitation

For the characterisation of rainfall fluctuations that have affected the District of Abidjan. The study conducted an analysis of the spatio-temporal variation of monthly and annual rainfalls (Figure 3.2).

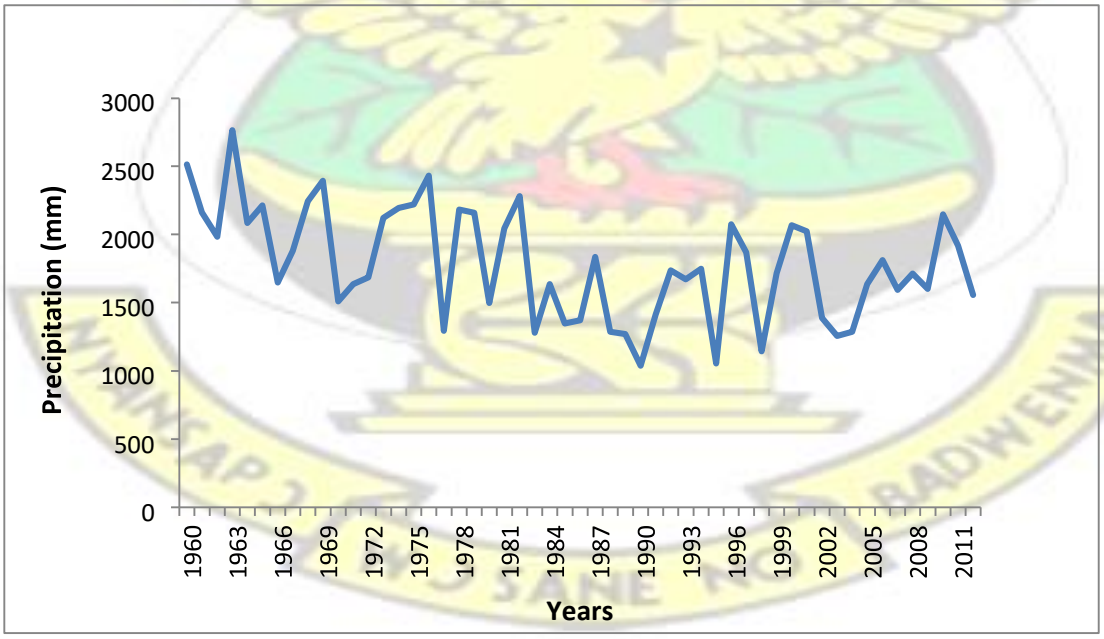


Figure 3.2: Annual rainfall trend from 1961-2012

The high annual rainfall recorded in the District of Abidjan during the period 1960-2012 ranged from 2800 mm in 1963 to 1020 mm in 1990, with an average of 1910 mm. Generally in the 1960s, the annual rainfall ranged between 2000 and 3000 mm. After 1987, there was a drop of this rainfall that oscillated between 1500 and 2200 mm. This is a reduction of more than 500 mm of rain compared to the 1960s.

Also, the observation of highest average monthly rainfall from 1960 to 2014 shows that June and sometimes May are the rainiest month of the District of Abidjan (Figure 3.3).

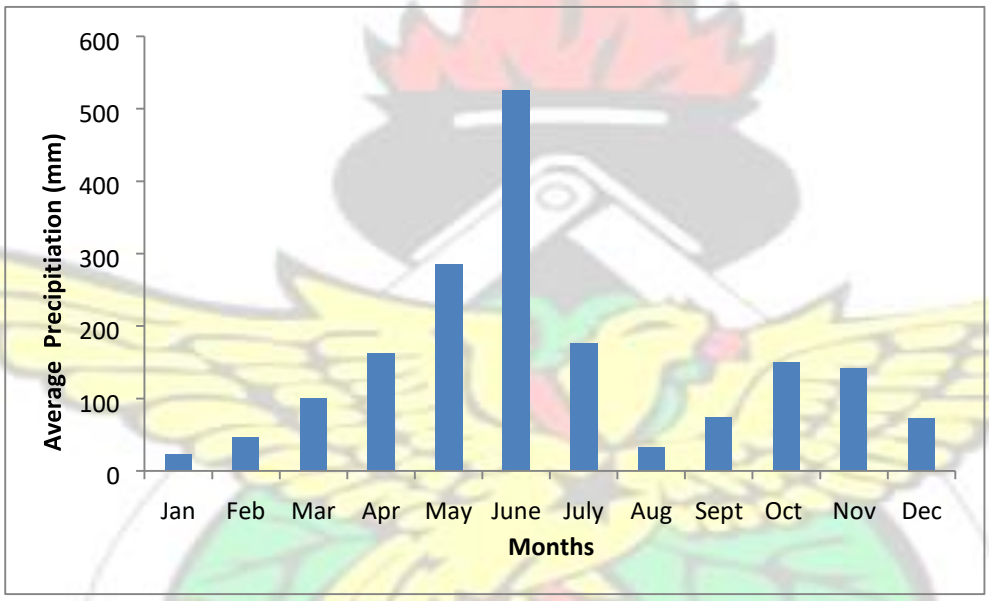


Figure 3.3: Variability of average monthly rainfall of Abidjan from 1961-2012

3.1.1.2. Relative humidity

The relative humidity of the Abidjan District is between 80 % and 90 % (Figure 3.4). The months of July, August and September are more humid with relative humidity above 86 % while those in November, December, January, February and March are less humid.

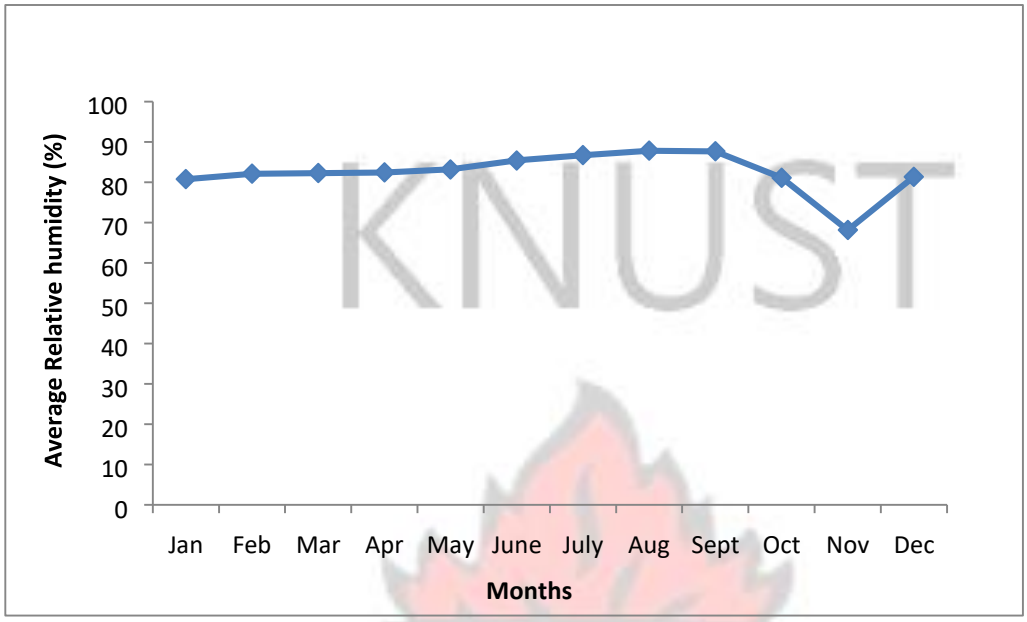


Figure 3.4: Average monthly relative humidity of Abidjan from 1961-2000

3.1.1.3. Temperature

The temperatures in the District are higher from February to March and November. There is a slight decline between the months of June and October. Figure 3.5 shows that the average monthly temperatures for the period 1960 - 2012 fluctuated between 24-28 °C. The months of March and April are the hottest months with a monthly average temperature above 27°C. The months of July to September (rainy season) are the least hot, with a maximum temperature equal to 24.5°C (Figure 3.5).

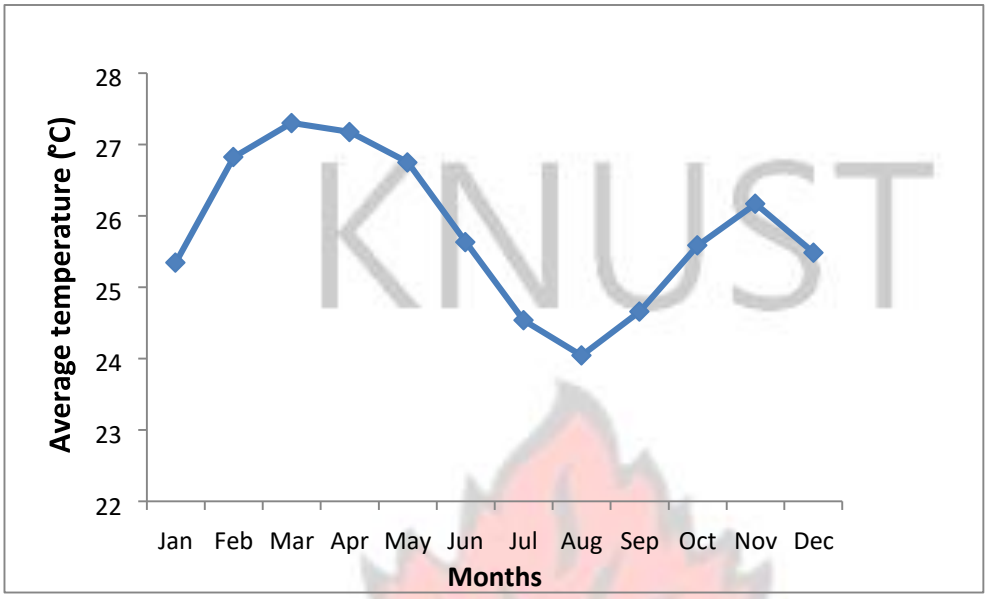


Figure 3.5: Average monthly temperature from 1961-2012

3.1.1.4. Relation between temperature and precipitation

After completing ombrothermic diagrams (comparison between temperature and rainfall charts) of Abidjan (Figure 3.6) over the period 1961-2012. It was noted that temperatures were low during the months of heavy rainfall and high during the months of low rainfall.

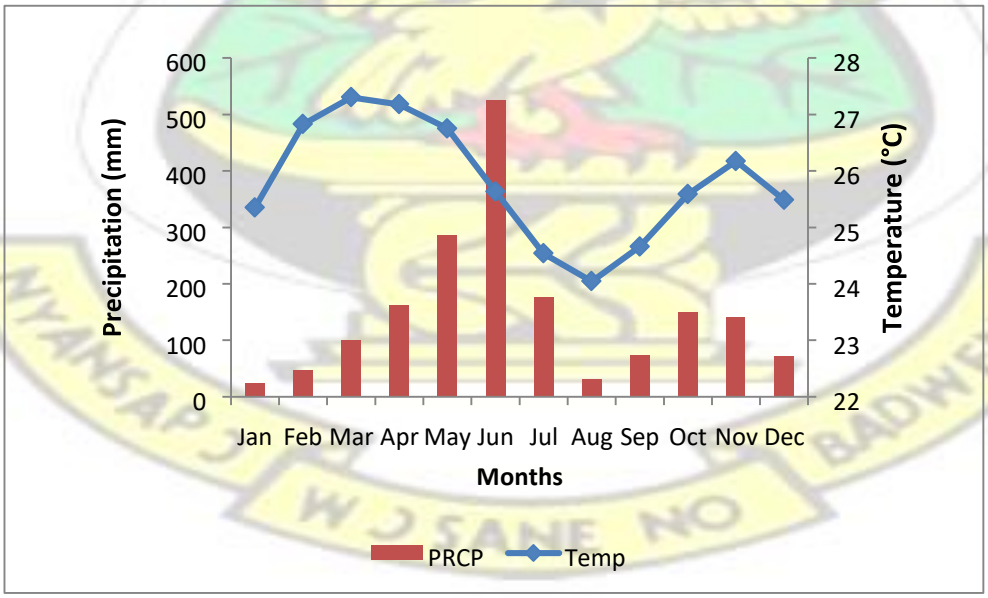


Figure 3.6: Ombrothermic diagram of Abidjan from 1961-2012

3.1.1.5. Relation between annual rainfall and two rainiest months

A comparison between annual rainfall and rainiest months of the respective years of the Abidjan District was carried out to analyse the trends from 1960 to 2012. The comparison revealed that, in general, the annual rainfall variability (rise and fall) is mainly related to the total rainfall recorded in the month of June (Figure 3.7).

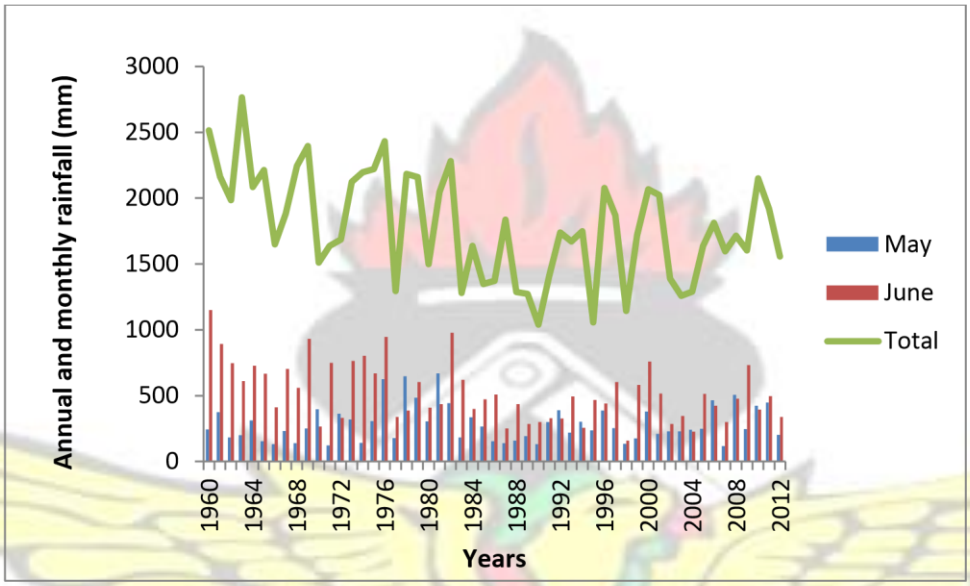


Figure 3.7: Plot of annual rainfall for two rainiest months (May and June) from 1960-2012

3.1.2. Topography

3.1.2.1. Relief

According to Tastet (1979), three geomorphological could be found in the study area (Figure 3.8):

- highlands into two levels, 40 to 50 m and 100-120 m, represented by the mounds of Continental Terminal north of the lagoon Ebrie;
- means plateaus ranging from 8 to 12 m, are the outcrops along the shoreline of the Quaternary;
- Plains and lagoons are all the more collapsed.

Tertiary high plateaus were cut by deep valleys and were covered with secondary forests and plantations in North and South Savannah Palmyra.

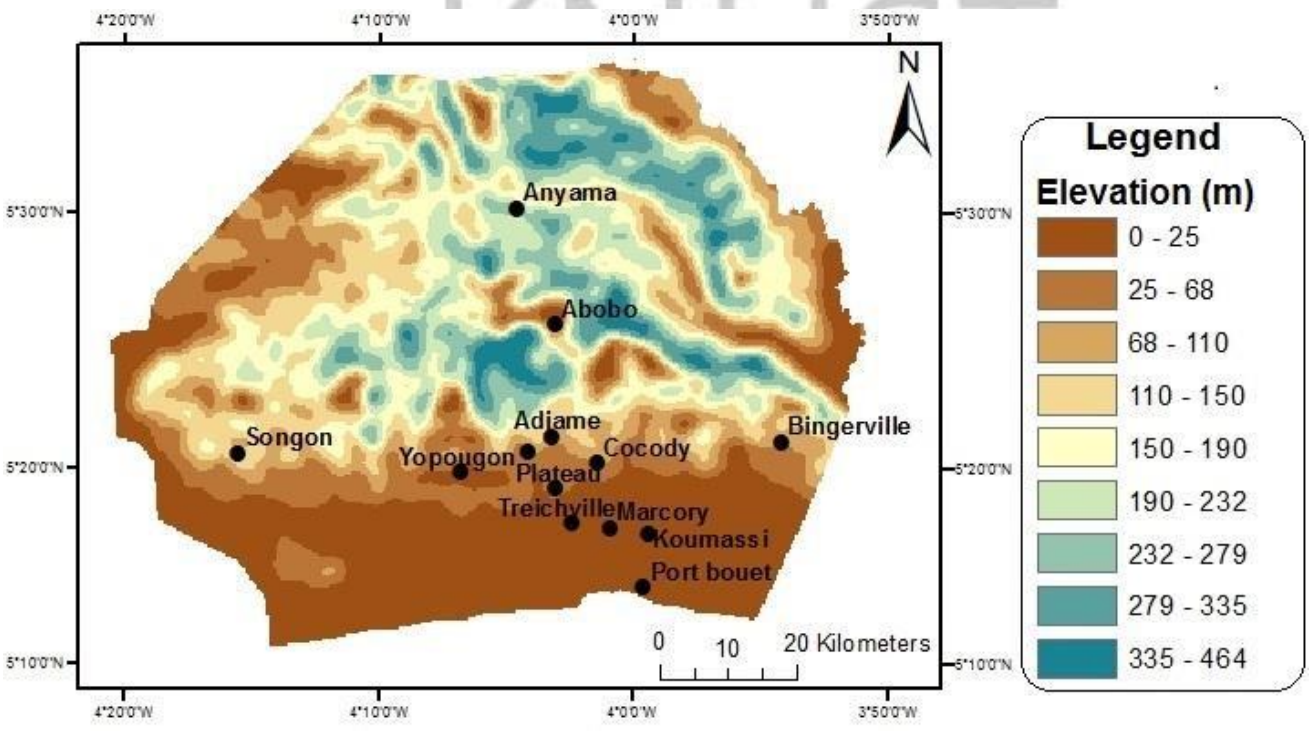


Figure 3.8: Digital Terrain Model (DTM) map of Abidjan

3.1.2.2. Soils

According to Papon and Lemarchand (1973), the soils of the study area belong to the class of highly desaturated lateritic soils, depleted-modal, on tertiary sands (continental terminal). However, the iron formations (levels gravel, fragments of armor and ironstone), classified in depleted soils are more or less reworked frequent in west of Abidjan in northern and southern border. Also, the sedimentary soil of Abidjan developed on Neogene collection consists of more or less clayey sands classified in the group of waterlogged soils. Hydromorphic soils in turn are at the estuary and near the main river. Depending on the importance of organic accumulation, two subclasses of waterlogged soils have been distinguished:

(i) Mineral hydromorphic soils that grow on alluvial river terraces and valley bottoms, periodically inundated by floods and ancient sands of the coastal band where the oscillations of water cover the entire profile (Humo-ferruginous layer). These soils are characterised by the presence of patches of waterlogging in the topsoil or in the underlying horizon depth pseudo-gley (mottled horizon grey rust and yellow ocher) reflecting alternating oxidizing and reducing conditions gley or (more or less mottled bluish gray horizon) reflecting reducing conditions can develop.

The pseudo-gley soils (to stains and concretions) and which most often gley (leached or all) grow in low funds and small valleys of colluvial-alluvial material. In floodplain soils pseudo-gley are more common and are associated with poorly developed soils and waterlogged modal input of alluvial material.

(ii) Organic hydromorphic soils that are represented in areas of swamp forest or grass origin, are permanently waterlogged throughout the year. These soils located on plateaus and moderate slopes (less than 3%) include two series: one series sandy and sandy loam series, the two sets are not separated on the sketch, only the depleted soil subgroup is modal noted. Soil slopes are more clayey in the top of the slope and very sandy in the lower slope. Fertility traits of these soils are medium, with soil depth, although its physicochemical properties are very low when it falls below a few centimetres of the topsoil.

3.1.3. Vegetation

Abidjan District has a dense forest vegetation type, and is part of attieen domain (Figure 3.9). There were many protected areas consisting of classified forests (M'brago, Djibi, Bedasso, Tagbadie, Languededou, Audoin, Mafe, and Ile boulay) and the Banco National Park. The vegetation which is characterised by the presence of large trees that may exceed a height of 50 m.

This forest has a closed canopy and as such maintains a warm and humid climate in southern of the study area. Thus, the defoliation of trees never affects the whole species' perpetual refoliation process is observed at the same time. However, there are few large trees, with thick woods. This degradation is caused largely by human activities including industrialisation, extensive agriculture, and also due to very poor soil or shallow soil. The shallow areas were characterised by the presence of palm oil, bananas, coconut and cashew plantations.

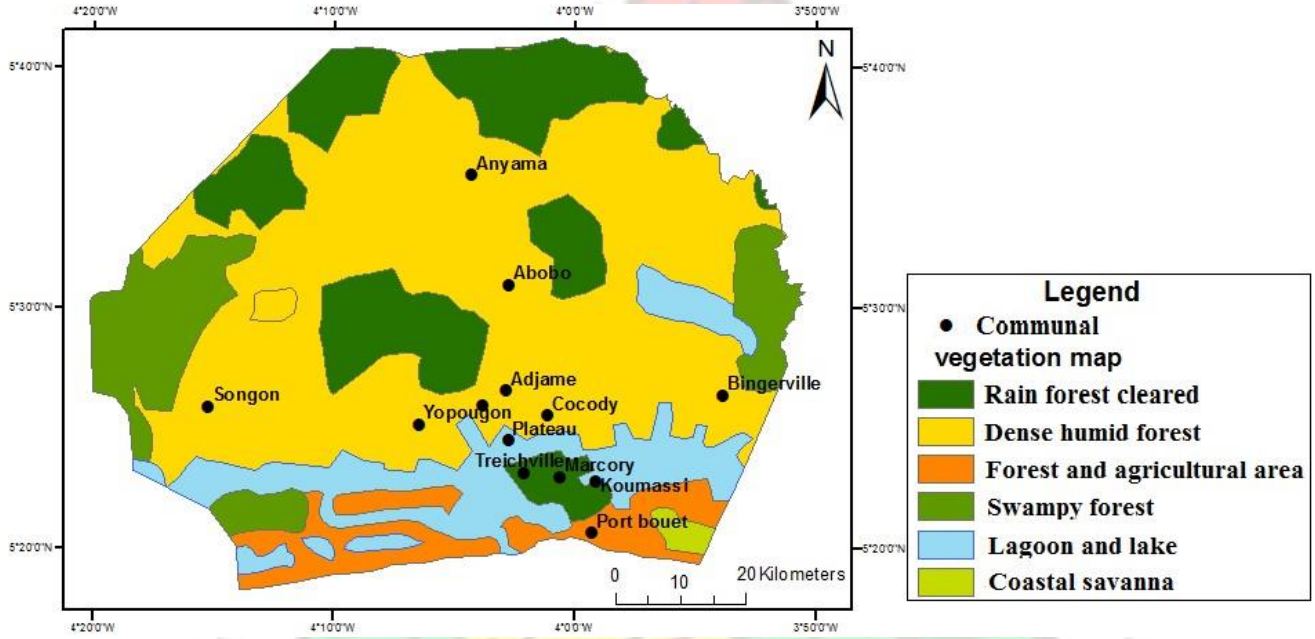


Figure 3.9: Vegetation map of Abidjan

3.1.4. Hydrogeological and geological context

3.1.4.1. Hydrological system and flooding Flow

- **Hydrological system**

Abidjan District has an equatorial transition system (Morell and Toillier 1973). This system covers the southern part of the Côte d'Ivoire on the south by a line Abengourou-Toumodi-Soubre (Sassandra region, Abidjan, etc.) in an area where the vegetation is a forest type (Morell and Toillier, 1973).

The temperature variations are low because they are highly buffered by the oceanic influence. The harmattan season has very little influence on annual averages. The flow of rivers depends on many factors including soil, the structure of the river system, evaporation, etc.

The area is drained by numerous rivers which have their hydrological regime influenced by precipitation (Figure 3.10). The influence of rainfall is very prominent on these factors. The hydrological regime is therefore apparently related to rainfall.

- **Drainage**

The drainage system of the District of Abidjan is average, and the regime is essentially irregular. This network is characterised by eight (8) streams orienting three (3) major directions:

(i) Banco, Gbangbo, Agneby and Anguédégou of north-south drain trays and empty into the lagoon Ebrie;

(ii) Nieke, a tributary of the Agneby, direction North-East to South-West;

(iii) Djibi, Bete and Lame, management northwest-southeast flowing into the lagoon Aghien.

All these rivers have essentially a drainage function vis-à-vis groundwater. During the rainy season, the flows are strong with large floods, and unlike in the dry season when the flow decreases and ponds dry up.

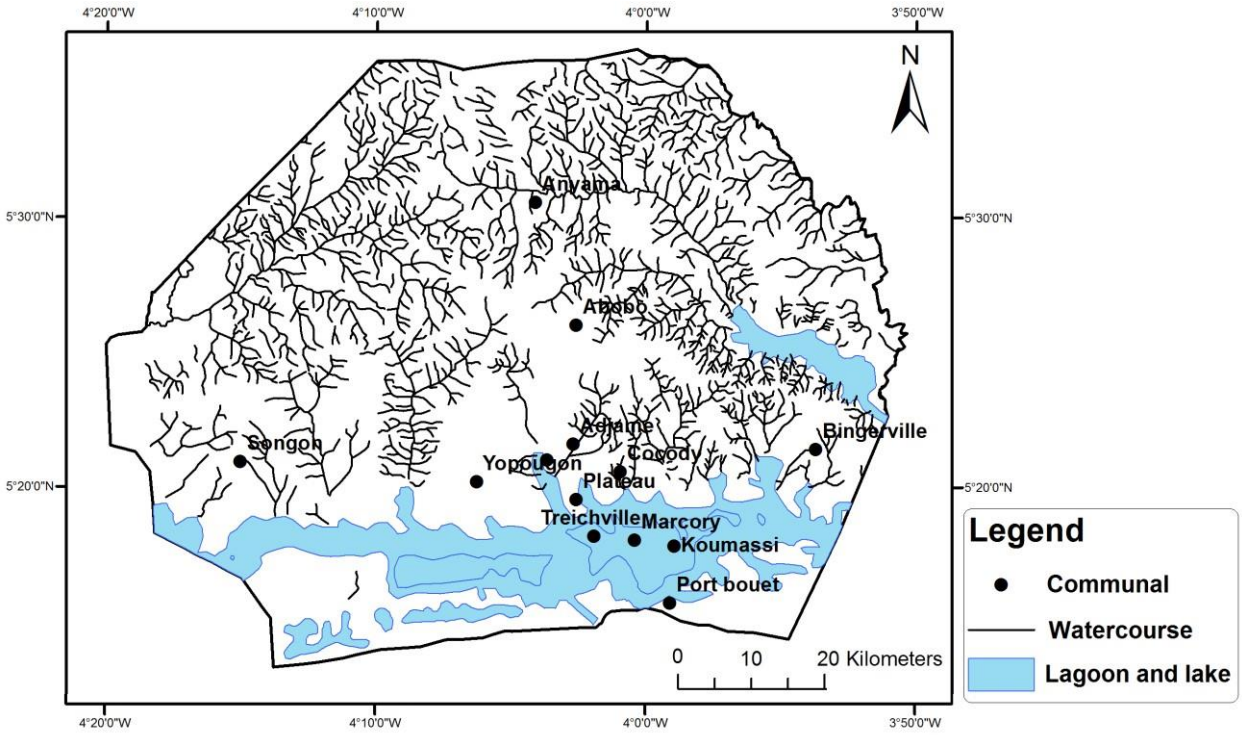


Figure 3.10: Hydrography of Abidjan District

3.1.4.2. Hydrogeology

The District of Abidjan is composed of homogeneous and highly permeable aquifers. The lithological column of the mainland sedimentary basin highlights sands, sandy clays and clays. The sedimentary basin reservoirs which have an important role in the hydrogeological network are three in number (Aghui and Biemi, 1984):

- Quaternary aquifer;

- Continental Terminal aquifer of Mio-Pliocene age; - Aquifer Maastrichtian.

3.1.4.3. Geology

The study area lies across the sedimentary basin in the south and the Precambrian basement in the

North. The Precambrian basement in the Abidjan area consists of Precambrian metamorphic schist age means (Birimian). The study belonging to the Ivorian coastal sedimentary basin (which represents only 2.5% of land area) area is Cretaceous-Quaternary and is composed of post-training Eburnean (Loroux, 1978). However the Mio-Pliocene age formations, commonly called Continental Terminal, from the Quaternary of the last episode of sedimentation basins of West Africa. The Continental Terminal has been characterized by (Aghui and Biemi, 1984) and consists of a lenticular stratification, coarse sand of variegated clays, ironstone and iron ore (Figure 3.11).

On the tectonic map, the visible part of the basin is divided into two unequal parts by a known fault "fault lagoons" of East-West direction (Tastet, 1979) with a rejection of up to 5000 meters and through Grand Lahou Akounongbe and Allangouanou (Ghana). This major accident lagoon is a normal fault extremely important distension, related to the opening of the Atlantic. This fault separates the basin into two distinct areas:

- North, sediment recovery has a monoclinic structure because all the beds dip to the south and the thickness is about 300 m. The Continental Terminal is major unconformity on the base through the basal conglomerate formed of gravel and quartz (Aghui and Biemi, 1984);

- In the South, a deep trench collapse where the foundation sinks to about 5000 m. Sedimentary formations in the Greater Abidjan consist of clays and sandy clays, sands and sandstones, conglomerates, glauconitic sand and marl (Aghui and Biemi 1984).

It should be noted that the sedimentary basin deepens from north to south with an average gradient of between 6 and 9%.

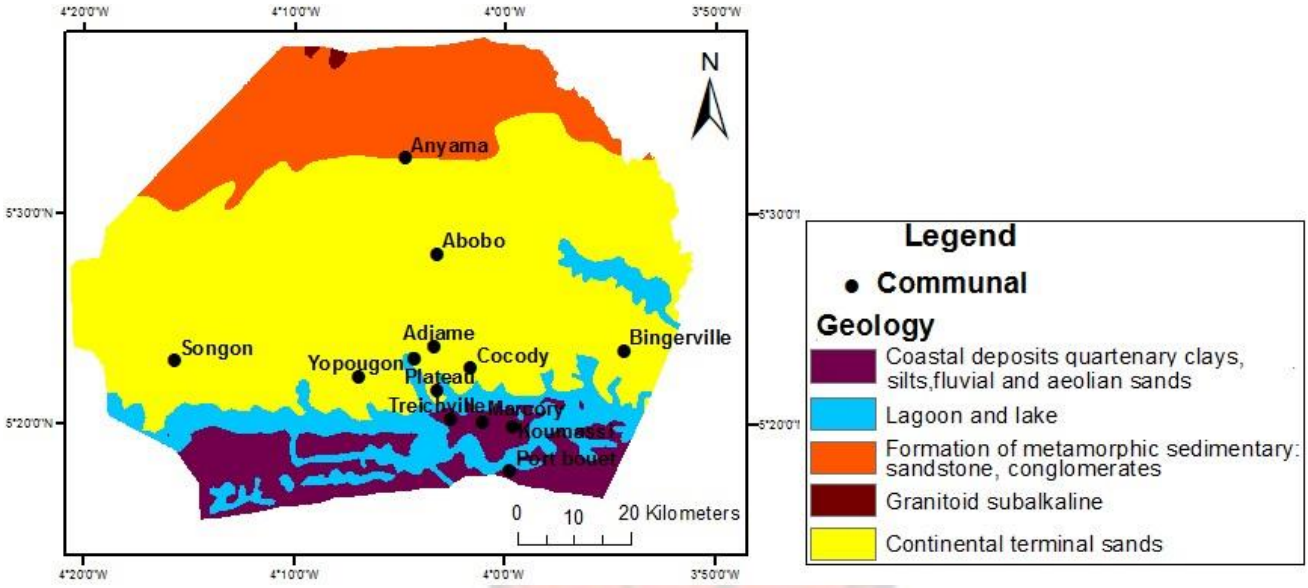


Figure 3.11: Geological Map of the District of Abidjan

3.1.5. Socio-economics and human environment

3.1.5.1. Socio-economic aspects

Abidjan District is the economic capital of Cote d'Ivoire and is the most populated city in Frenchspeaking countries within West Africa. It is also the second largest French-speaking city and the third largest metropolitan area. Considering West African or African cultural centre, Abidjan area knows a perpetual growth characterised by high industrialisation, business and urbanisation, added to the political crisis that the country has gone through in recent years; urban sprawl has increased due to mass displacement of population to the capital and its surroundings (Figure 3.12). According to the national statistical institute (INS, 2013), it has a population of about 5 million inhabitants, an urbanisation rate of 95.8%. It has four urban centres: The main city Abidjan is composed of ten (10) municipalities as cosmopolitan city and the municipalities of Anyama, Bingerville and Songon are the other three urban centres of the District. Abidjan is also characterised by continuous uncontrolled urbanisation growth (near rivers, the drainage networks

and even in areas prone to natural disasters) due to demography growing which creates gaps in the context of climate change and anthropogenic impact related to safe environment and healthy life.

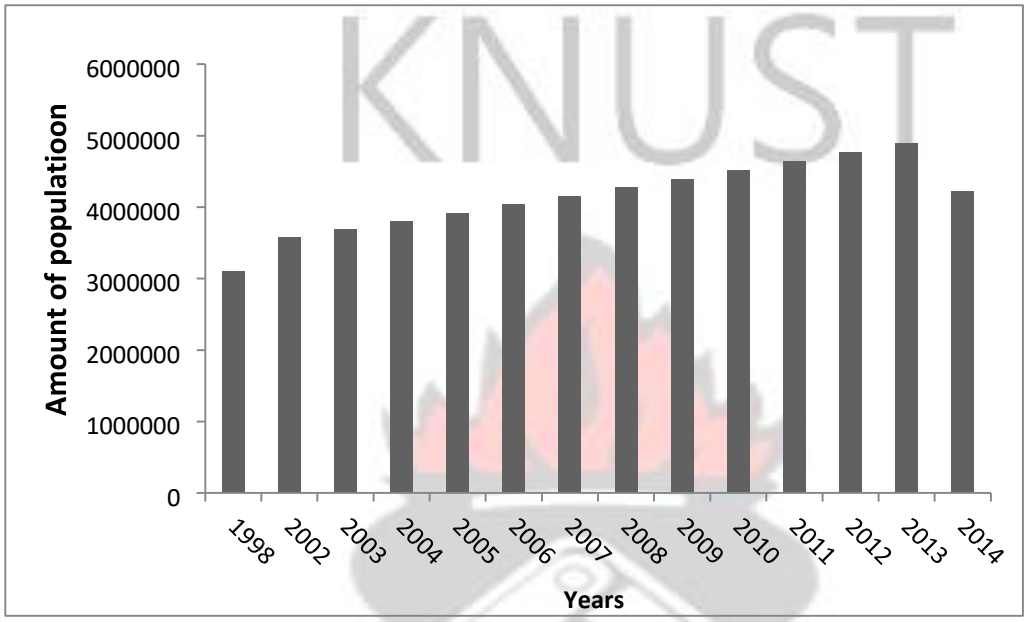


Figure 3.12: Population growth of Abidjan from 1998-2014 (INS, 2014)

3.1.5.2. Human Environment

The estimated population of Abidjan's District which is about 5 million is composed of more than 160 nationalities and Ivorian people, especially indigenous Ebrie, Attie and M'Batto live in perfect harmony with a large foreign community, mainly from the ECOWAS countries. The crisis situation experienced by Cote d'Ivoire from 2002 to 2011 has had serious repercussions on the population of the study area. Indeed, the crisis led to a vast movement of population from northern, central and western regions to the southern part of the country especially in Abidjan District where the population grew as a consequence of migration creating a framework for environmental unhealthy and unsuitable lives for the majority of the population.

3.2. Dynamic of Land use / land cover

The land use and land cover (LULC) dynamics is an important component to better understand the land patterns induced by human activities and therefore to understand its implications in climate change (Lambin, 2001). Several methods have widely been developed to study the land use / land cover changes.

KNUST

3.2.1. Data acquisition and Pre-treatment

In order to analyse the trends in land use/ land cover change in Abidjan District, three Landsat imagery were used. These images were selected based on time coverage, and amount of clouds.

The study area is covered by two (2) different Landsat scenes 196-56 and 195-56. Landsat TM and ETM+ images for the years 1990, 2002 and 2014 were downloaded from the United States Geological Survey's (USGS) (Table 3.1). Images that had a cloud cover of less than twenty percent (20 %) were considered for download specifically from Climate Data Record (CDR) which was defined by the National Research Council (NRC) as a time series of measurements with sufficient length, consistency, and continuity to identify climate variability and change. It was assumed that, 12 years between the images is large enough to allow identifying dynamism and changes in land use and land cover.

Table 3. 1: Landsat satellite data acquired for the years 1990, 2002 and 2014

Scene ID	**Date of acquisition**		
196 - 056	1990/12/14	2002/03/18	2014/04/12
195 - 056	1989/01/02	2001/02/02	2013/06/05

Legend: TM: Landsat Thematic Mapper, ETM+: Landsat Enhanced Thematic Mapper Plus, OLI: Landsat 8 Operational Land Imager

The first step of the pre-processing procedure was to do radiometric correction on each Landsat scene, using Landsat 8 OLI as reference. Afterwards, all bands were combined as one file using

layer stacking follow by mosaicking of the two scenes. After these steps the study area was masked from the mosaic image. Different color composite was generated to differentiate each class with various color band combination using remote sensing and GIS guide from the center for biodiversity and conservation and geospatial innovation facility collaboration. For instance, the band combination R7, G5, and B3 was very useful in identifying. Later, image enhancement was done to improve visual identification and interpretation of the possible land use/cover classes. However, several other image composites or bands combination were done to find and improve land use/land cover class identification and reduce confusion among classes. This procedure helped to have better view for each identified land use/cover class during the field data collection.

3.2.2. Data collection and processing

From this historical Landsat data, three land use/cover classes were finally identified and described broadly as follow:

- Vegetation: Forest (land cover dominated by trees with important crown density and National park), cropland (Cashew plantation, Palm oil plantation, banana plantation, coconut plantation, and food crop), and newly cleared land for agricultural purpose;
- Water body: lagoon Ebrie and Aghein and some other rivers;
- Settlement: represents built up areas and bare soil (because of their close reflectance value). The number of classes was kept to a minimum since this study focused more on urbanisation dynamics and also reduced the confusion between classes and improved classification accuracy.

Afterwards, field campaigns to generate reference data (for validating results) were organised within the study area for each identified land use/cover class. Several ground control truth point were recorded randomly with GPS based on each land use/land cover classes.

3.2.3. Image classification and Validation

The three Landsat data were classified to reveal changes in land use/land cover between 1990, 2002 and 2014. Supervised classification was carried out for each satellite image (1990, 2002, 2014) separately using the maximum likelihood algorithm based on the collected training data site. For each land use/cover class, the maximum training and validation samples were implemented. The number of region of interest built in each classification was more than 3000 respectively.

Hence, more than 100 ground truth points were randomly selected for all identified land use/land cover classes collected from the field for validation and accuracy assessment for 2014 years. The same classification algorithm was used to classify images of the years 2002 and 1990. However, for these periods, validation of classification was relied essentially on sites where there was no change (identified from the current image and the oldest ones), using existing land use maps in that period or near. Also, historical LULC information was recorded to derive knowledge of the LULC changes that have occurred on the surveyed sites between 1990 and 2002 from the national center of mapping and remote sensing. Sample from spot image from 1990 with 10 m resolution too was recorded. Accuracy assessment was performed independently for each image period using Envi post classification assessment.

3.2.4. Post-classification

Image classification accuracies were determined by applying statistical analysis for validation based on confusion matrix and Kappa. Overall accuracy, producer's accuracy and user's accuracy were also determined. The confusion matrix provides information on the correct and incorrect prediction made by a classification algorithm by comparing a classified map with ground information. The 2014 classified image was validated using the ground truth data collected during the field campaign. However, because there was no sufficient past land cover information and no

aerial photography at these specific period, a different approach was used to assess the reliability of the 1990 and 2002 images classification based on areas with no change, maps , sampling within high resolution image (spot) as GCT and historic land cover information from years nearly close. From visual observation and all these information recorded, areas with similar characteristics and spectral signature between these old images have been selected. This allows classification for these previous dates and enhances the accuracy of the classification process. At the end of the classification process, all files have been saved as Geotiff before further GIS analysis.

3.2.5. Land Use Change Detection

From aforementioned, in this study technique for image classification and post-classification were applied in Envi (Figure 3.13) while land use change detection was applied in Geographic Information System (GIS) interface. The three (3) classified images were saved to TIFF format and opened in ArcGIS. The new land use TIFF images were then converted to polygon for change detection analysis, and later extracted by mask using the study area polygon in spatial analyst tools. Then in the same spatial analyst tools, the three (3) classified were compared two by two as initial and final images using combine method. The resulting combined image obtained table attribute allowed land use change detection analysis by observing where there was change and no change.

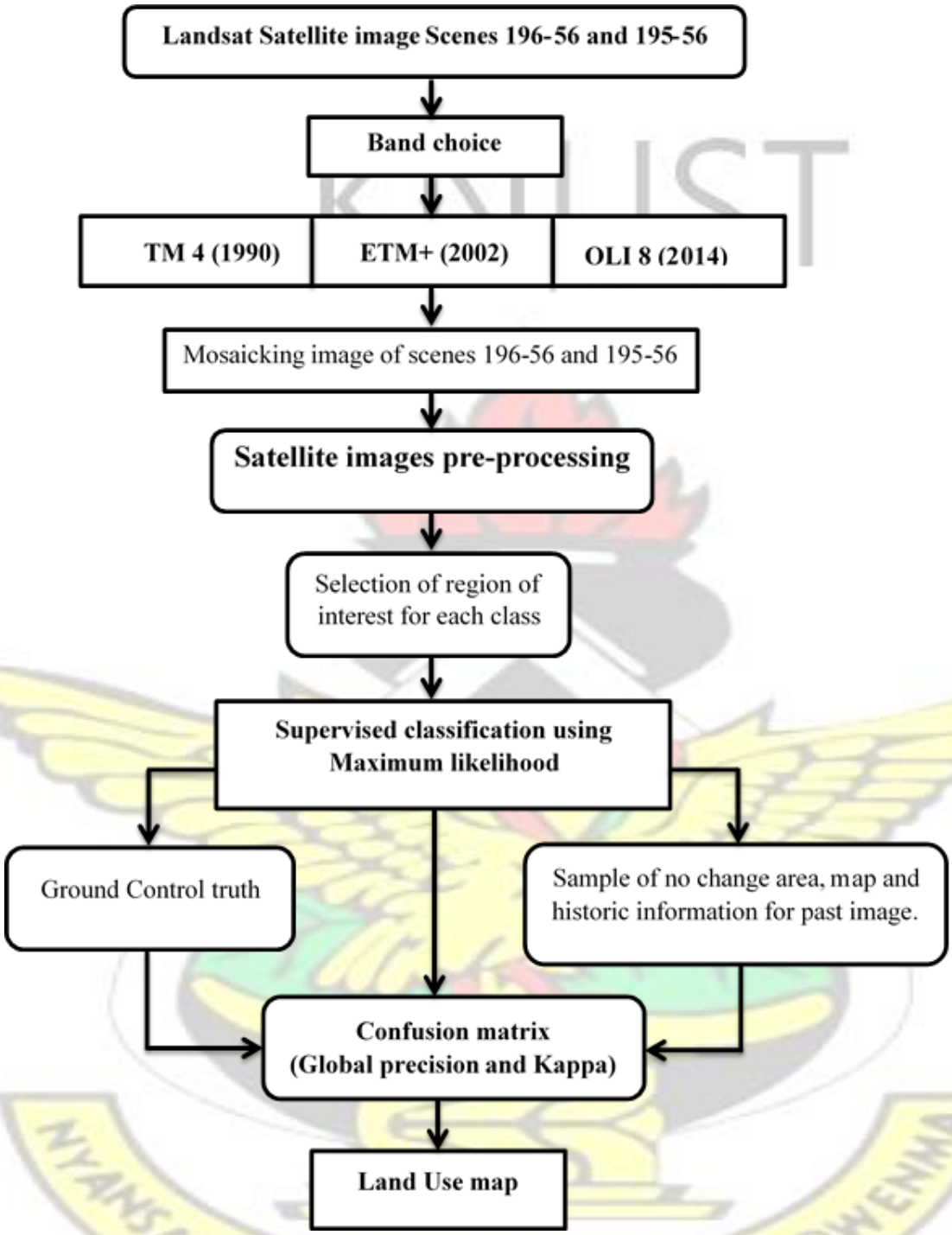


Figure 3.13: Flow chart for spatio-temporal dynamic of land use/land cover in Abidjan

3.3. Normalized Difference Build-up Index (NDBI)

Normalized Difference Build-up Index (NDBI) data were obtained from Landsat 5, 7 and 8 images in 1990, 2002 and 2014 respectively and comprises the composites of the Near-Infrared (NIR), Mid-

Infrared (MIR). This NDBI was applied in this study to highlight urban area compared to other classes such as vegetation and water bodies. According to Singh *et al*., 2014, Normalized difference building Index (NDBI) is used to increase the accuracy of classification and also it assumes that the use of spectral indices has many advantages:

− highlights a particular type of land cover (e.g. vegetation, water, etc.);

− compensate background effects;

− normalize the effects of atmospheric distortion caused due to sun angle, viewing angle etc.

The computation of NDBI is described by the given equations (*3.1*)

$$NDBI = \frac{mir - nir}{mir + nir} \qquad (3.1)$$

where, *NIR* and *MIR* are, respectively, the near infrared and the middle infrared and correspond to Band 4 and 5 for Landsat 5, 7 and Band 5 and 6 for Landsat 8. NDBI generally is brightness sensitive.

3.4. Urban Structure Types classification

In order to analyse the urban structure types in Abidjan District, spot 5 image with 10 m of resolution from 2013 has been used and apply in eCognition version developer 9 software. This image was selected based on available data. Get deeper comprehend of current Abidjan urban structure types under land use dynamic and vulnerability to flood risk using Oriented Based Image Analysis (OBIA) approach. Up to now, the use of OBIA method and eCognition developer software to do urban structure type classification in Cote d'Ivoire is practically not existent. So this new approach of classification bring more details in urban area classification by being able to

discriminate vegetation, industry area, public services, formal residences and informal settlement areas.

In this study, the classification of SPOT data set was based on OBIA approach using a rule set based method which consists of several steps. Estimate scale parameters, the so called multiresolution segmentation and classification. The rule set based method through process tree serves for clarity and illustrates the steps carried out when and how.

3.4.1. Estimation of scale parameter

After several training, three scale parameters were used which are 20, 30 and 50 in the multiresolution image segmentation. This was the best selected scale parameters to discriminate the different area and classes before doing the classification. However there is an existing tool for estimate the scale parameter (Dragut *et al*., 2014) but it is not applicable in the last version eCognition Developper 9 (Trimble) that was used in this study. Normally, this ESP tool automatically segments the user defined data with fixed increments of scale parameter, and calculates a local variance (LV) as the mean of standard deviation (SD) of the objects for each object level obtained through segmentation (Dragut *et al*., 2014). Then the Graphics of local variance (LV) are used to evaluate the appropriate scale parameters, relative to data properties of the scene.

3.4.2. Image segmentation

Segmentation is the process of dividing remotely sensed images into discrete regions or objects that are homogeneous with regard to spatial or spectral characteristics. The first step in the object based image analysis (OBIA) was segmentation of the SPOT image into several objects as homogeneous objects (cluster of pixels) with multiresolution segmentation tool in eCognition

Developer 9 software (Trimble). Multiresolution segmentation allows for flexibility in output object sizes.

In this study, three segmentations were done: S1, S2 and S3 based on the multiresolution segmentation algorithm. In addition to multiresolution segmentation, spectral difference segmentation was used to differentiate and merge objects with the same spectral difference using the spectral difference 5 and 7 as scale parameter to couple them with the two first segmentations.

After segmentation using both methods, areas of homogeneous morphology within the study area were grouped together based on their physical appearance and image object information existing in object feature such as customized where some index calculation including NDVI and Ratio (NIR/Red) were done; layer value including mean of Brightness, Green, Red, NIR and maximum difference and standard deviation of Green, Red, and NIR; then geometry extent (Number of pixel) and geometry shape (compactness, density, rectangular fit values), (Figure 3.14). All these image object information were used in the final step which was object classification.

KNUST

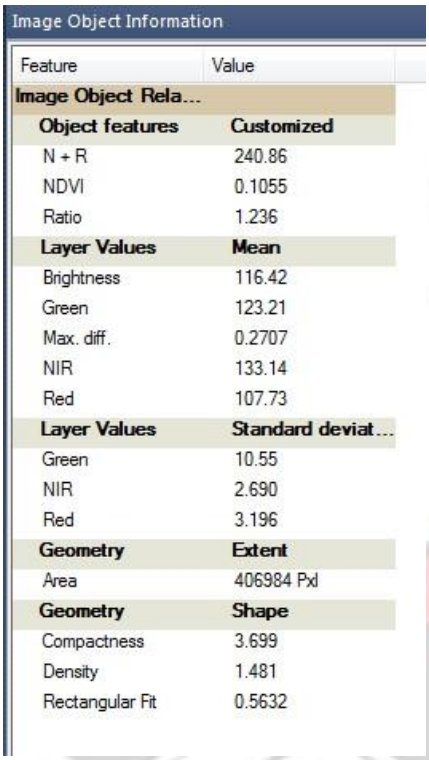


Figure 3.14: Image object information

3.4.3. Oriented object classification

Urban structure type's classification was also conducted using process trees method to do hierarchical image classification (Figure 3.15). The image objects were assigned to a class based on its individual membership value that means image object information to the corresponding class. The classification process is a hierarchical process where objects in the optimized segmentation level are classified first until the final classification is reached on the basic segmentation level by merging homogeneous urban morphology selected object in one class industry, high and medium residences as formal residence and informal residence, publics' services, bare soil, vegetation and water respectively. This method requires specifying a set of class discriminating attributes a priori from a potentially large number of various object variables

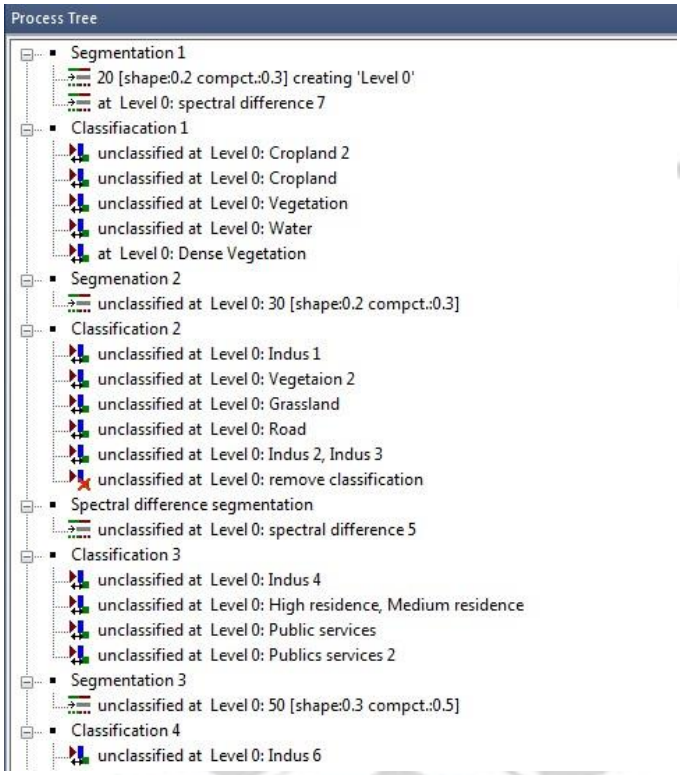


Figure 3.15: Process tree development for segmentation and classification

3.5. Climatic variability methodology approaches.

Several statistical methods were used to assess the variability of hydroclimatic data within the study area. A long time series of rainfall and temperature data of about 52 years from 1960 to 2012 were used to compute: mean ($\overline{X}$), minimum, maximum and standard deviation (σ).

3.5.1. Standardised precipitation index (SPI)

For the analysis of hydro-climatic variables, the annual rainfall average was calculated and rainfall index (RI) through SPI, which is a reduced centre variable calculated on annual precipitation to highlight fluctuations in rainfall patterns. It is the ratio of the difference in inter-annual to average standard deviation of annual precipitation amounts. Standardised precipitation index (SPI) play a very important role in determining precipitation fluctuations (wet, normal and dry period). Nicholson *et al*. (1988) cited by Paturel *et al*. (1997) have defined an index which is calculated for each year and expresses itself, given by the following equation (3.2):

$$RI = \frac{X_i - X}{\sigma} \qquad (3.2)$$

Where:

RI: Rainfall Index

Xi: Rainfall year i (mm)

X: Height of average rainfall over the period of study (in mm) σ

= standard deviation of the rainfall over the study period.

Standardised precipitation index (SPI) determines a reduced centred variable (Lamb, 1982) cited by Servat *et al*., (1998).

Inter-annual average of a series is the index zero (0) by the method of SPI.

- A normal period is a period during which the same fluctuation observe either side of the abscise axis. In this case, the average is approximately equal to average of the total rainfall. For a wet period, the annual average is greater than the average of total rainfall.
- Finally, the dry season is a period where the annual average is less than the total average rainfall.
- Later, rainfall index (RI) were filtered using the low-pass Hanning filter of order 2 and it was applied to remove seasonal fluctuations. Each term of the series was weighted as follow:
- $X_{(t)} = 0.06X_{(t-2)} + 0.25X_{(t-1)} + 0.38X_{(t)} + 0.25X_{(t+1)} + 0.06X_{(t+2)}$ *pour* $3 \le t \le (n-2)$ *(3.3)*

where X(t) are the weighted of total rainfall observed in the term t; X(t-2), X(t-1): are the observed total rainfall of the two terms immediately preceding the term t; X(t+1) and X(t+2) are observed total rainfall of the first two terms following the term t.

- The total rainfall weighted for the first to X(1) and X(2) and the last two terms X(n-1) and X(n) of the series is determined as follow:

- $X_{(1)} = 0.54X_{(1)} + 0.46X_{(2)}$ *(3.4)*
- $X_{(2)} = 0.25X_{(1)} + 0.50X_{(2)} + 0.25X_{(3)}$ *(3.5)*
- $X_{(n-1)} = 0.25X_{(n-2)} + 0.50X_{(n-1)} + 0.25X_{(n)}$ *(3.6)*
- $X_{(n)} = 0.54X_{(n)} + 0.46X_{(n-1)}$ *(3.7)*

3.5.2. Detection of changes within rainfall series

KHRONOSTAT software program developed at the Science House of water (ESM) of Montpellier (Lubès *et al.*, 1998) includes various statistical tests. These analyses are specific for variable change behaviour within the time series. The first category was testing the randomness of the series (correlation test on the rank and auto-correlogram). They cover the constancy of the mean of the series throughout its period of observation. Then, the time series was analysed using four (4) statistics test methods for detection of breaks within time series: Buishand test (1982), Pettitt test (1979), the procedure of segmenting series of rainfall so called Hubert test (Hubert *et al.*, 1989) and the Bayesian of Lee and Heghinian test. These entire tests were following at end by a normality test.

- **Buishand test**: is a parametric test and supposes, under the null hypothesis that the values of the testing variable are independent and identically normally distributed. Under the

alternative hypothesis, it assumed that a step-wise shift in the mean (a break) is present. This test is capable of locating the period (month or year) where a break is likely.

- **Pettitt test**: recognised by its robustness, the test is non-parametric and derived from the wording of the Mann-Whitney test. The null hypothesis is that the data is independent, identically distributed random quantities, and the alternative is that a stepwise shift in the mean is present.
- **Procedure for segmentation (**Hubert *et al***,** 1989**)**: this method is to cut the series **m** segments (m >1) so that the average calculated on any segment is significantly different from the average of the adjacent segment. This procedure is seen as a test of stationary. If the procedure does not accept segmentation of order greater than or equal to 2, then the hypothesis invalid (stationary series) and is accepted.
- **Bayesian from Lee Héghinian (1977)**: this procedure is used for searching average change in the sequence of independent random variables. It assumes that a change in average exists in a time series, and then considers the probable date of this change and the magnitude of the change made. A significance level of 10% was used for testing.

3.5.3. Gumbel distribution method

Gumbel method or frequency analysis of a long series of precipitation using statistical adjustment to estimate the return period of a particular value of these data series. This prediction is based on the definition and implementation of a frequency which is a model equation describing (modelling) the statistical behaviour of a process. These models describe the probability of occurrence of an event of a given value. It is the choice of the frequency model (and in particular its type) that depend the validity of the results of the frequency analysis. A frequency model often used to describe the statistical behaviour of extreme values is the statistical distribution of Gumbel (double

exponential law or Gumbel). The distribution function of the Gumbel distribution F (x) is expressed as follows:

$$F(x) = \exp(-\exp(-(x-a)/b)) \quad (3.8)$$

reduced with the following variable: $u = (x-a)/b$ (3.9)

Where **a** and **b** are the parameters of the model Gumbel.

The distribution is then written as follows:

$$F(x) = \exp(-\exp(-u)) \quad (3.10)$$

$$u = -\ln(-\ln(F(x))) \quad (3.11)$$

The advantage of using the reduced variable is the expression of a linear quintile given by this equation:

$$Xq = a + bu_q \quad (3.12)$$

Accordingly, when the series of points to be adjusted may be carried in a system of axes **x – u**; it is possible to adjust a line that best passes through these points and to derive the two parameters **a** and **b** of the law. Two different methods of adjustment have been used in this study: graphical method (adjustment to the eye or using a statistical regression) and moment's law method.

In practice, it is essentially to estimate the probability of exceeding **F (x_i)** to be assigned to each x_i value. There are numerous formulas for estimating the distribution function using empirical frequency. They are all based on sort of the series by increasing values for associating with each value its rank **r**. Various simulations have shown that for the Gumbel distribution, it is better to use the empirical distribution of Hazen. It is given by this formula:

$$\frac{r - 0.5}{n} \qquad (3.13)$$

Where **r** is the position in the data set sorted by increasing values, **n** is the sample size, x [r] the value of rank **r**.

Let us recall that the return period **T** of an event is defined as the inverse of the frequency of occurrence of the event. Either:

$$T = \frac{1}{1 - F(xi)} \qquad (3.14)$$

This study, limited itself to the estimation of annual maximum daily precipitation and appreciated the correlation coefficient between the measured and estimated precipitation. This procedure follows different steps:

Step 1: Preparation of the data series: means reorganisation in ascending order and ranking each value.

Step 2: Calculate the empirical frequency for each row (Hazen, equation *(3.13)*).

Step 3: Calculate the reduced variable "**u**" of Gumbel (equation *(3.9)*).

Step 4: Graphical representation of pairs (u_i, x_i) in the series to be adjusted.

Step 5: Fitting a linear relationship such couples **(u_i, x_i)** and deduced the two parameters **a** and **b**. With an adjustment of graphical method, estimation were made for the parameters **a** and **b** values.

The method of moments is to match the times of the samples with the theoretical moments of the law. By the method of moments the parameters a and b were calculated according to the formulas:

$$\hat{b} = \frac{\sqrt{6}}{\pi} \hat{\sigma}$$

$$\hat{a} = \hat{\mu} - 0.5772\,\hat{b} \qquad (3.15)$$

with: 0.5772 (Euler's constant).

With: **σ**: standard deviation of the sample values.

μ: mean of sample.

Therefore it is possible to estimate the annual maximum daily rainfall whose graph is a straight line equation: $Q = \hat{a} + \hat{b}u$ *(3.16)*

Where **u**: reduced variable (see equation *(3.9)*).

3.6. LARS-WG and rclimdex models

3.6.1. LARS-WG model processing

LARS-WG is a model for simulating times series weather data for a station. In this study, 50 years of observed daily weather data (precipitation, maximum and minimum temperature and solar radiation) have been used with LARS-WG (a stochastic weather generator model) and considered

as baseline for the different process. Precipitation was considered as the primary variable in this study for analysing flood event occurrence in the future and the other three variables come as secondary variables to obtain an overall understanding of future hydro-climatic events.

In LARS-WG, the process of generating synthetic weather data can be divided into three distinct steps: calibration or site analysis, validation or Q-test and Generator or generation of future data based on normal distribution. The seasonal cycle of means and standard deviations was removed from the observed performance, and the residuals approximated by a normal distribution. These residuals were used to analyse a time correlation of each variable.

3.6.1.1. Model calibration

Model calibration is done in LARS-WG by implementing SITE ANALYSIS which analyses observed daily weather data (precipitation, maximum and minimum temperature and solar radiation) of Abidjan to determine their statistical characteristics. The resulting information is stored in two parameters files and later used in the generation process.

3.6.1.2. Model validation

In this step, the statistical characteristics of observed data are compared with those of synthetic data generated using the parameters derived from the original observed data by applying the Qtest. Several statistical tests: chi-squared test, Student's T-test and F-test were used in order to determine whether the distributions mean values and standard deviations of the synthetic data were significantly different from those of the original observed data set. Then, the ability of LARS-WG to simulate the data at the chosen site was assessed.

3.6.1.3. Generation of Climate Scenario

LARS-WG model generates synthetic future weather data by combining a scenario file containing information about changes in hydro-climatic data (precipitation, minimum/maximum temperature, solar radiation and PET) based on baseline weather data (50 years of observed data) at Abidjan site. Baseline parameters were adjusted by the changes for the future period and the emissions predicted by IPCC Global Climate Model for each climatic variable of the grid covering the site. In this study, IPCC Global Climate Model: HadCM3 and SRA1B emission were used to generate fifty (50) future years predicted weather data for the periods of 2011-2030, 2046-2065 and 20652099.

3.6.2. Rclimdex model processing

27 different climate indices recommended by a joint WMO CCI/CLIVAR Expert Team and ETCCDMI team for Climate Change Detection Monitoring Indices. These indices have been developed to characterise the intensity, duration and frequency of extreme events via daily information, and / or define relevant derived variables. The software "rclimdex" provides an appropriate template to calculate these indices efficiently. The originality of rclimdex is to make quality control tests even on daily data that do not follow a normal statistical distribution.

The calculation of climate indices requires first making quality control test and secondly homogenization test on the data sets used. The periods 1960-2010 and 2011-2100 were chosen as climate normal period to calculate the indices of climate extremes of Abidjan District.

3.6.2.1. Quality Control test

The method of quality control is to help the user to identify registry errors that may exist on his daily data. The main steps for the quality control of the data in rclimdex can be summarised in the following steps:

- replace missing data by -99.9 values which is code that rclimdex model required for missing data,

- have not more than 365 to 366 daily observations per year;
- Negative rain (prcp <0)
- Tmax <Tmin
- Repeat on consecutive days in the same variable value (Tmin, Tmax or rain)
- sudden jump in the time series (rupture or average change)
- Detection of aberrant values defined as a value outside the range climate known in the locality

3.6.2.2. Homogenization

Homogenization means correction of data sets with artificial discontinuities due to changes in observation networks (moving station, change instrument measuring change in the immediate vicinity of a station, changing observer, etc.). These artificial discontinuities are present in most climate records and may interfere with the actual climate variations. Detection and correction of these breaks are needed to build climate databases that will be used to analyse the climate variability under present condition and its evolution in time later because the artificial discontinuities that can occur involves the risk that future projections based on past observations are biased.

Homogeneity test was implemented using RHtestV3 software from the package r (Wang and Feng, 2010). RHtestsV3 function handle daily, monthly and annual series of Gaussian errors except daily precipitation series where RHtests_dlyPrpc procedure was used because the homogenization of daily precipitation series are typically non-Gaussian (Wang and Feng, 2010). According to Wang 2008 and Wang *et al.,* 2010; it is based on the penalised maximal t test and the penalised maximal F test, fixed in a recursive testing algorithm applied to the time series. The advantage of homogeneity test was to correct data series as homogeneous climate data series and systematically involved a diagnosis on average analysis of extremes because between that date and

the end of the series, the series becomes daily reference series (QAS). The RHtestV3 software is already incorporated into the rclimdex model.

3.6.2.3. Indices

Indices, developed at the annual level by the rclimdex program are 27 indices and can be grouped into several categories.

- The indices based on percentiles provide information on the temperature of cold nights (*TN10p*), warm nights (*TN90p*) cold days (*TX10p*) and hot days (*TX90p*);
- The indices represent the absolute maximum or minimum values of temperature during a given period of time (season, year) as the highest maximum temperature (*TxX*) , the highest minimum temperature (*TNx*), the most maximum low temperature (*TXn*) or the lowest minimum temperature (*TNn*) ,
- Total daily above the 95 percentile (very wet days (*R95p*)) and 99 (extremely wet days (*R99p*)) rainfall totals for these figures vary from one station to another even when the various stations are influenced by the same type of climate , so it is impossible to have a common value for all stations define by the *R95p* and *R99p* .
- Indices of maximum 1 day (*RX1day*) and 5 consecutive days (*RX5day*) precipitation;
- The indices of the maximum duration of dry periods (daily R < 1mm: *CDD*) and wet periods (R > = 1mm: *CWD*).

The advantage of using these indices for the detection of climate change is that they can be applied to different climate parameters such as minimum temperature, maximum temperature and precipitation at a daily time. Also, indices of climate extremes are easily understandable and manageable for studies of climate change impacts.

In this study, to analyse extreme rainfall events in Abidjan, instead of 27 indices, only the ten (10) rainfall indices were calculated and analysed (Table 3.2).

KNUST

Table 3. 2: Daily extreme precipitation indices

Precipitations indices			
Identification	**Indicators name**	**Definitions**	**Units**
PRCPTOT	Annual total wet-day precipitation	Annual total PRCP in wet days (RR>=1mm)	mm
RX1day	Max 1-day precipitation amount	Monthly maximum 1-day precipitation	Mm
Rx5day	Max 5-day precipitation amount	Monthly maximum consecutive 5-day precipitation	Mm
SDII	Simple daily intensity index	Annual total precipitation divided by the number of wet days (defined as PRCP>=1.0mm) in the year	Mm/day
R10	Number of heavy precipitation days	Annual count of days when PRCP>=10mm	Days
R20	Number of very heavy precipitation days	Annual count of days when PRCP>=20mm	Days
Rnn	Number of days above nn mm days	Annual count of days when PRCP>=nn mm, nn is user defined threshold	Days
CWD	Consecutive wet days	Maximum number of consecutive days with RR>=1mm	Days
R95p	Very wet days	Annual total PRCP when RR>95th percentile	mm
R99p	Extremely wet days	Annual total PRCP when RR>99th percentile	mm

3.7. Analytic Hierarchic Process (AHP) approach for flood risk assessment

Flood risk mapping is a vital component for appropriate land use planning in flood areas and mitigation measures (Bhatt *et al*., 2014). Flood risk map is important to provide basis information and must be effectively communicated to various target groups: decision makers and the public. The concept of risk is a complex concept that can be modelled using the combination of two separate components, Hazard and Vulnerability (Ouma & Tateishi, 2014). This model is suitable for most natural hazards, which is represented by the equation:

$$Risk = Hazard \times Vulnerability \qquad (3.17)$$

3.7.1. Hazard

Hazard is considered a physical phenomenon, natural and non - manageable, occurrence and intensity that can cause damage by overflow stream and the extension of the field in the water flood. Hazard refers also to hydro-climatic phenomena and their impact on the flow of water.

Geomorphological characteristics (slope, drainage, soil types) and mainly rainfall (because it is the intense rainfall that triggered flooding) were the various factors taken into account under hazard criteria. The data processing for these factors allowed establishing thematic layers maps. One of the maps is the slope extract from Aster DEM with resolution 30 m. Three latest maps are drainage density map obtained after a meshed (discretization) of hydrography network of the study area and this meshing measuring 5 km x 5 km was obtained from the Linwin software. Isohyet map was obtained from annual precipitation and soil types. Classes of very low, low, medium, high and very high were defined for slope, drainage density and isohyet maps.

- **Rainfall**

Rainfall amount, duration and intensity are part of the major causes of floods. Flooding occurs most commonly from heavy rainfall when natural watercourses do not have the capacity to absorb excess water. In urban area, floods are associated with extremes in rainfall which cannot immediately seep into the ground as runoff. The occurrence and intensity of rainfall, and natural settings that are not manageable, whatever the prevention provisions are overriding parameters of the flood ability (Saley *et al*., 2005). From annual rainfall, isohyets map was drawn from Surfer 11 software. The kriging interpolation method type was used for the preparation of isohyets curves. Each given point, with the geographic coordinates and rainfall measurement, were used for this purpose. The study period was divided into five (5) phases in order to understand its spatial and temporal variations. However, for the combination with other parameters within the AHP method, the mean annual rainfall from 1961-2010 was considered and interpolated using Inverse Distance

Weighting (IDW) in ArcGIS software to create a continuous raster rainfall data within and around Abidjan District to generate isohyets map of the study area. Five classes were defined: very low, low, moderate, high and very high.

- **Slope**

Slope plays an important role in the stability of a terrain and in the same time influences the direction and amount of surface runoff or subsurface drainage. Slope has a dominant effect on the contribution of rainfall to stream flow and controls the duration of infiltration within subsurface. Slope reflects the geomorphology of the study area and the slope map was generated using the digital elevation model (DEM) from Aster with resolution 30 m and spatial analyst tools in ArcGIS software. The risk of flooding is high in very low and low slope areas.

- **Drainage density**

Drainage is an important factor shaping the physical characteristics and controlling the hazards. Drainage density denotes the nature of the soil and its geotechnical properties under the study area. It is also used for modelling of major and minor beds in the propagation of floods (Sharon and Burnett, 2003). This means that, the higher the density, the higher the study area is susceptible to erosion, resulting in sedimentation at the lower grounds. In this study, higher weights were assigned to poor drainage density areas and lower weights were assigned to areas with adequate drainage because hazard increase with lower drainage density and lower infiltration.

- **Soil type**

Soil types define the amount of water that can be infiltrated into the ground, and later the amount of water which becomes flow based on its nature. Soil type which includes texture and structure are an important component and characteristics of hazard. Soil textures have a great impact on flooding because sandy soil absorbs water soon and few runoffs occurs where inversely clay soils are less porous and hold water longer than sandy soils. This implies that, areas characterised by clay soils are more affected by flooding. On the other hand, soil structure too has great impact on infiltration capacity because the chance of flood to occur is when heavy rainfall increase with decrease of soil infiltration capacity. Soil type map was extracted from national soil map and validated through soil profile description and analysis through field work (Plate 3.1).



Plate 3.1: Soil profile description

The combination of these four factors (Isohyet, slope, drainage density and soil type) has been used to map the spatial extent and areas potentially exposed to hazards that could cause flooding.

The flood-prone areas are those located in areas of low permeability and slope, below reliefs, where the drainage is weak (low infiltration, rapid concentration of water), high rainfall and where they were clay as soil types.

3.7.2. Vulnerability to flooding

Vulnerability expresses the level of foreseeable consequences of a natural phenomenon on issues (MATE, 1998). On the other hand is the most crucial component of risk in that it determines whether or not exposure to a hazard constitutes a risk (Ouma & Tateishi, 2014). Flood vulnerability mapping is the process of determining the degree of susceptibility and exposure of a given place to flooding. These issues include people, goods and socio-economic activities likely to be affected both quantitatively and qualitatively by a natural phenomenon. In this study, vulnerability criteria

include three major components: population density, sewer system network and urban structure type (UST) as land use.

- **Urban Structure Types (UST)**

Obtaining information about land use which concerns the management of urban areas is predominantly important to determine and reduce physical and social vulnerability (hulk *et al*., 2013). Also physical structure and the composition of urban area are key factors in urban planning issues (Netzbind and Jurgens, 2010). For this reason it is essential to take into account the typology of land use /land cover in the vulnerability mapping. To highlight the role play by the different land use/land cover tenure instead of using the classic land use map, Urban Structure Type's (UST) map of Abidjan was developed within eCognition software using oriented based image analysis (OBIA) method. Eight (8) classes: vegetation, water, publics services, industrial, medium and high residence, informal residence and bare soil were retained to perform urban structure types (UST) as a current land use map.

- **Population density**

Population in urban area is an important factor which can influence climate change. The demographic development is high and uncontrolled near water courses; valley and low land because settlements in these flood-prone areas is easier and less expensive to build. Also, the study area is the economic capital of the country; hence demand of welfare and population growth is very important. Estimating the population density in the District could help better manage the land in its current situation and in the future. Population data was obtained from national statistical institute (INS) and then imported into ArcGIS.

- **Drainage system network**

Drainage (sewer) system map was obtained from map bought with National Water Company and drainage system station inventory through field work (Plate 3.2), the same approach aforementioned for density of drainage was carried out. Drainage system of Abidjan was digitize by the polyline entity in the Mapinfo software and combines with plotting point of drainage system inventory. The drainage system density was obtained after meshing (discretization) the sewerage network and the calculation of the cumulative length per cell.



Plate 3.2: Sewer system inventory

UST, sewer system and population density maps, crossed with their different weights (according to importance) in the GIS using raster calculator in spatial analyst tool allow the development of vulnerability map of flooding in Abidjan District.

3.7.3. Spatial mapping of multi-combination

Parameters including rainfall, soil type, slopes, drainage density, land use, drainage system and demography involved in the occurrence of flooding by combining anthropogenic and natural variables that produce susceptibility to flooding to be effective. This was to elaborate maps of slopes, soil type, drainage, drainage system and population densities, UST, and rainfall. The analysis of these factors led to the present hazard and vulnerability of the land to flooding. In this study, the considered factors did not have the same importance, and therefore occurred with different weights when crossed into the GIS. According to Mulders, (2001), using a multi-criteria approach allows the spatial prediction of superficial movements (floods) and the application of multiple analyse to provide reliable thematic maps.

3.7.3.1. Development factors

For the development of flood risk map of Abidjan District, these several factors were identified and clustered under hazard and vulnerability criteria. These are the different weighted elements combined to others under each criterion. Afterwards, the two criteria were also crossed and the resulting map will be area at risk of flooding. The selected factors included:

- **Hazard criterion**
  - Slope;
  - Drainage density
  - Isohyets
  - Soil type
- **Vulnerability criterion**
  - Population density
  - Urban structure Types (Land Use)

- Drainage system network

All elements under each criterion were set based on literature and the definition of hazard (physical phenomenon, natural and non- manageable) and vulnerability (degree of susceptibility and exposure due to man-made) concepts that were used in this study.

3.7.3.2. Classifying factors

For best performance, the number of classes were reduced to five (5) classes:

- Very low
- Low
- Medium
- High
- Very High

3.7.3.3. Analytic Hierarchy Process (AHP) approach

The multi-criteria analysis methods provide a framework which can handle different views on the identification of the elements of a complex decision problem, organise the elements into a hierarchical structure. For this study, the method used to determine the weight of parameters is the multi-criteria analysis (MCA) method: Analytic Hierarchy Process (AHP). AHP assumes complete aggregation among criteria and develops a linear additive model. The weights and scores are basically achieved by pairwise comparisons between the indicators with each other. This method allows effective decisions relating to complex by decomposition and structuring problems more accessible to decision makers to refine their decision-making process. It can be very interesting in the quantification and prioritization of criteria and sub-criteria characterising the mapping of areas

at risk for flooding. This technique is based on experience and theoretical expert knowledge (Papaaioanounou *et al*., 2015). Thus a questionnaire was drawn and submitted to 15 experts. Expert knowledge was considered an important tool as it provides flexibility in the weight aggregation of each element depending on each expert point of view.

The basic procedure to carry out the AHP consists of the following steps:

i) Decompose a complex and non-structured situations by developing its hierarchy;

ii) Classification of the variable parts in a hierarchy by binary combination; iii) Assigning numerical values to subjective judgments on the significance of each variable; iv) Synthesize judgments to determine the priority variables;

v) Test the consistency of assessments and judgments.

Thus, the approach adopted by the AHP can be summarized in three main parts:

❖ **Development of the hierarchy**

For the development of the hierarchy, the parameters identified above were grouped in a homogeneous and all disposed in different levels. Each element of the same given level is then compared with all others elements in that level. The different levels of AHP were:

Level 0: General objective

Level 1: decision criteria or analysis. In this study, criteria analysis selected were two (2). Saaty recommends limiting the number of decision criterion to seven (7) more (Saaty, 1980);

Level 2: Characteristics of criteria: The characteristics of the criteria in this study were the various parameters influencing hazard and vulnerability to flooding;

Level 3: different alternatives under each criterion.

In this respect, it should define key terms involved in the comparison elements (Anonymous, 1990):

- Alternatives: main choices which can be referred to ;
- Criteria or attributes: following aspects which alternatives considered. These latter can be quantitative or qualitative ;
- Units: an expression to express the performance criteria ; tangible or intangible;
- Weight: importance attributed to criteria (subjective).

The hierarchy established in the case of this study is shown in Figure 3.16.

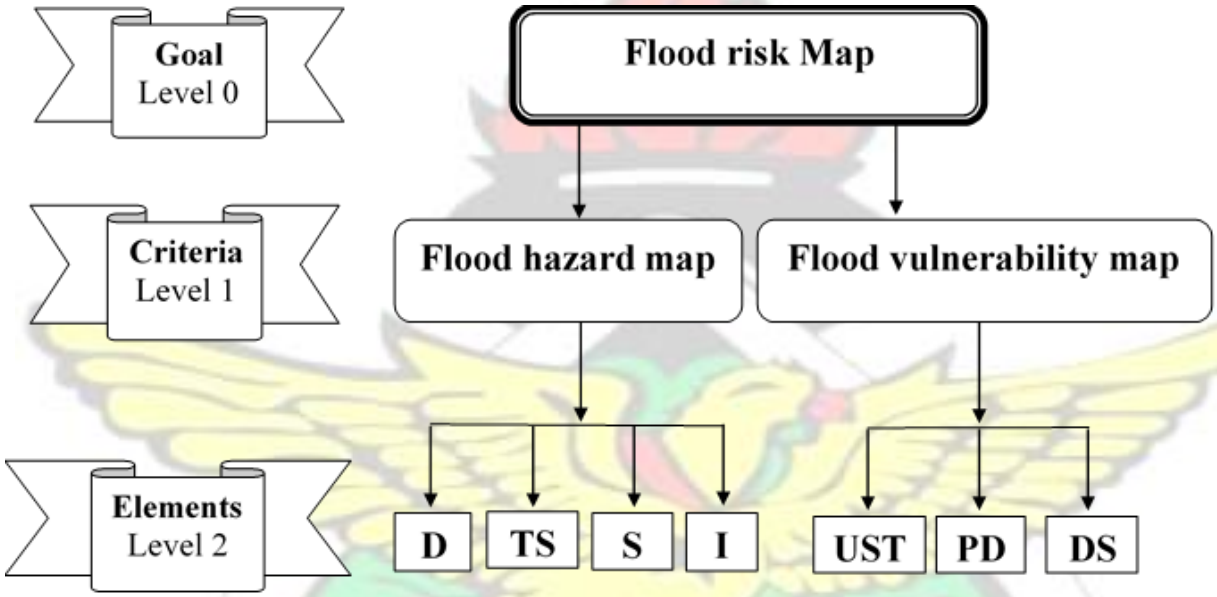


Figure 3.16: AHP model use in the process flood risk map

❖ **Binary combination**

In the case of the structure shown in Figure 3.16, three matrices are distinguished. The first two matrices, allow comparisons to be carried out between elements of each criterion and the last will allow comparison between the two criterions to reach the goal.

Following the binary comparisons, checking the consistency of judgments through prioritization is needed (Table 3.3). Indeed, setting priorities can synthesise our assessments of a mathematical

way to verify the consistency. Thus, in a matrix, the element of the column is left successively compared to each element of the row of the matrix. If the comparison is not supported by the element on the left column in relation to an element of the line, assessment is expressed using the fraction and otherwise using a whole.

Table 3. 3: Reports the scale of the various elements of comparison (Saaty, 1980).

Scale	Judgment of preference	Description
1	Equally important	Two factors contribute equally to the objective
3	Moderately important	Experience and judgment slightly favour one over the other
5	Important	Experience and judgment strongly important favour one over the other
7	Very strongly important	Experience and judgment strongly important favour one over the other
9	Extremely important	The evidence favouring one over the other is of the highest possible validity
2, 4, 6, 8	Intermediate preference between adjacent scales	When compromised is needed

❖ **Development and prioritization matrix**

The principle of development is the following matrix:

- determine the eigenvectors (Vp) of each criterion for each item :

$$Vp = \sqrt[K]{W1 \times \ldots \times Wk} \qquad (3.18)$$

With k: number of parameters and compared W_k ratings main parameters;

- Calculate the weighting coefficients (Cp) :

$$Cp = \frac{Vp}{Vp1 + \ldots + Vpk} \qquad (3.19)$$

The sum of Cp of all parameters of a matrix must be equal to 1 (one).

- Normalize the matrix by dividing each element by the sum of the column;
- Averaging each line to determine the priority vector [C];
- Multiply each column of the matrix by the priority vector corresponding there to determine the overall priority [D];
- Divide each global priority by the priority vector corresponding to it and determine the rational priority [E]; [*E*]

$$\square \max \square ___ \quad (3.20)$$

- Determine the maximum Eigen value (λ_{max}): k
- Calculate the consistency index (CI): $CI \square \frac{\square}{_____} \max \square k \quad (3.21)\ k \square 1$
- Determine the consistency ratio (CR). The ratio of coherence can be interpreted as the probability that the judgement is completed in a random manner. In fact, the responses often have a certain degree of incoherence. The AHP method does not require that judgments are consistent or transitive, hence, Saaty (1980) has defined the value of consistency ratio. In the case where the value of consistency ratio exceeds 10%, the assessments may require some revisions.

$$CR \square \frac{CI}{___} \quad (3.22)$$

With *RI*: random index

Values of the random index (*RI*) are shown in Table 3.4.

Table 3. 4: Random Index matrix of the same dimension (Saaty, 1980)

Number of criteria	2	3	4	5	6	7	8	9	10	11

RI	0.00	0.58	0.90	1.12	1.24	1.32	1.41	1.45	1.49	1.51

With the number of criteria = number of parameters compared

3.7.3.3.1. Hazard matrix

The test of hazard consists of:

- Drainage density;

- Type of soil;

- Slope map.

- Isohyets.

Determining the weight of parameters of the matrix obtained after conducting a survey from various experts based on the comparison between these parameters themselves. Table 3.5 shows the values of the eigenvectors and the weighting parameters of the hazard test. These values corresponding to the matrix level 1, will be determine from the previous level (level 0).

Table 3. 5: Hazard matrix [A]

	D	**TS**	**S**	**I**	**V_P**	**C_P**
D	1	3	1/3	1/5	0.67	0.13
TS	1/3	1	1/3	1/5	0.38	0.08
S	3	3	1	1/3	1.31	0.26
I	3	5	3	1	2.59	0.52
Sum	7.33	12	4.66	1.73	4.95	1

Application: Example of calculation of the eigenvector (Vp) and the weighting coefficient (Cp) of the density of the drainage in table 3.5.

Vp = $\sqrt[4]{1 \square 3 \times (1/3) \square 1/5} = 0.67$ and **Cp** = $\frac{0.67}{4.95} = 0.13$

View the values of hazard criterion Cp, It was noted that soil type weight (0.08) is low in the study of mapping hazard. As against, the weighting coefficient of rainfall (0.52) is the most highest. Although the total amount of Cp is 1, a check of the consistency of judgments recommended by the Analytical Hierarchy Process (AHP). The different results of the check are summarized in Table 3.6.

Table 3. 6: Normalized Matrix [A]

	D	**TS**	**S**	**I**	**∑ ranges**	**[C]**	**[D] = [A]* [C]**	**[E] = [D]/ [C]**	**λmax**	**CI**	**CR**
D	0.14	0.25	0.07	0.12	0.58	0.15	0.58	3.87			
TS	0.04	0.08	0.07	0.11	0.3	0.08	0.32	4			
S	0.41	0.25	0.21	0.19	1.06	0.26	1.12	4.31	**4.09**	**0.03**	**0.03**
I	0.41	0.42	0.64	0.58	2.05	0.51	2.14	4.20			
Sum	1	1	1	1	3.99	1		16.38			

[A] = Original matrix

After normalization of the matrix and determining the amount of standard lines, calculate [C] of the first line, [D], λ_{max}, CI, RI and CR:

- C ____30..9958 →[C]= 0.15

- $$[D] = \begin{bmatrix} 1 & 3 & 1/3 & 1/5 \\ 1/3 & 1 & 1/3 & 1/5 \\ 3 & 3 & 1 & 1/3 \\ 3 & 5 & 3 & 1 \end{bmatrix} * \begin{bmatrix} 0.15 \\ 0.08 \\ 0.26 \\ 0.51 \end{bmatrix} = \begin{bmatrix} 0.58 \\ 0.32 \\ 1.12 \\ 2.14 \end{bmatrix}$$

- $\max = \frac{16.38}{4} = 4.09$

- CI = $\frac{09-4}{4-1}4.$ = 0.03
- CR = $\frac{0.03}{0.90}$ = 0.033

CR = 3 % □ 10 %

KNUST

Therefore judgments are consistent.

Table 3. 7: Weight of Hazard indicators

Hazard indicators	**Weight**
Drainage density	0.13
Type of Soil	0.08
Slope	0.26
Isohyet	0.52

The relative hazard map is obtained from equation 3.23:

$$Hazard_map = 0.13_Dd _0.08_TS _0.26_S _0.52_I \quad (3.23)$$

3.7.3.3.2. Vulnerability matrix

The test for the vulnerability of land to flooding consists of:

- Population density;
- Urban structure types
- Drainage system network

Table 3. 8: Vulnerability Matrix

	UST	PD	DS	V_p	C_P	λ_{max}	CI	CR
UST	1	1/3	3	1	**0.26**			
PD	3	1	5	2.47	**0.64**			
DS	1/3	1/5	1	0.4	**0.1**	3.03	0.02	**0.03**
Sum	4.33	1.53	9	3.87	**1**			

The matrix is coherent because **CR = 3 % < 10 %**

Table 3. 9: Weight of the vulnerability indicators

vulnerability indicators	**Weight**
UST	0.26
Population density	0.64
Drainage system	0.1

The relative map of vulnerability of the land to flood is obtained from equation 3.24**:**

$$Vulnerability\ map = 0.26 UST + 0.64 PD + 0.1 DS \quad (3.24)$$

3.7.3.3.3. General objective relative Matrix

Table 3. 10: General objective matrix

	V	H	V_P	C_P	λ_{max}	CI	CR
V	1	1	1.73	0.5			
H	1	1	0.58	0.5	**2**	**0**	**0**
Sum	2	2	2.31	1			

Where: V = Vulnerability and H = Hazard

The matrix is coherent because CR = 0% <10%

Table 3. 11: Weight of flood criteria

Criteria	Weight
Vulnerability	0.50
Hazard	0.50

The relative AHP map of flood risk is obtained from the equation 3.25

$$Flood\ risk\ map = 0.5 Vulnerability\ map + 0.5 Hazard\ map \quad (3.25)$$

The analysis of natural phenomenon based on knowledge of the hydrological, geomorphological, and anthropogenic parameters functioning within the study area is summarized in Figure 3.17. Thus, it is possible to determine the often flooded areas, frequently flooded or not flooded areas. A first map of the hazard can be established: it has all the areas likely to be affected by floods. The vulnerability map shows the land: water, vegetation, urban (Residence, industrial, commercial, publics services, informal) areas. Physical vulnerability depends on man-made of land. However, urban vulnerability vis- a-vis of flood risk is a function of land tenure. It represents the degree to which social level and property in urban areas are likely or resistant to the impact of natural hazards. By superimposing these two criteria or a combination of these two components, the study obtained a synthetic map that shows the areas at risk. The resulting maps highlight areas that are most exposed to flooding compare to those where flooding is tolerable and low.

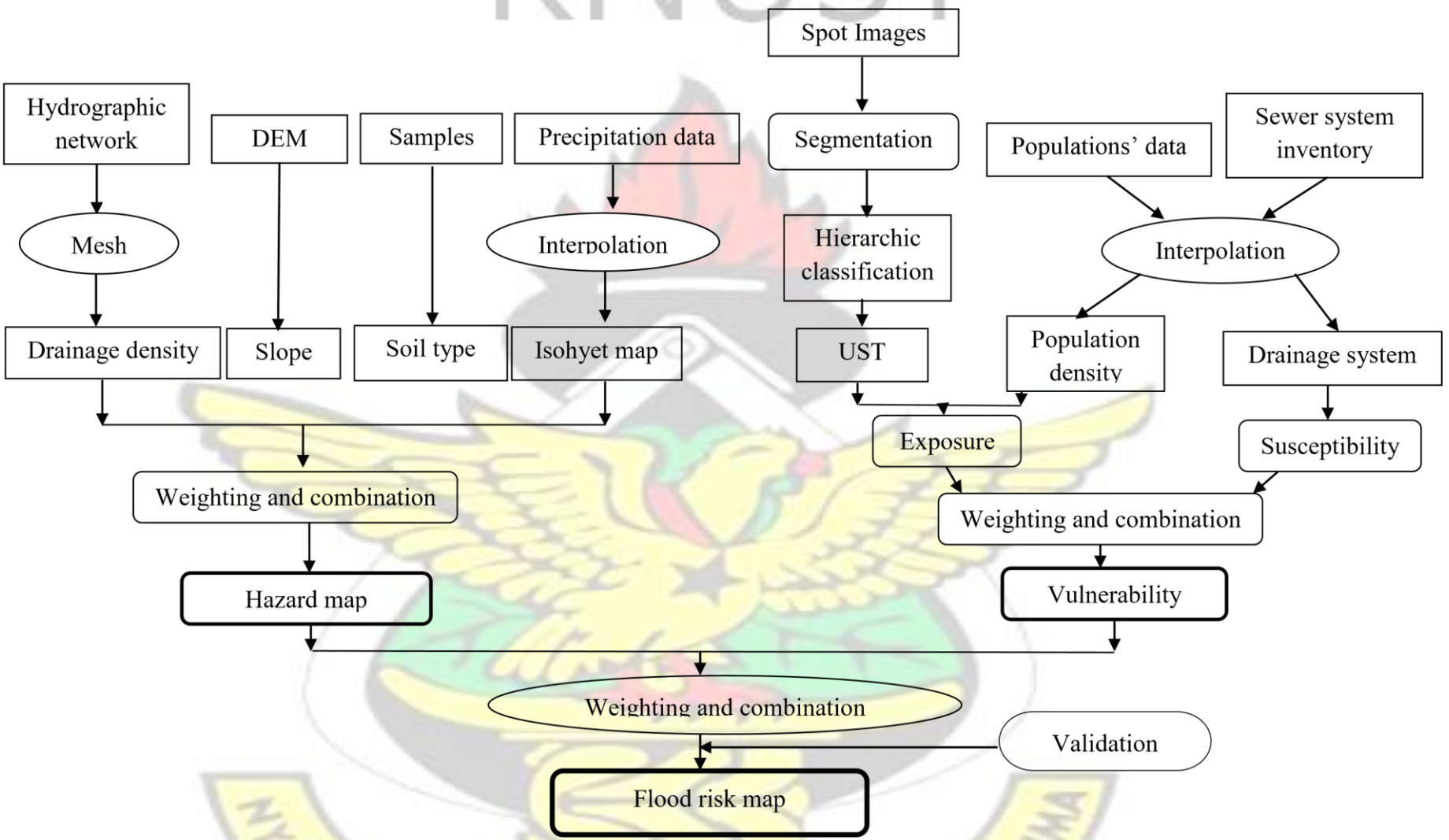


Figure 3.17: Flood risk flowchart for development of flood risk map

KNUST

3.8. Flood hazard index model

In this study, both hydrological (rational method) and statistical model approaches are combined to estimate the spatial extent of flood hazard index at District level. Coupling the two flood modelling approaches compensate the limitations associated with each of them (Asare-Kyei *et al.*, 2015). This combination enables a better identification of flooded areas in Abidjan District.

Other benefits to be derived from the coupled approach include:

- Getting reliable estimates without using a purely empirical model
- Use of historical flood records and knowledge of flood causal factors which are readily available
- Application in Geographic Information System (GIS)
- Considers both the susceptibility of each area to be inundated and flood emergency management.

3.8.1. Rational model

The Rational Method is an important hydrological model used to determine the peak surface runoff rates in small urban watershed or catchments for design of variety of drainage structures (Bengtson, 2010). Peak of runoff depends on three data values: runoff coefficient, drainage area and rainfall intensity. However, in this study the challenge is to apply the rational method at
District level and by replacing rainfall intensity by annual rainfall within the model.

3.8.1.1. Determination of runoff coefficient

The main factors affecting the rational method runoff coefficient value are the land use, the soil type and the slope. The physical interpretation of the runoff coefficient for a District is the fraction of rainfall on that District that becomes storm water runoff.

In this study, the U.S. Soil Conservation Service (SCS) coefficient tables was used for a classification of land uses, slopes, and soil types to determine the runoff coefficient. It has four soil group identifications that provide information helpful in determining runoff coefficients. The four soil groups are identified as A, B, C, and D (see appendix 1). In order to find a representative runoff coefficient within given land covers, an overall runoff coefficient was determined using the areas of the different hydrologic soil group and slope complexes as weighting factors. This was done in a GIS environment by first reclassifying the soils map into a map based on SCS soil classification groups; followed by land use map reclassification too. Finally, all reclassified map were crossed (land use map, soil map and slope map) to determine the drainage area and runoff coefficient values of each cover type of the study area because runoff differ per soil group.

3.8.1.2. Determination of peak runoff

The Rational Formula to determine the runoff peak rate is given by the equation.

$$Qp = 0.28 C I A \qquad (3.26)$$

Where,

Q_p = Peak runoff rate (m^3/sec)

C = Runoff coefficient (-)

I = Annual Rainfall (mm)

A = Drainage area (Km^2)

In application of rational model important assumption were considered. These assumptions include

- The entire District was considered as a single unit,
- Rainfall is uniformly distributed over the drainage area.
- Predicted peak runoff has the same probability of occurrence as the used rainfall variability

(*I*),

- The runoff coefficient (*C*) is constant during the rain storm

3.8.1.3. Development of peak runoff map

After generating runoff coefficient map, the data requested by the hydrological model as input variables which is runoff coefficient (*C*), annual rainfall (*I*), drainage area (*A*) and land use were generated and rasterized with a cell resolution of 30m to correspond to the spatial resolution of the DEM layer into GIS. Then crossing them based rational formula in map algebra tools specifically using raster calculator to elaborate peak runoff map.

3.8.2. Categorisation of maps

After creating the peak runoff rate map, the peak runoff values was categorised by applying the natural breaks (Jenks) method into ArcGIS. This procedure results in a categorised runoff values on a scale of 1 to 5; with one being the lowest probability for a flood to occur and 5 for the categories with the highest probability. Then, DEM of the study area was also categorised using the same natural breaks (Jenks) method and reclassified on a scale of 1 for high (93 – 141 m) to 5 for low (-59 – 20 m) elevation. This reclassification of the elevation is based on the theoretical principles underlying the relationship between elevation and flood occurrence. Flood occurrence is high in low slope areas and inversely, Flood occurrence is low in greater slopes areas.

3.8.3. Flood hazard index (FHI) map

Using the two categorised layers (peak runoff and DEM); the distribution of the intensity level of flood hazard was realized by overlaying them using the raster calculator in GIS to elaborate the flood hazard index (FHI) map (Figure 3.18). For each pixel, this method multiplies the categorised peak runoff score with the score of the categorised DEM to produce the distribution of runoff at different elevations which is indicative of flood hazard. The Flood Hazard Index was finally

derived again by applying the natural (Jenks) breaks method which reclassified the data into five classes: very low, low, medium, high and very high.

Flood Hazard Index (FHI) = Peak runoff □DEM *(3.27)*

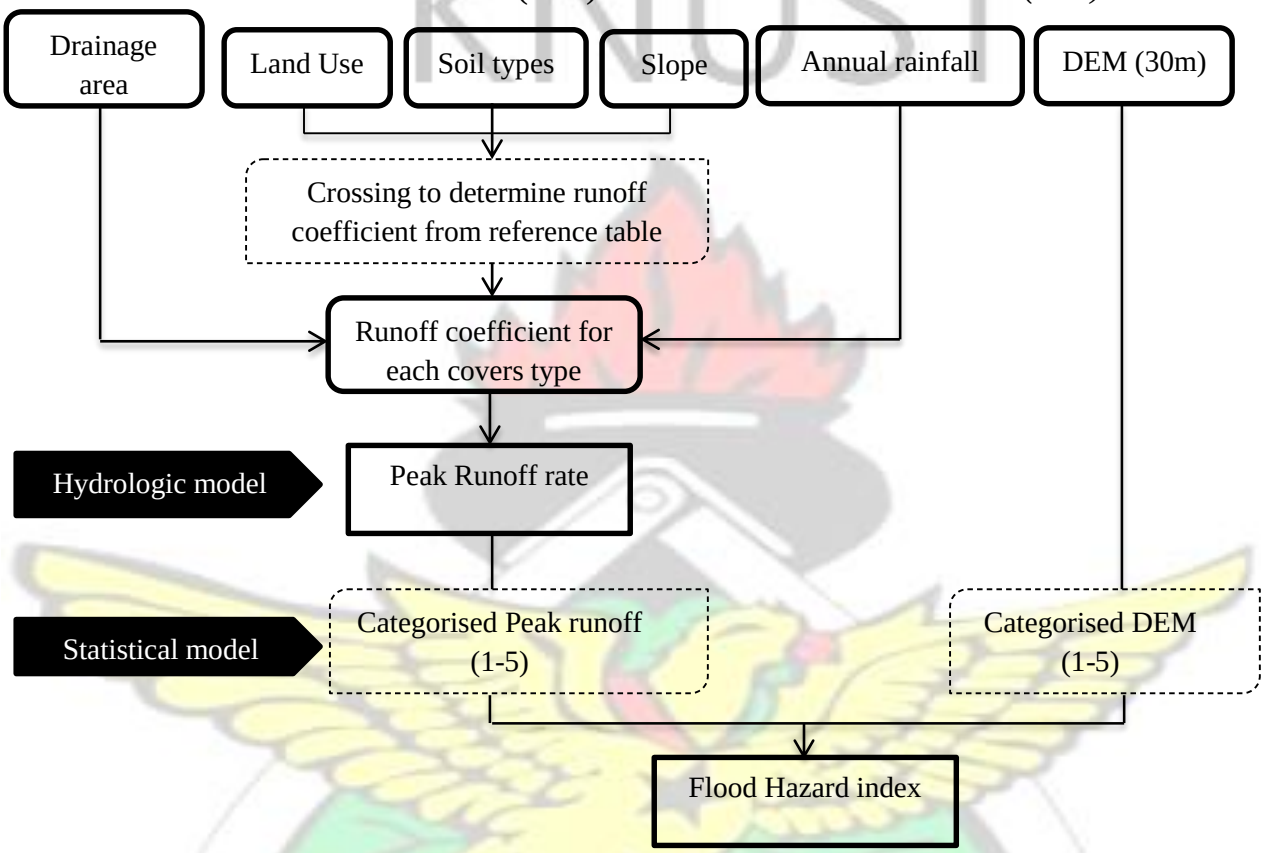


Figure 3.18: Flood hazard index (FHI) framework

CHAPTER 4: RESULTS

4.1. Land Use/ Land Cover dynamic of Abidjan District

Three land use/ land cover classes were identified in this study:

- Vegetation: include Natural forest, national park, cropland, green space, fallows.
- Water: include river and lagoon
- Settlement: include built up areas and bare soil (because of their close reflectance value)

4.1.1. Land use/ land cover classification between 1990, 2002 and 2014

At the end of image analysis and classification, three land use/ land cover maps were generated for each year.

The land use/ land cover map for the year 1990 was mainly dominated by vegetation (Figure 4.1). The area covered by vegetation, water and settlement, was 129,521 ha, 16,657 ha and 24,607 ha, respectively. These represent 75.84%, 9.75% and 14.41% of the total land areas, respectively.

For the year 2002, the land use/ land cover map (Figure 4.2) showed that LULC was still dominated by vegetation. However, a decrease in vegetation followed by an increase in settlement area. Vegetation areas were about 128,009 ha (74.98%), water 16,962 ha (9.93%) while settlement covered 25,751 (15.08%), respectively.

In the land use/ land cover map for the year 2014 (Figure 4.3), vegetation covered 117,191 ha (68.66%) of the landscape, then water area was 16,954 ha (9.93%) and the area covered by settlement was equal to 36,548 ha (21.41%).

KNUST

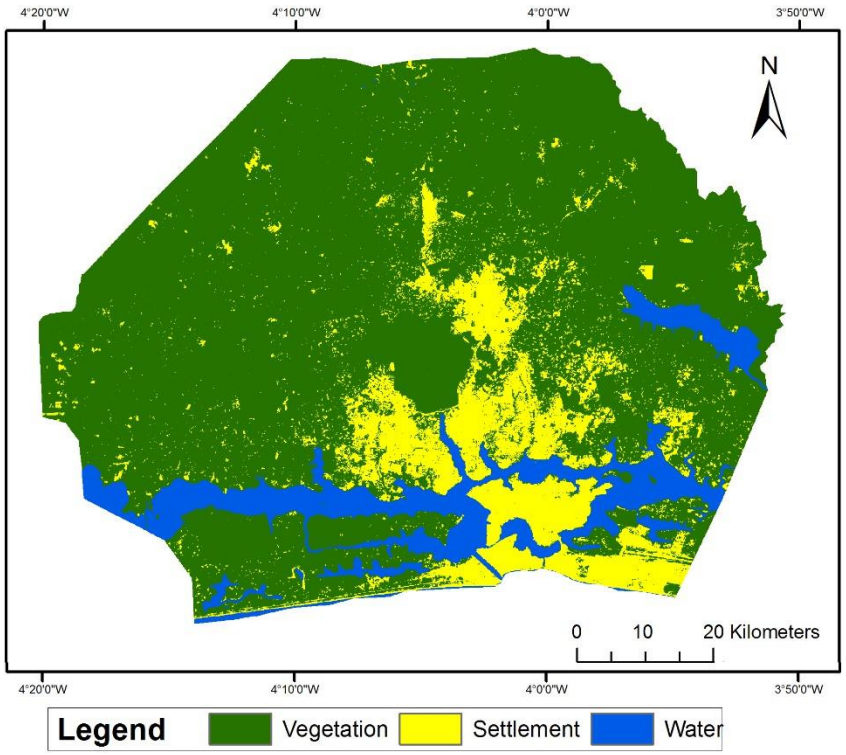


Figure 4.1: Land use/Land cover dynamic of Abidjan District in 1990

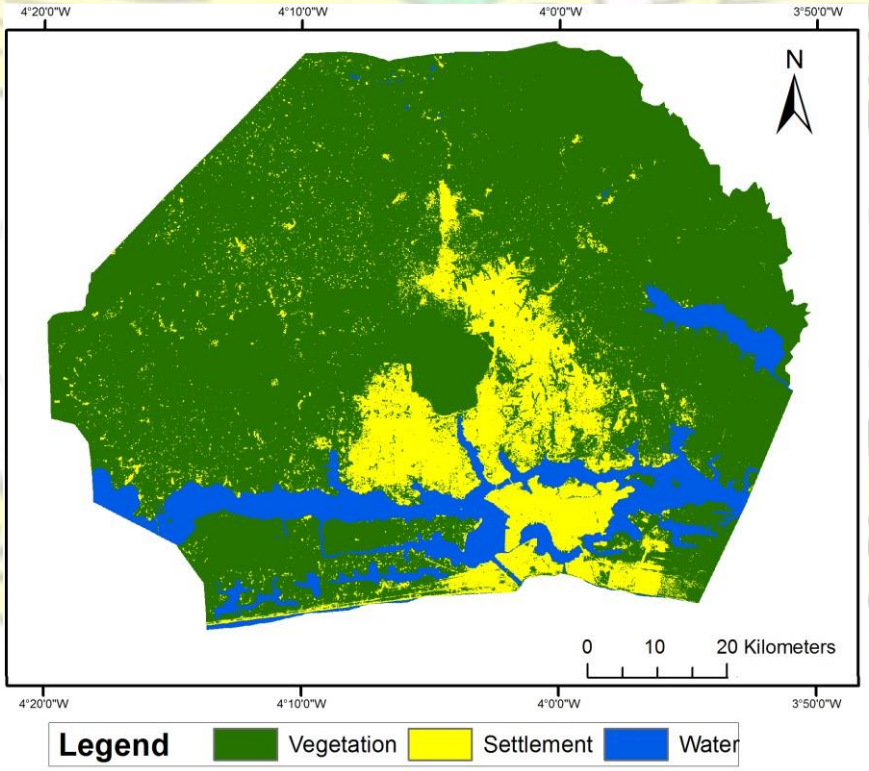


Figure 4.2: Land use/Land cover dynamic of Abidjan District in 2002

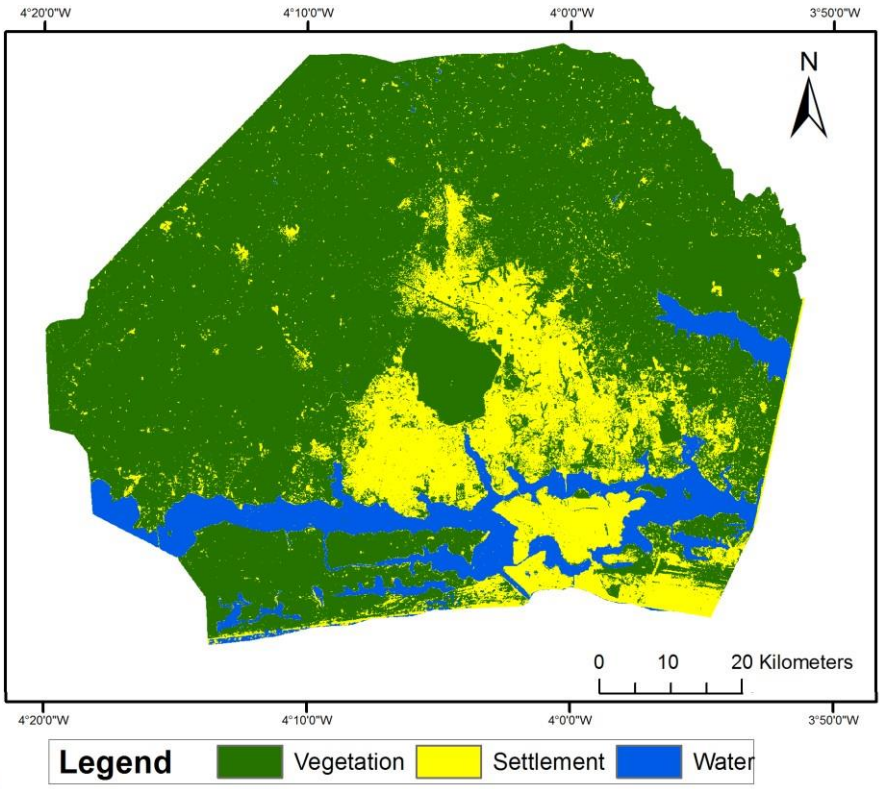


Figure 4.3: Land use/Land cover dynamic of Abidjan District in 2014

4.1.2. Validation of land use /land cover classification

For the year 1990, the accuracy assessment results showed an overall accuracy of 93.9 % and a *Kappa coefficient* of 0.90 with a producer accuracy of 93.32 % and a user accuracy of 95.56 %.

For the year 2002, the overall accuracy was 99.58 % with a *Kappa coefficient* of 0.99 and the overall producer and user accuracy of 99.58 % and 99.59 %, respectively.

For the year 2014, the overall accuracy was 98.96 % and a *Kappa coefficient* of 0.98 with an average producer and user accuracy of 99.04 % and 98.9 %, respectively.

For these three (1990, 2002, 2014) years, all land use/ land cover classes were well identified and classified with very low class confusion. The overall accuracy of the classification derived from

confusion matrix was estimated to be 93.9 %, 99.58 % and 98.96 % for 1990, 2002 and 2014 images, respectively (Table 4.1).

Table 4. 1: Confusion matrix (percentages) for classified land use land cover map of the years 1990, 2002 and 2014

1990	Vegetation (Pixel)	Water (Pixel)	Settlement (Pixel)	**Total**	**Producer's accuracy (%)**	**User's accuracy (%)**	**Kappa**
Vegetation	14,822	125	1,256	16,203	97.67	91.48	
Water	0	4,924	0	4,924	97.5	100	0.90
Settlement	353	1	7,000	7,354	84.79	95.19	
Total	15,175	5,050	8,256	28,481	**Overall Accuracy = 93.9**		
2002	Vegetation (Pixel)	Water (Pixel)	Settlement (Pixel)	**Total**	**Producer's accuracy (%)**	**User's accuracy (%)**	**Kappa**
Vegetation	2,580	15	17	2,612	100	98.77	
Water	0	2,601	0	2,601	99.43	100	0.99
Settlement	0	0	2,498	2,498	99.32	100	
Total	2,580	2,616	2,515	7,711	**Overall Accuracy = 99.58**		
2014	Vegetation (Pixel)	Water (Pixel)	Settlement (Pixel	**Total**	**Producer's accuracy (%)**	**User's accuracy (%)**	**Kappa**
Vegetation	2,066	11	8	2,085	100	99.09	
Water	0	2259	0	2,259	97.54	100	0.98
Settlement	0	46	1,876	1,922	99.58	97.61	
Total	2,066	2,316	1,884	6,266	**Overall Accuracy = 98.96**		

4.1.3. Land Use/ Land Cover dynamic

For aforementioned, the overall accuracy of the post classification derived from the confusion matrix was estimated to be 93.9 %, 99.58 % and 98.96 % for 1990, 2002 and 2014 LULC maps, respectively. The study area has known important land use/cover conversion from one type to another.

4.1.3.1. Land Use/ Land Cover change between 1990 and 2002

In 1990, the size of the vegetation was significant compared to the present. Land use/land cover trends from 1990 to 2002 are presented in Table 4.2. There was a decline in area of vegetation class. On the other hand, increase of water body area (1.83%) and a most significant increase of urban area from 1,144 ha (4.65%) after 12 years covered by built-up and some bare soil, which means that urbanisation of the Abidjan District at this time, was mainly due to the conversion of vegetation area to settlement area.

Table 4. 2: Change in areas of each land use/ land cover class between 1990 and 2002

	Area in 1990		**Area in 2002**		**Change 1990-2002**	
	ha	%	ha	%	ha	%
Vegetation	129,521	75.84	128,009	74.98	-1512	-1.17
Water	16,657	9.75	16,962	9.93	305	1.83
Settlement	24,607	14.41	25,751	15.08	1144	4.65

4.1.3.2. Land Use/ Land Cover change between 2002 and 2014

Analysis of the land use/ land cover change trends from 2002 to 2014 showed two main trends which are presented in Table 4.3. During this period, there was a decrease of vegetation area from 8.45 % followed by an important increase in settlement area (41.93 %) and irrelevant decrease in water body area from 0.05 %. This implies that urbanisation process converted vegetation area into settlements following a significant reduction in the vegetation area. In the land use dynamics of Abidjan, vegetation undergoes a speedy decrease and conversion to settlement area during the 2002-2014 decade, compared to 1990-2002.

Table 4. 3: Change in areas of each land use/ land cover class between 2002 and 2014

	Area in 2002		**Area in 2014**		**change 2002-2014**	
	ha	%	ha	%	ha	%
Vegetation	128,009	74.98	117,191	68.66	-10,818	-8.45
Water	16,962	9.93	16,954	9.93	-8	-0.05
Settlement	25,751	15.08	36,548	21.41	10,797	41.93

4.1.3.3. Land Use/ Land Cover change between 1990 and 2014

Land use/ land cover changes that occurred during the 24-years period is presented in Table 4.4. The land use/ land cover classes showed a negative change in vegetation meaning a decrease in its area while settlement and water area were increased to 48.53 % and 1.78 % respectively. It means that urban area sprawls inside the District occurred during this 24-years period. Over 9.52 % of vegetation area was transformed to settlement area.

Table 4. 4: Change in areas of each land use/ land cover class between 1990 and 2014

	Area in 1990		**Area in 2014**		**Change 1990-2014**	
	(ha)	%	ha	%	ha	%
Vegetation	129,521	75.84	117,191	68.66	-12330	-9.52
Water	16,657	9.75	16,954	9.93	297	1.78
Settlement	24,607	14.41	36,548	21.41	11941	48.53

4.1.3.3. Overall Land Use/ Land Cover change from 1990 - 2014

The statistical details of the Land use/land cover changes during the various years 1990, 2002 and 2014 is shown in Figure 4.4. There was a decline in vegetation cover during these periods, especially from 1990 to 2014. While there was no change in water area from 1990 to 2014, settlement area expanded importantly from 1990 to 2014.

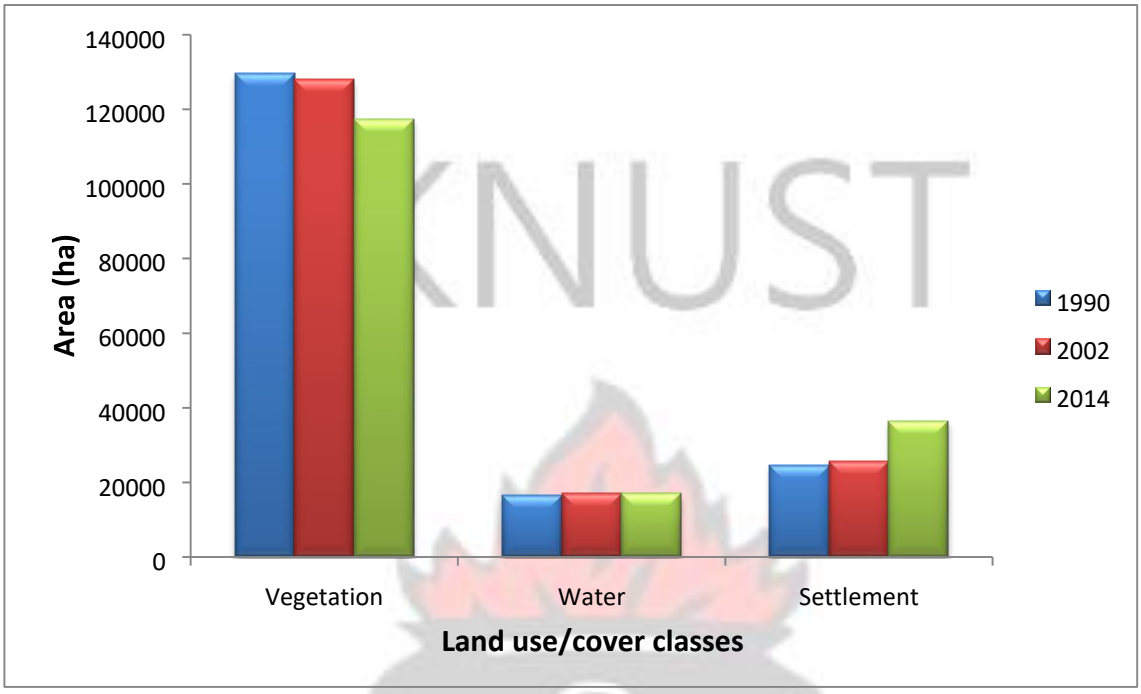


Figure 4.4: Land use/land cover change for the years of 1990, 2002 and 2014 in Abidjan

4.1.4 Land use/ land cover change detection

Transition matrix, between 1990-2002; 2002-2014 and 1990-2014 in Table 4.5 shows that all land use/ land cover classes changed during these periods. From 1990-2002, nearly 6.17 % and 1.6 % of vegetation and water, respectively, decreased and was mainly degraded and converted to settlement area. During 2002-2014, around 7 % and 4 % of vegetation and water areas, respectively, decreased as a result of settlement purpose while 9.59 % of settlement area was reconverted to vegetation area.

From 1990 to 2014, an average of 9.6% and 5.3% of vegetation and water areas, respectively, were converted to settlement area.

Table 4. 5: Land use / land cover change detection in Abidjan

Change 1990-2002 (%)	Vegetation	Water	Settlement
Vegetation	93.11	0.65	6.17
Water	2.14	96.23	1.63
Settlement	28.32	0.42	71.26
Change 2002-2014 (%)	Vegetation	Water	Settlement
Vegetation	82.03	11.01	6.96
Water	12.75	83.31	3.94
Settlement	9.59	0.54	89.87
Change 1990-2014 (%)	Vegetation	Water	Settlement
Vegetation	88.87	1.49	9.64
Water	1.38	93.31	5.31
Settlement	24.05	0.58	75.37

Analysis of the general land use/land cover dynamics and change showed vegetation area was taken over by settlements (build up and bare soil). The dynamics of settlement area between 19902002 and 2002-2014 were different. Settlement area in 2014 was higher than that in 2002 which implies a fast increase in urbanisation sprawl. The explanation of the rapid urbanisation sprawl from 2002-2014 is due to the civil war that was experienced in the country from 2002-2011 and which resulted in the migration of people from affected areas during the civil war. Also, there was an increase in infrastructure projects during this period, hence an increase in settlement area. Finally, Abidjan, being the economic capital of Cote d'Ivoire with developmental projects including construction of roads, houses and industries, as well as population growth, is still ongoing and therefore vegetation area is still expected to be transformed further into urban area.

4.2. Normalized Difference Build-up Index (NDBI)

From the data collection based on the study focus, all classes including vegetation, bare soil and water under others class were merged to have a better appreciation of settlement dynamic and change through NDBI calculation over the three periods in this study:

- Others: include vegetation, bare soil and water classes
- Urban: Settlement

At the end of NDBI processing on 1990, 2002 and 2014 Landsat images, three NDBI maps were generated for each year (Figure 4.5). After observation, it was realised that, there was a significant increase in settlement area in 2014 (39.91 %) compared to 2002 (36.44 %) and 1990 (31.4 %). This result shows that rapid urbanisation has really taking place from 2002 to 2014 in the 13 municipalities which means there was a lot of conversion of other classes' area. The NBDI calculation of settlement area in 2002 is less than settlement area in 2014 (Table 4.6). This confirmed and validated results from land use/ land cover dynamics and change detection state previously.

Table 4. 6: NDBI for 1990, 2002, 2014 years in Abidjan

	1990		**2002**		**2014**	
Classes	pixel	%	pixel	%	pixel	%
Others	1301383	68.6	1335473	63.56	1140192	60.09
Settlement	595677	31.40	765598	36.44	757303	39.91
Total	1897060	100	2101071	100	1897499	100

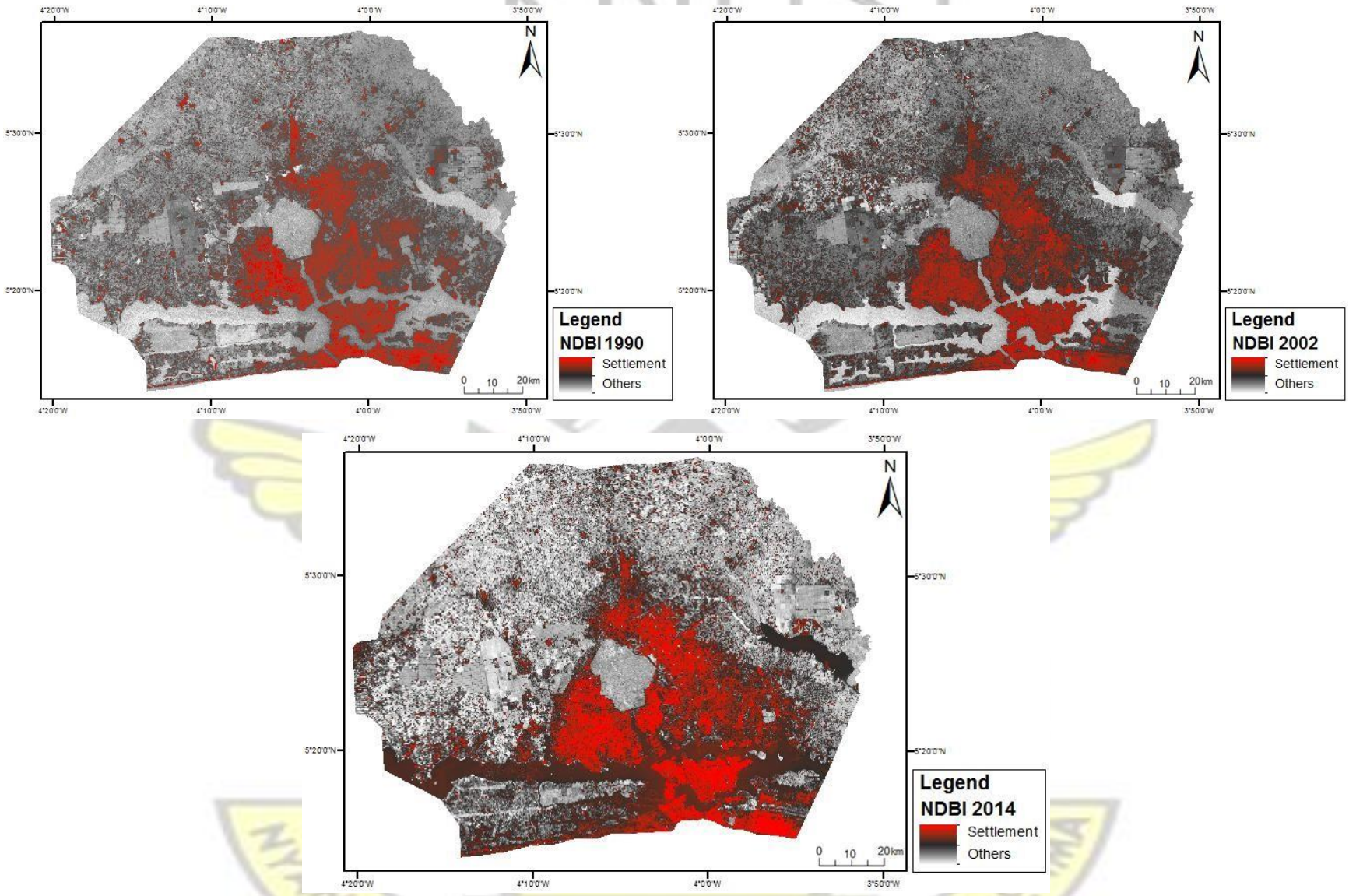


Figure 4.5: Normalized Difference Build-up Index (NDBI) of 1990, 2002 and 2014

KNUST

4.3. Urban Structure Types Classification

The result by processing urban structure types classification of Abidjan District using Spot 5 image with 10 m resolution from 2013 through rule set based method and hierarchical classification is shown in the Figure 4.6. Based on image resolution and literature, eight (8) urban structure types (UST) classes were identified within the study area. These were:

- informal residence
- industry area
- high residence
- medium residence
- Public's services (administration, hotels, church, etc.)
- bare soil
- Vegetation (forest, vegetation, cropland and grassland)
- Water (lagoon, lake and river)

The analysis of UST classification revealed a disproportion in all classes' areas coverage with 2.97 % of industrial area, 3.21 % of public services, bare soil are of 2.03 %, informal, medium and high level residences areas covered 0.28 %, 7.83 % and 3.2 % respectively, and they were surrounded by 70.35 % of vegetation area (forest, vegetation, cropland and grassland) and 10.13 % of water body (lake, lagoon and river). The overall accuracy of the classification derived from confusion matrix was estimated to be 62 %.

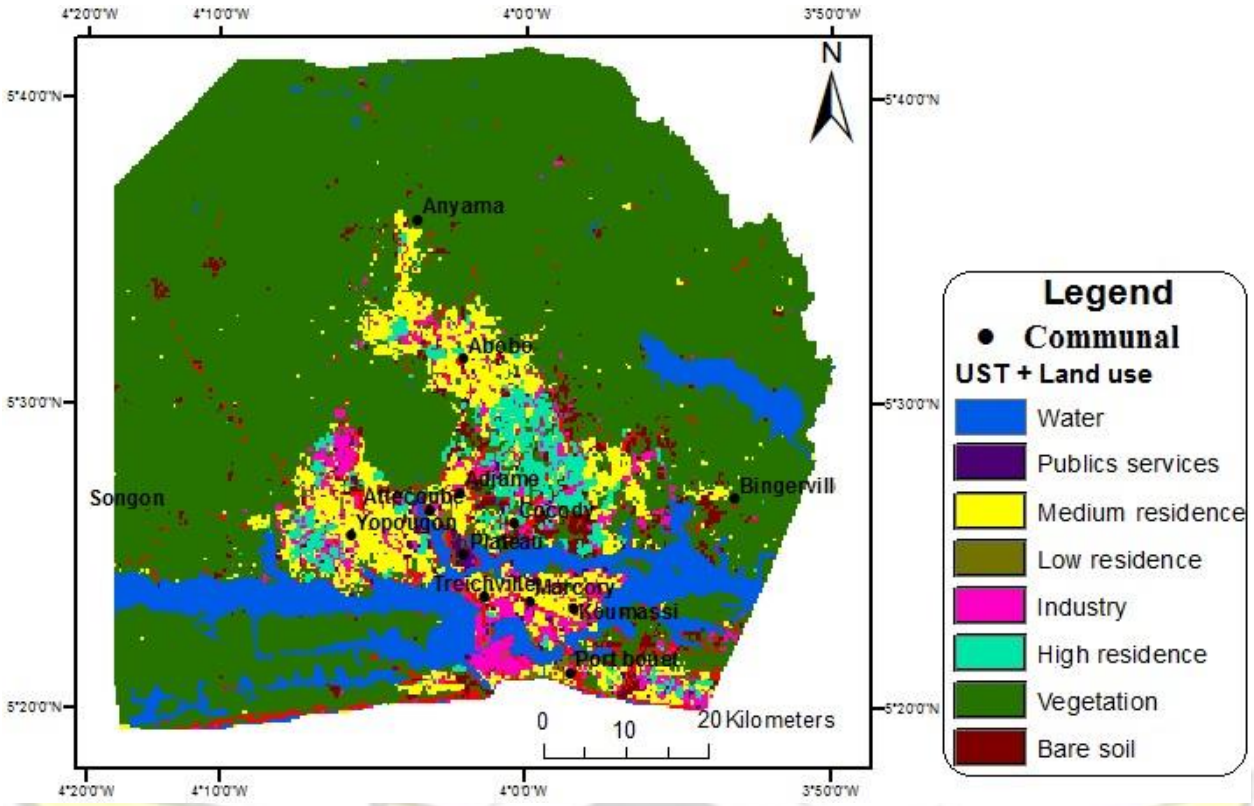


Figure 4.6: Urban structure types of Abidjan from spot image

4.4. Rainfall Variability Analysis

4.4.1 Standardised Precipitation Index (SPI)

Graphical representations of standardised precipitation index (SPI) of annual rainfall series averages permit to determine different precipitation fluctuations (wet, normal and dry period) at Abidjan (Figure 4.7). Three periods were identified in all:

- Wet period from 1960 to 1969 with an average annual rainfall of 2190 mm. This represents more than 22 % of total rainfall greater than the total annual average of 1787 mm. It was noted that, this period has a remarkable year 1963 with a rainfall of 2765 mm or 978 mm excess over the average for the study period.

- Normal period 1970 – 1982, with an average rainfall of 1944 mm. This represents over 8 % of total rainfall above the average annual total.

- Dry period from 1983 to 2012. This period is characterised by an average rainfall of 1585 mm, a shortfall of 11 % compared to the average of the study period.

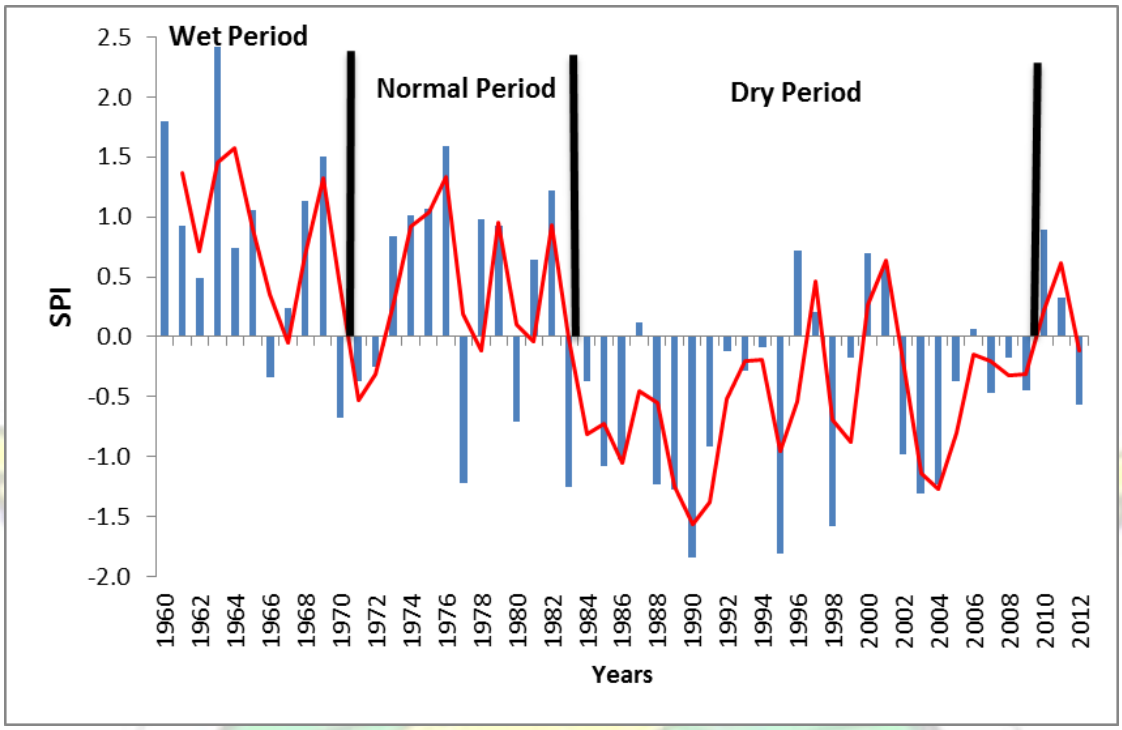


Figure 4.7: Standardised Precipitation Index of Abidjan station from 1960 - 2012

Curves fluctuation in rainfall by SPI and weighted indices clearly reflect the high rainfall variability in the District of Abidjan during this period (Figure 4.8). These indices show a general wet period from 1960 to 1983, followed by a dry period from 1983 to 2010 throughout the District. This results show an upward trend from1960 to 1983 and a downward trend from 1983 to 2010 as observed through the weighted indices. However, there has been an increasing rainfall trend since 2010 at Abidjan.

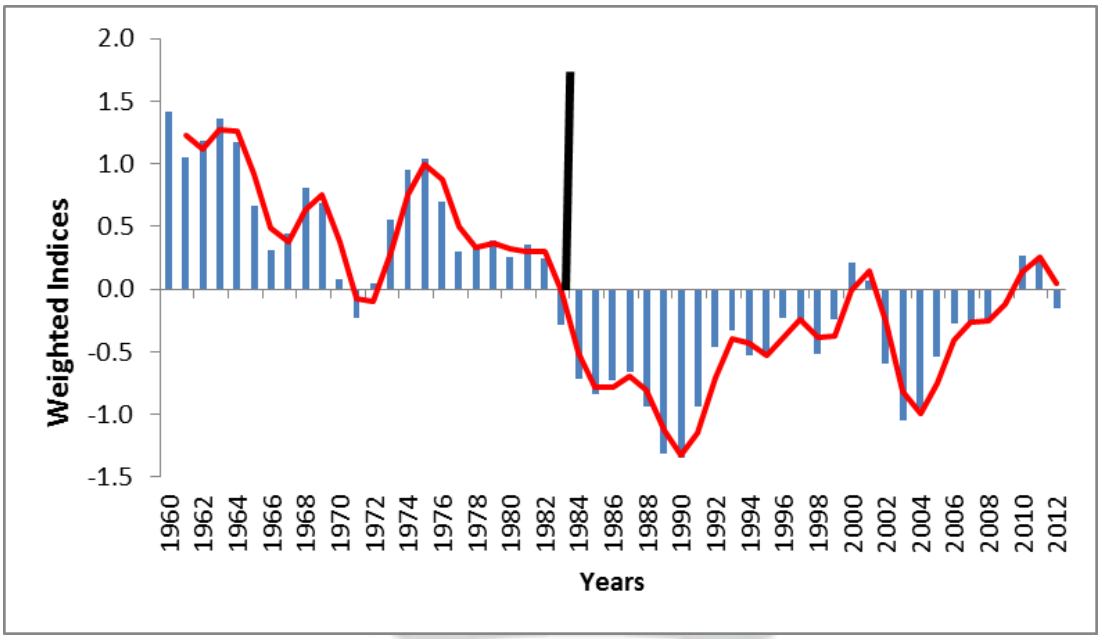


Figure 4.8: Curve weighted indices of Abidjan station from 1960-2012

4.4.2. Change detection tests

Based on statistical methods, years of break in the rainfall pattern of the District of Abidjan were defined. Buishand's test allowed accepting or rejecting the hypothesis of no break in the series (H_0), while Pettitt test permitted to specify the year of break. Here, the study considered only the primary or main breaks.

4.4.2.1. Buishand's test

Under the Null Hypothesis H_0, it is possible to define a confidence region containing a given confidence level, the series of S_k^* This region is called confidence ellipse control. When S_k^* is out of this ellipse, H_0 hypothesis is rejected at confidence level $1-\alpha / 2$ (variable reduced the probability of not exceeding normal). Ellipsoids control of Abidjan is shown in Figure 4.9.

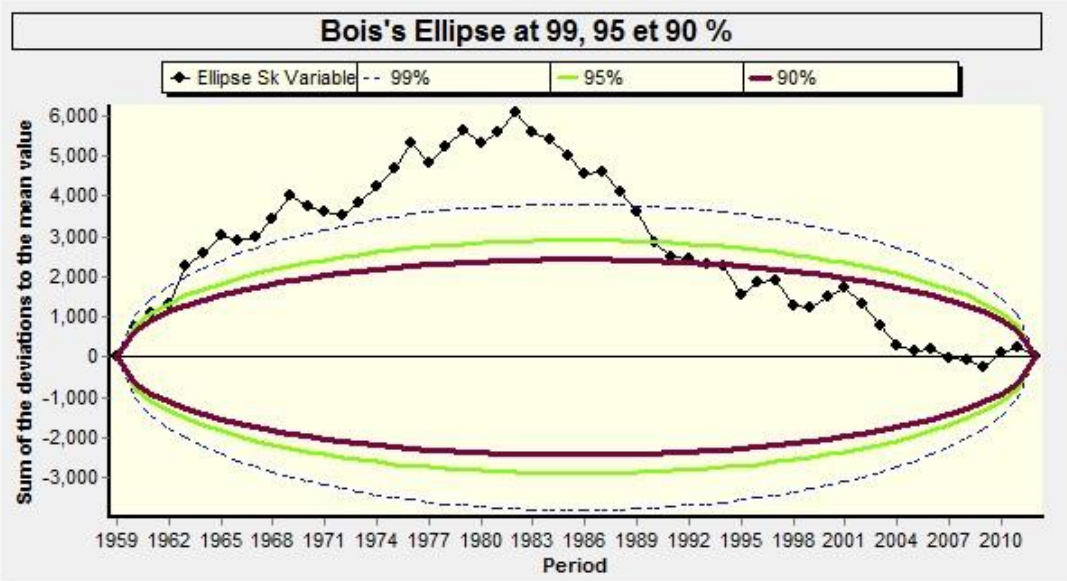


Figure 4.9: Buishand's test of Abidjan from 1960-2012

The analysis of these ellipsoids permitted to realise that the hypothesis of no break H_0 is rejected at confidence levels of 90, 95 and 99 % in the rainfall series of Abidjan, respectively. Therefore these series show a break and the year of break was 1982 in Abidjan.

4.4.2.2. Pettitt test

The break is here embodied by the point at which the curve of the variable U of Pettit test changed trend by passing from positive (1960-1982) to negative (1982-2010), (Figure 4.10). Thus, the analysis of curves showed that the rainfall series have ruptures. However, the main break was detected in 1982 at Abidjan.

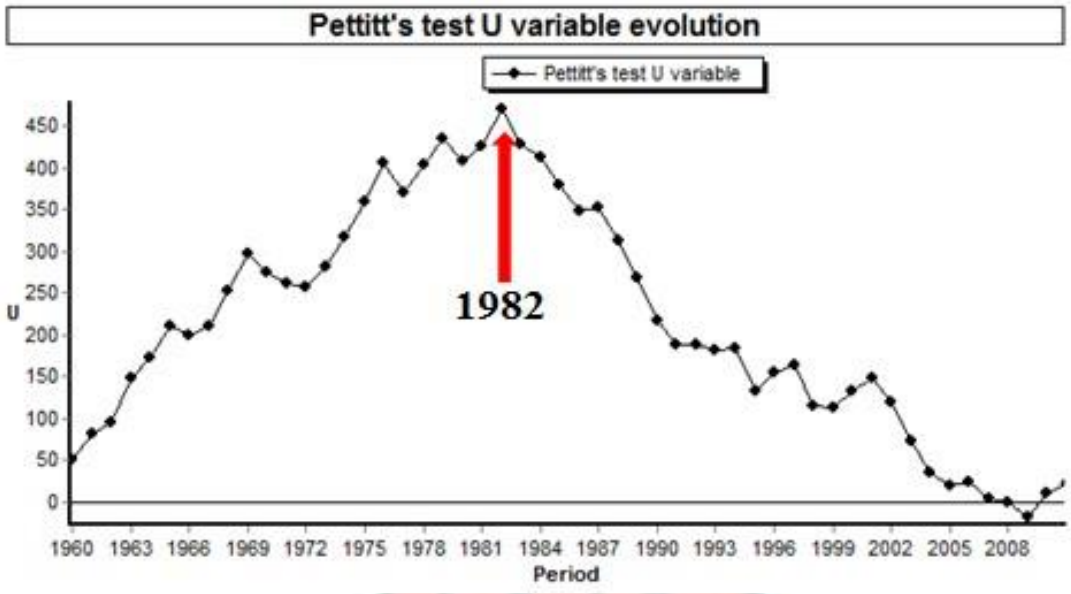


Figure 4.10: Pettit test of Abidjan from 1960-2012

After analysis, it was observed that Buishand and Pettit tests clearly confirm the presence of breaks in the rainfall series of Abidjan District. In the end, these tests demonstrate and validate the different divisions obtained with SPI and weighted indices.

4.5. Gumbel Approach

Gumbel statistical methods applied in the rainfall pattern of the District of Abidjan by using Graphical method and moment law method are shown in Figure 4.11a and 4.11b. The analysis shows that, in general the, Gumbel distribution provide an acceptable fit to the measured and estimated annual maximum daily precipitation distribution.

	a

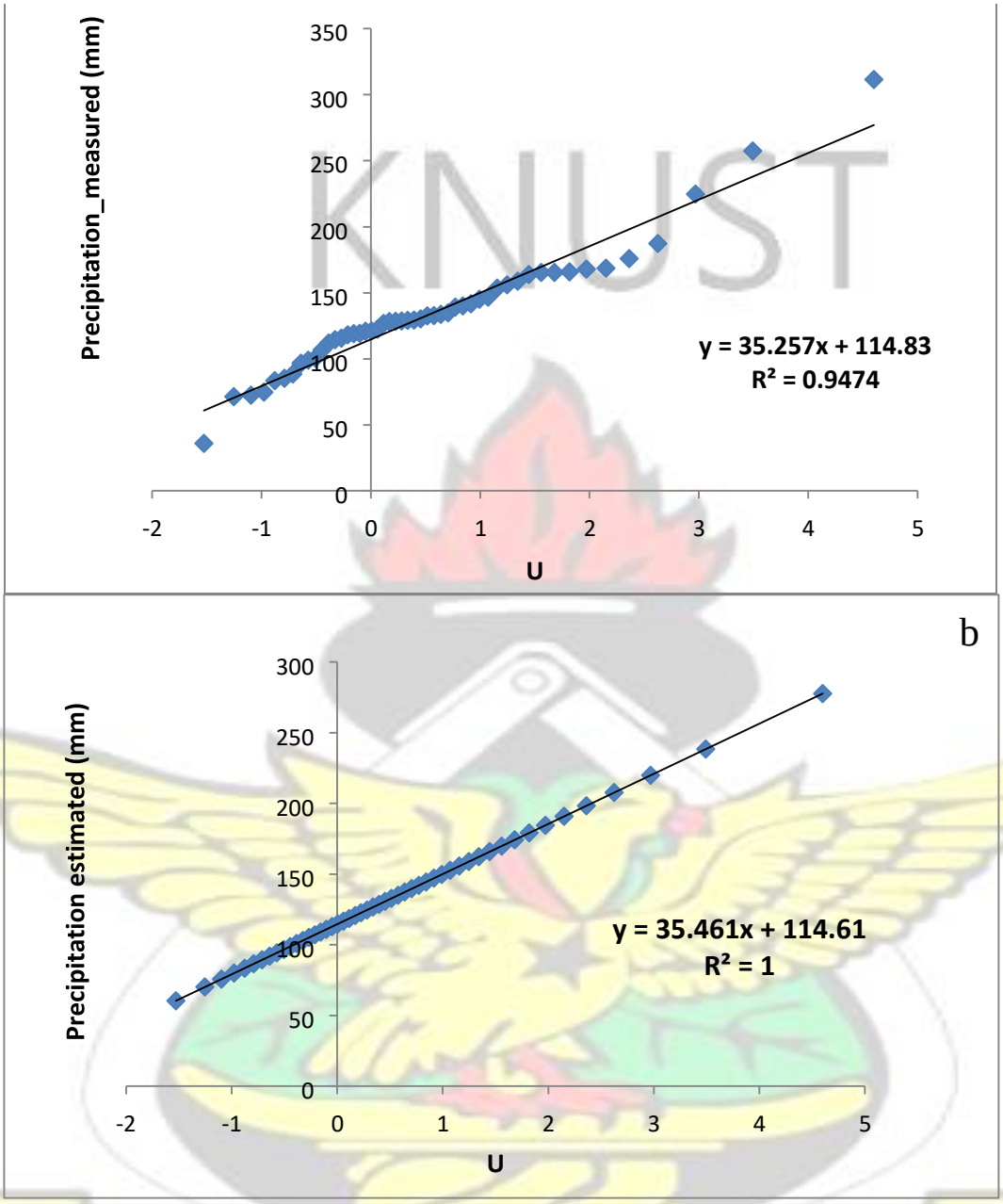


Figure 4.11: Gumbel test of measure (a) and estimate (b) precipitation at Abidjan The scattered lines in Figure 4.11 (a and b) are the ordinary linear regression approximations. The linear approximation equations and coefficients of linear determination (R^2) of each graph shows that measured and estimated precipitations are highly correlated (Table 4.7). The visual interpretation of the graph is that the Gumbel distribution is appropriate to estimate return period (Table 4.8).

Table 4. 7: Correlation between measured and estimated annual daily maximum rainfall

Variables	Graph	Moment law	Average
b	35.26	35.67	35.46
a	114.83	114.39	114.61

Table 4. 8: Precipitation returns period for 100, 50, 20, 5, 2 years

Return preiod T	**100**	**50**	**20**	**5**	**2**
Xq	0.99	0.98	0.95	0.8	0.5
U	4.60	3.90	2.97	1.50	0.37
Xq for Tperiod	278.45	253.55	220.32	167.88	127.46

Where: **Xq**= (1- (1/T) :

U= -ln (-ln (Xq)): Reduced variable

Xq for Tperiod = a + bu: linear quintile

T: Return period

4.6. Temperature, Precipitation, Solar Radiation and PET Predictions in LARS-WG model

The Table 4.9 shows results of minimum and maximum temperature, rainfall, solar radiation and PET change between the baseline (1961-2010) and three future scenarios:

- Scenario 1: 2011-2030,
- Scenario 2: 2046-2065;
- Scenario 3: 2065-2099.

As shown in Table 4.9 and Figure 4.12 (a, b, c, d, and e), the variability trend and change of each weather data between the baseline and generated future scenario revealed that, weather data will change from the baseline to one scenario to another scenario. These predictions were made using the global model HadCM3 and the optimistic emission scenario SRA1B.

Table 4. 9: Minimum/maximum temperature, precipitation, solar radiation and evapotranspiration change prevision at Abidjan.

	Tmin (°C)	Tmax (°C)	Rain (mm)	RAD	PET
Baseline (1961-2010)	24.18	27.40	3.62	16.91	4.44
Scenario 2011-2030	24.50	27.72	3.75	16.82	4.43
Change 1	**0.32**	**0.32**	**0.04**	**-0.09**	**-0.01**
Scenario 2046-2065	25.54	28.77	3.82	16.81	4.49
Change 2	**1.36**	**1.37**	**0.06**	**-0.10**	**0.05**
Scenario 2080-2099	26.72	29.95	3.97	16.76	4.54
Change 3	**2.54**	**2.55**	**0.10**	**-0.15**	**0.10**

With:

Tmin: Minimum temperature

Tmax: Maximum temperature

Rain: Rainfall

RAD: Solar radiation

PET: Potential evapotranspiration

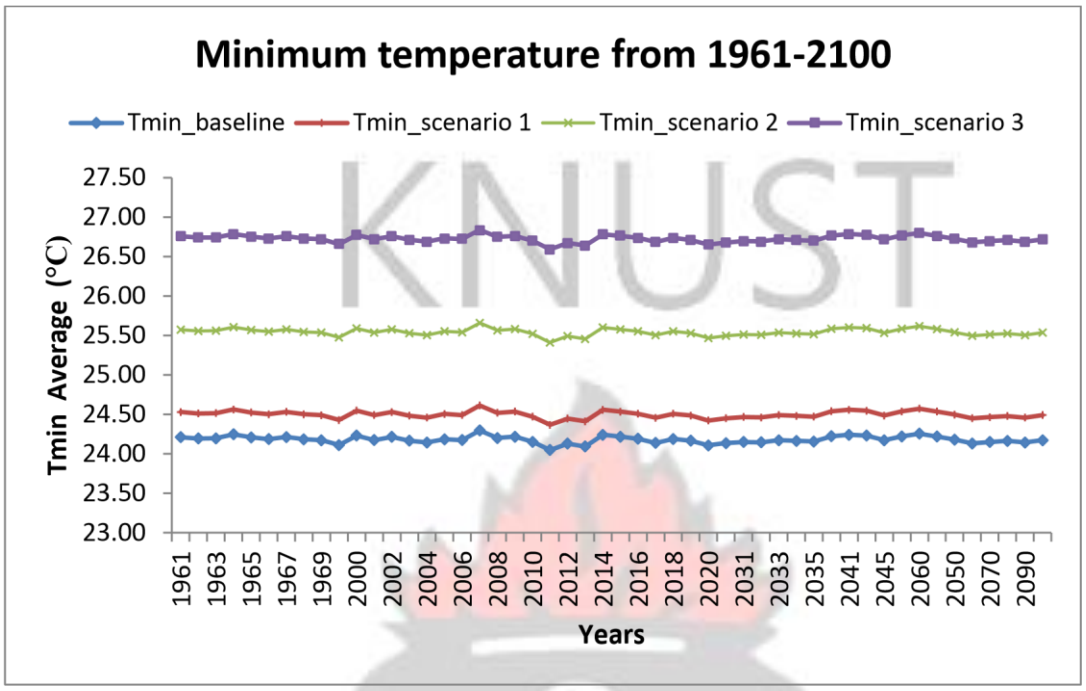


Figure 4.12a: Minimum temperature variability from 1960 to horizon 2100

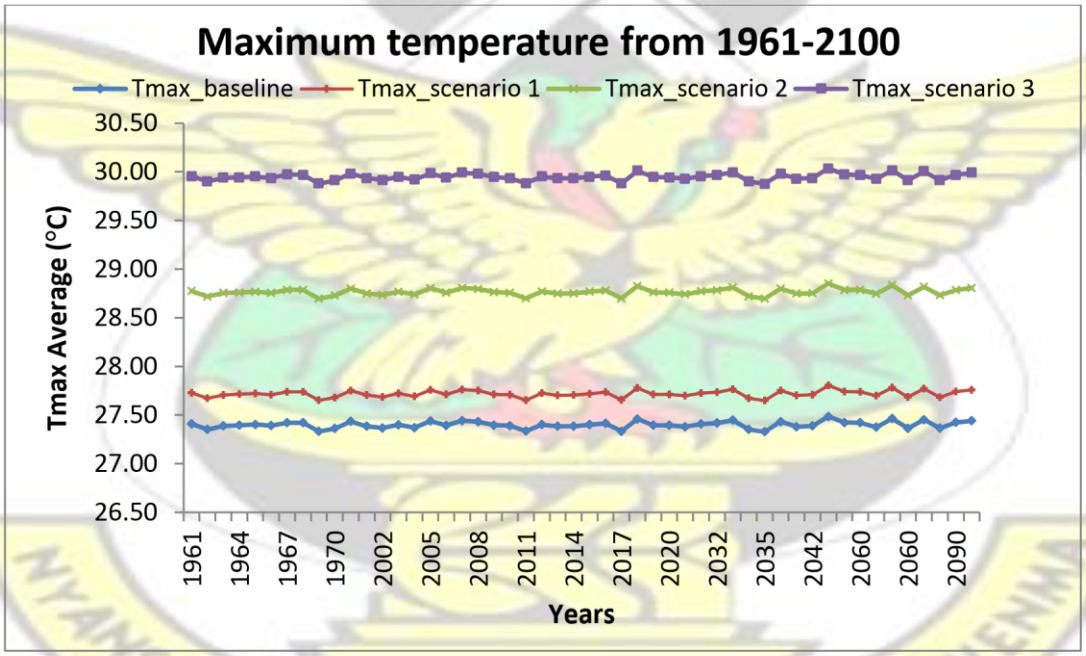


Figure 4.12b: Maximum temperature variability from 1960 to horizon 2100

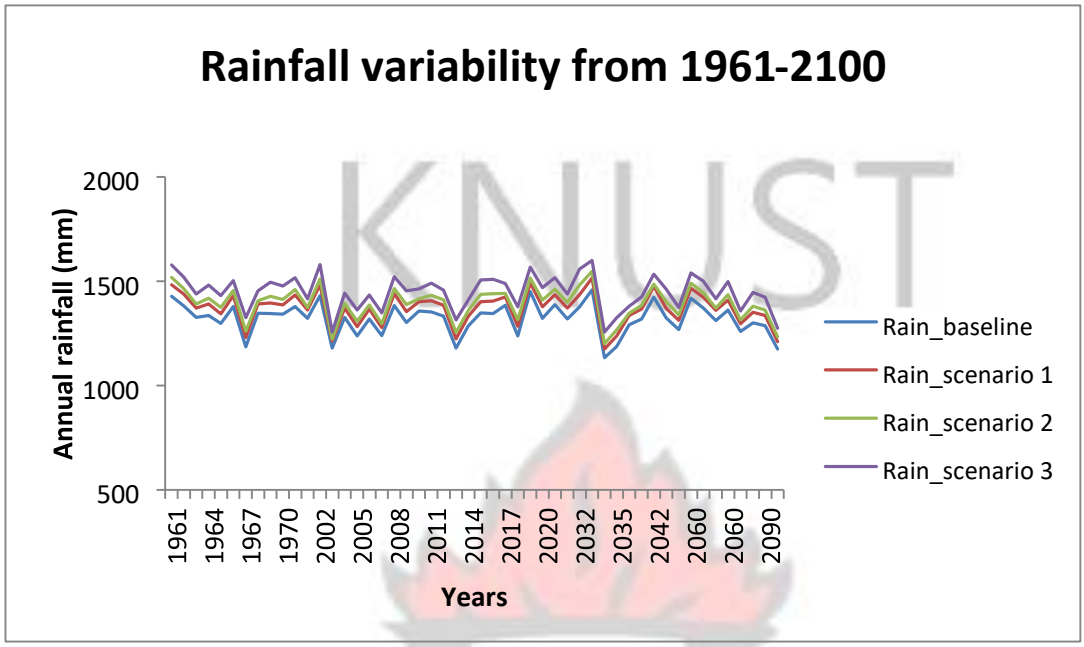


Figure 4.12c: Rainfall variability from 1960 to horizon 2100

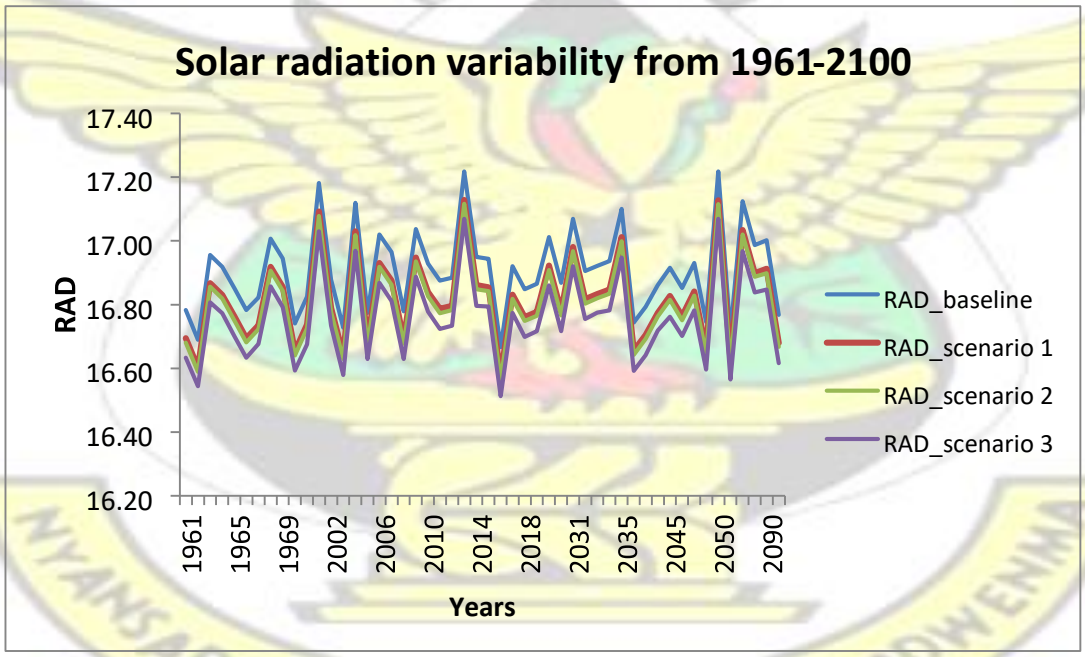


Figure 4.12d: Solar radiation variability from 1960 to horizon 2100

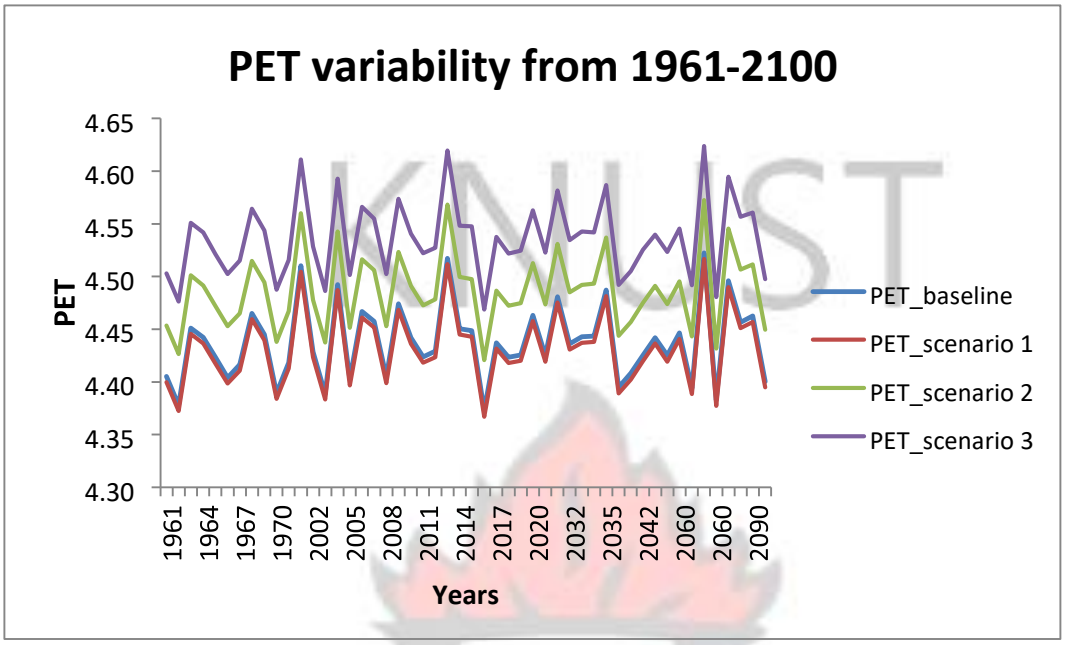


Figure 4.12e: Potential evapotranspiration variability from 1960 to horizon 2100

Scenario 1: 2011-2030

The result of this analysis shows that, for the scenario 1 compared to the baseline, there was an increase of 0.32°C in both the minimum and maximum temperatures, an increase of 4 % in the precipitation and a decrease of 0.09 and 0.01 in solar radiation and evapotranspiration, respectively, in the Abidjan District.

Scenario 2: 2046-2065

The second scenario shows an increase from the baseline of 1.36°C of the minimum and 1.37°C of the maximum temperatures. For this same scenario, there was also an increase of 6 % in precipitation from the baseline and a decrease of 0.1 in solar radiation and an increase of 0.05 of the evapotranspiration.

Scenario 3: 2065-2099

The third scenario shows an increase from the baseline of 2.54°C of the minimum and 2.55°C of the maximum temperatures. Then, an increase of 10 % of the precipitation and a decrease of 0.15 of solar radiation and an increase 0.10 of the evapotranspiration compared to the baseline.

Globally, climate predictions for the locality of Abidjan show an increase compared to the baseline of the temperatures and the precipitation for short term and long term periods with the longer one being higher than the shorter one. For the PET, the short term predictions show a decrease while the long term prediction shows an increase. In contrast, the solar radiation shows a decrease for the short term and long term periods. The implication of the different scenarios being modelled is that flood risk will occur more and more with high intensity due to the increase of precipitation in short and long term.

4.7. Rclimdex Rainfall Indices

From the daily weather data, ten (10) rainfall indices were calculated based on observed data from 1960 to 2010 and future data from 2011 to 2100 through Rclimdex model in this study.

KNUST

4.7.1. Consecutive wet days (*CWD*)

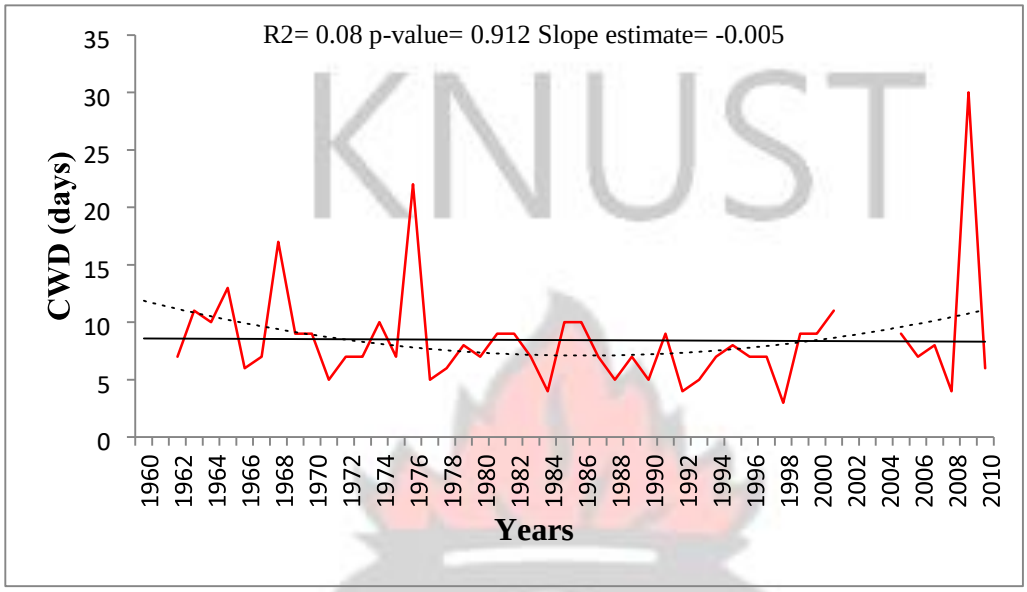


Figure 4.13a: Consecutive wet days (*CWD*) from 1960 to 2010

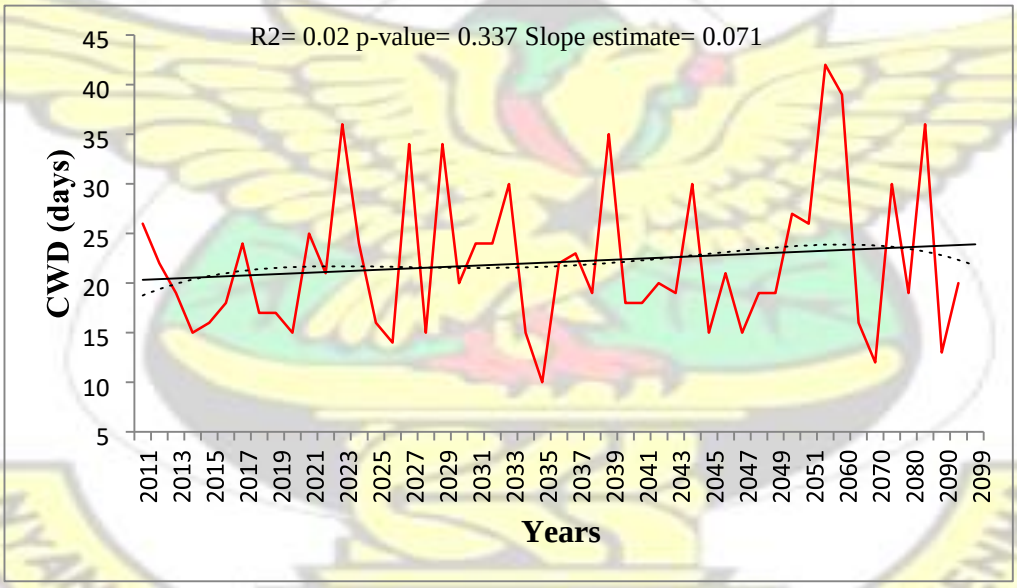


Figure 4.13b: Consecutive wet days (*CWD*) from 2011 to 2100

Figure 4.13 (a and b) shows the evolution of consecutive wet days (*CWD*) in Abidjan between the period 1960-2010 and 2011-2100. Observation of Figure 4.13a indicates that there was no important

inter-annual variability of *CWD* from 1960 to 2010 based on the general trend represented by the straight line. The *CWD* index fluctuated between 2 - 30 days. Except in 1968, 1975 and 2010 where there was a peak of 17, 23 and 30 of wet days, respectively. This directly means important amount of rainfall during these years.

In Figure 4.13b, *CWD* from 2011 to 2100 present a fluctuation between 10-40 wet days. This Figure shows an important variability of wet days under several observed peak (20-45days) which is opposite to results in Figure 4.13a. Average trend of this period indicates an increase of wet days which assume that rainfall intensity will be more persistent in future.

4.7.2. Annual total wet-day precipitation (*PRCPTOT*)

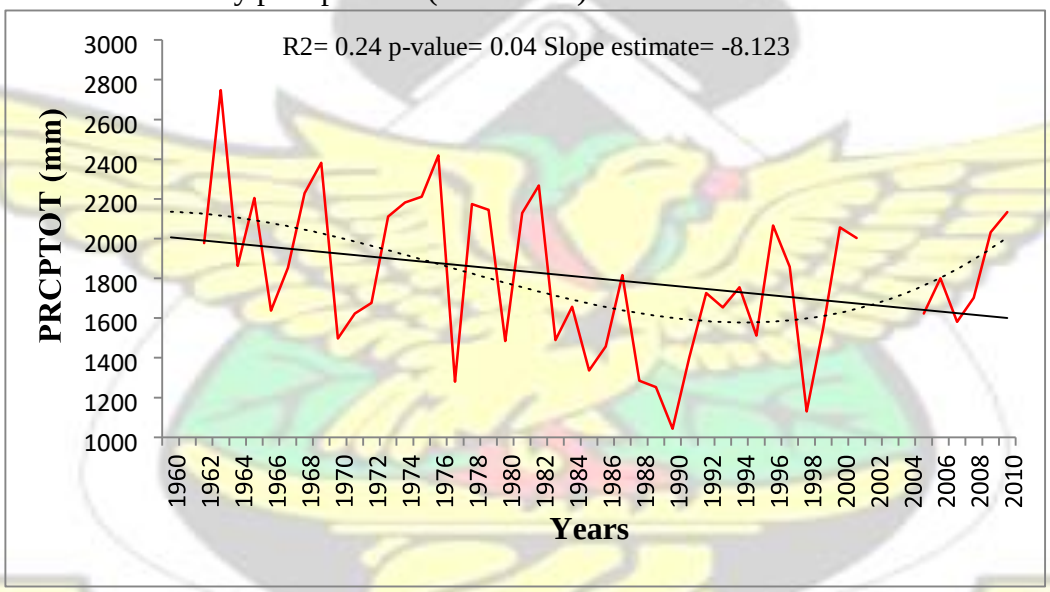


Figure 4.14a: Annual total wet-day precipitation (*PRCPTOT*) from 1960 to 2010

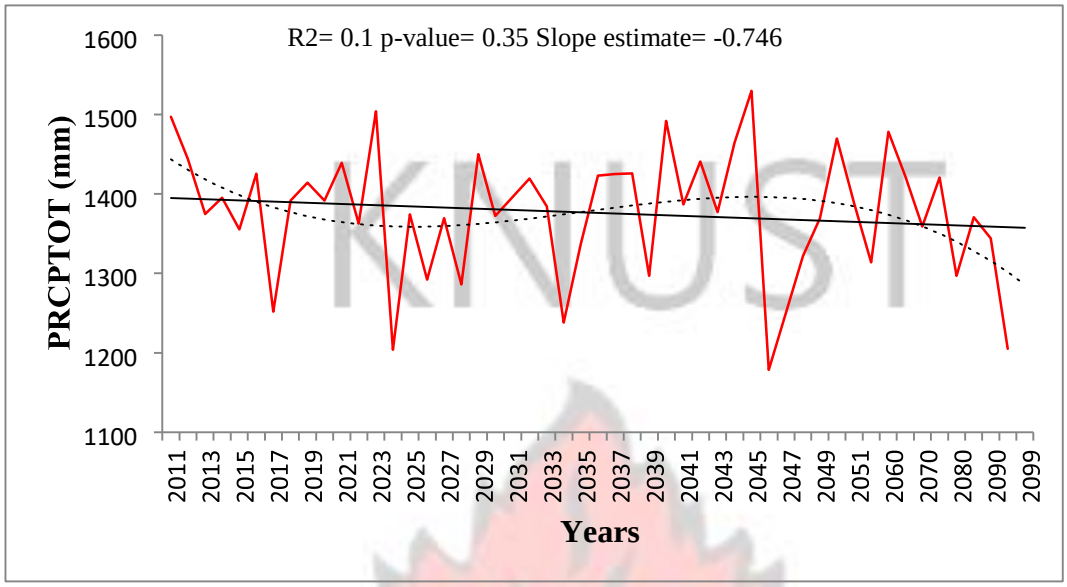


Figure 4.14b: Annual total wet-day precipitation (*PRCPTOT*) from 2011 to 2100

The result of Annual total wet-day precipitation (*PRCPTOT*) index from 1960 to 2010 in Figure 4.14a was characterised by a general downward trend with a decline amount of *PRCPTOT* from 2900-1000 mm during the period 1960-1990. Followed by an upward trend of *PRCPTOT* (10002200 mm) from 1990 to 2010 (Figure 4.14a). *PRCPTOT* result is very significant (p-value=0.04 <

0.05) from 1960 to 2010. However, in Figure 4.14b representing the same index from 2011 to 2100, there was a difference compared to previous in Figure 4.14a. The overall range of *PRCPTOT* (1000-1500 mm) was slightly lower than *PRCPTOT* from 1960 to 2010. However, *PRCPTOT* fluctuation in 2011-2100 is more pronounced and reveals a short decrease of *PRCPTOT* from 2011 to 2030 followed by an increase of the same index from 2030 to 2045 and finally a decrease from 2045 to 2100 (Figure 4.14b). The overall trend of this period shows an insignificant downward trend of *PRCPTOT* while in Figure 4.14a (1960-2010) there was an important decrease of *PRCPTOT*.

4.7.3. Number of heavy precipitation days (*R10*)

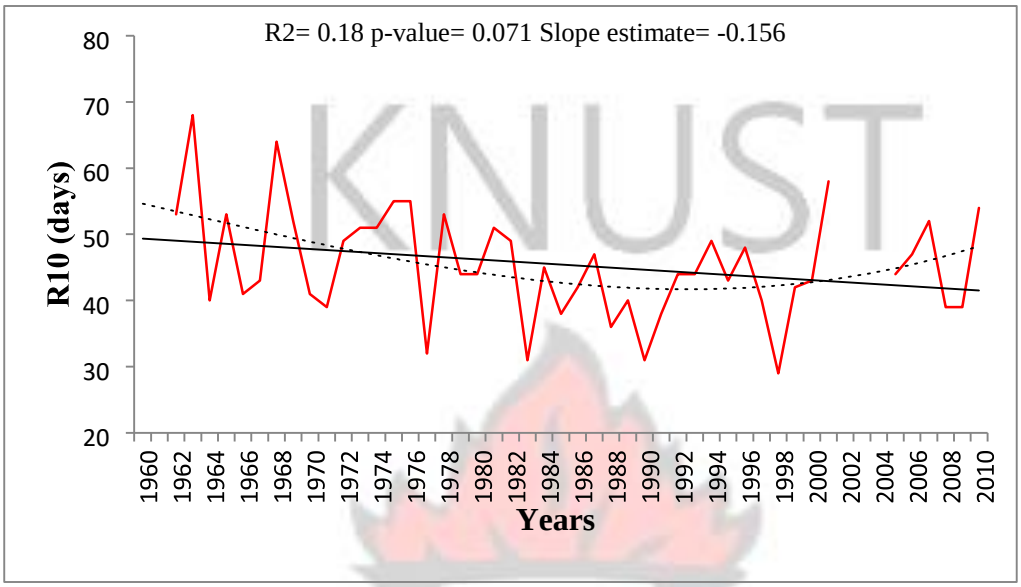


Figure 4.15a: Number of heavy precipitation days (*R10*) from 1960 to 2010

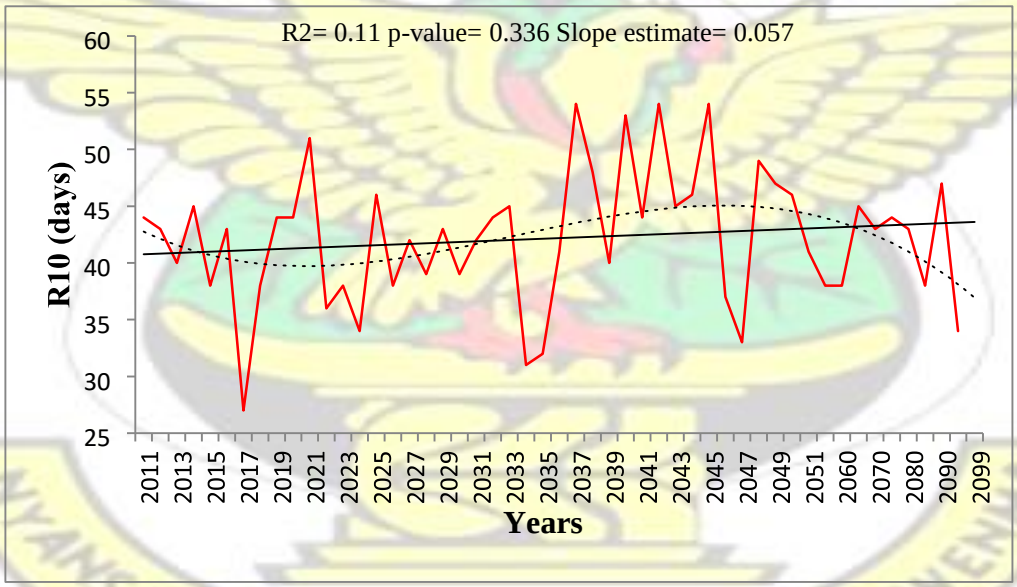


Figure 4.15b: Number of heavy precipitation days (*R10*) from 2011 to 2100

The number of heavy precipitation days over 10 mm (*R10*) index in Abidjan District show opposite trends from 1960 to 2010 (Figure 4.15a) and 2011 to 2100 (Figure 4.15b). In Figure 4.15a, general

tendency trend of *R10* present a decrease trend from 1960 to 2010. First of all, a medium decline of *R10* from 1960 to 1990 between 60-30 days was observed. Then, secondly from 1995 to 2010, the curve shows a resumption of *R10* between 42–50 days. Inversely, *R10* index from 2011 to 2100 increase based on the general observe trend (Figure 4.15b). Hence, *R10* index reached the most important peak from 2030 to 2045 with 52-54 days.

This index *R10* under present and future condition indicated that rainy days over 10 mm started increasing from 1995 to 2010 and will continue until 2100. This can be an explanation for the current heavy precipitation days

4.7.4. Number of very heavy precipitation days (*R20*)

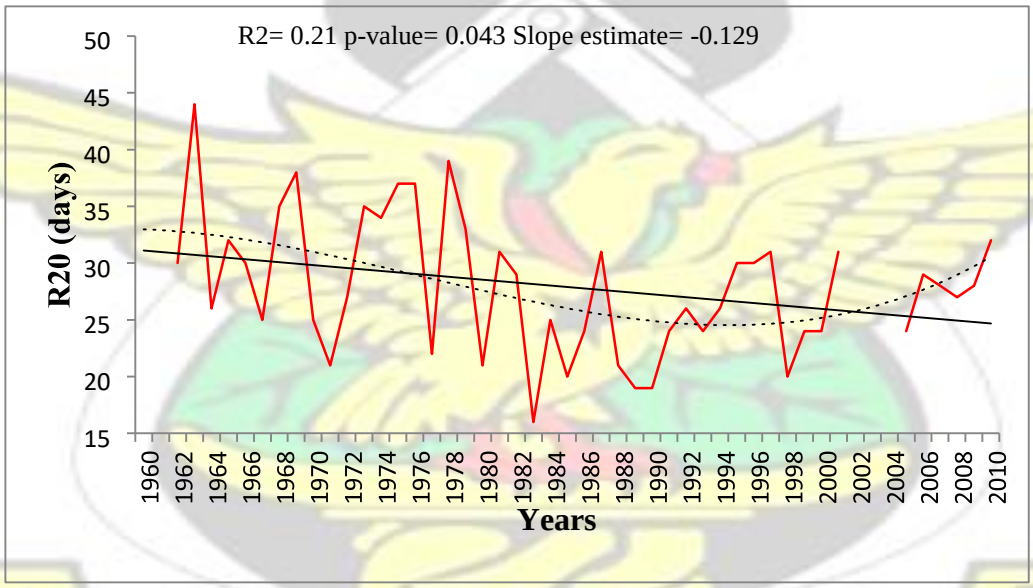


Figure 4.16a: Number of very heavy precipitation days (*R20*) from 1960 to 2010

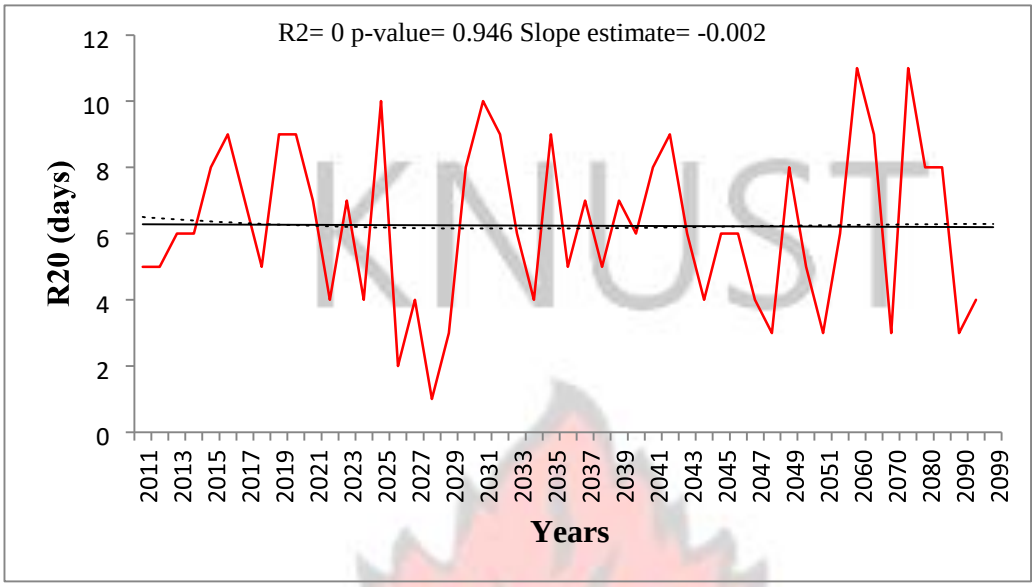


Figure 4.16b: Number of very heavy precipitation days (*R20*) from 2011 to 2100

The number of very heavy precipitation days over 20 mm (*R20*) index in Abidjan District also shows opposite trends between 1960-2010 (Figure 4.16a) and 2011-2100 (Figure 4.16b). From 1961 to 2010, the number of very heavy precipitation days over 20 mm (*R20*) show a decrease trend (Figure 4.16a). But, two (2) periods were distinguished: a decrease of *R20* from 1961 to 1995 between 43-18 days, followed by an increase of the same index between 18-25 days especially from 1995 to 2010. *R20* index result was very significant (p-value=0.043 < 0.05) from 1960 to 2010. While in Figure 4.16b, this *R20* index, average trend is constant means no decrease or increase from 2011 to 2100. However, the amount of *R20* during this period will be too small (010 days) compared to baseline *R20* (10-45 days) and means that *R20* index will be minimal in future (2011-2100).

4.7.5. Number of days above 25 mm (*Rnn*)

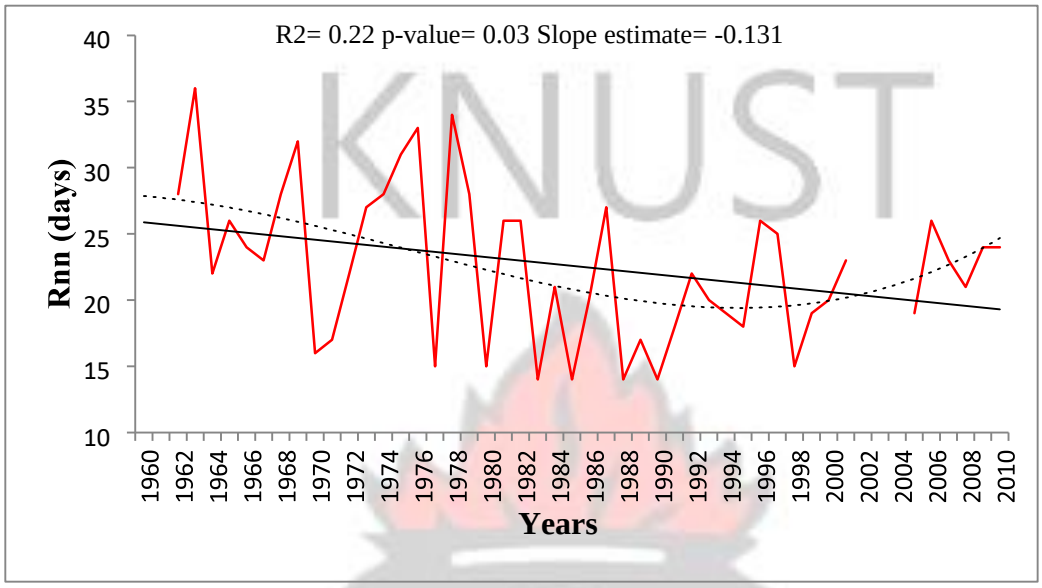


Figure 4.17a: Number of days above 25 mm (*Rnn*) from 1960 to 2010

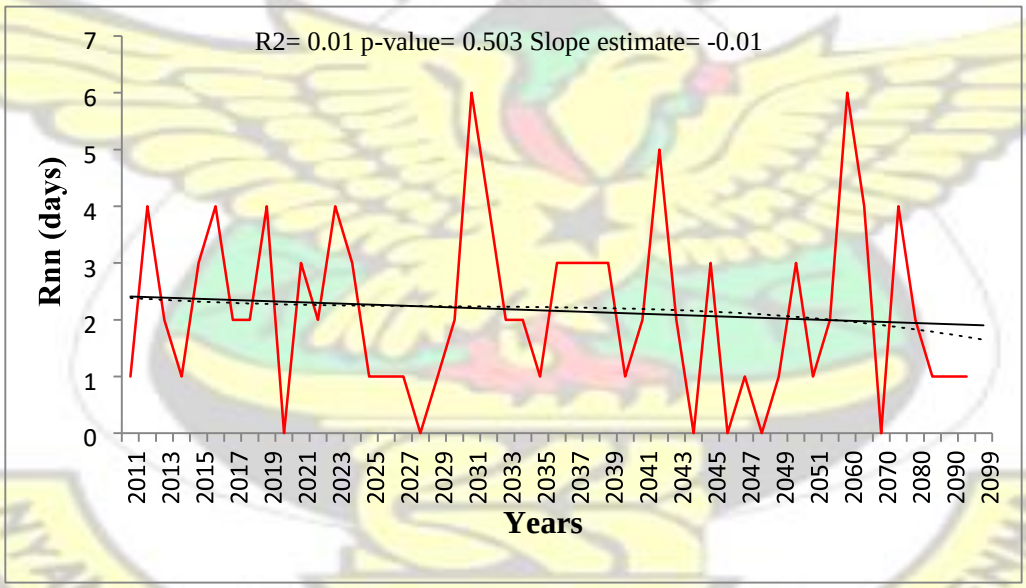


Figure 4.17b: Number of days above 25 mm (*Rnn*) from 2011 to 2100

From 1961 to 2010, the trend of the number of days above index 25 mm (*Rnn*) generally declined in Figure 4.17a. But as *R20* two big periods were characterised in *Rnn* index: a decrease number of

days above 25 mm (*Rnn*) from 1961 to 1995 between 5-40 days, followed by a rise of *Rnn* between 15-25 days especially from 1995 to 2010. *Rnn* index like *PRCPTOT* and *R20* result is very significant (p-value=0.03 < 0.05) from 1960 to 2010. This same index *Rnn* in Figure 4.17b showed a slight decrease from 2011 to 2100 and its range will be too small (0-6 days) compared to baseline *Rnn* range (10-45 days). The significance of *Rnn* index results could support heavy precipitation observed nowadays based on *Rnn* increase from 1995 to 2010.

4.7.6. Very wet days (*R95p*)

Very wet days (*R95p*) index from 1960 to 2010 is presented in Figure 4.18a. There was a general decrease trend from 1961 to 1995 of *R95p* with important fluctuation between 1000-40 mm. Then, a rise of this *R95p* index is identified (30-1000 mm) from 1995 to 2010. While *R95p* index trend from 2011 to 2100 in Figure 4.18b also present an overall decrease with a range (400-50 mm) less than *R95p* range (100-1000 mm) from 1960 to 2010.

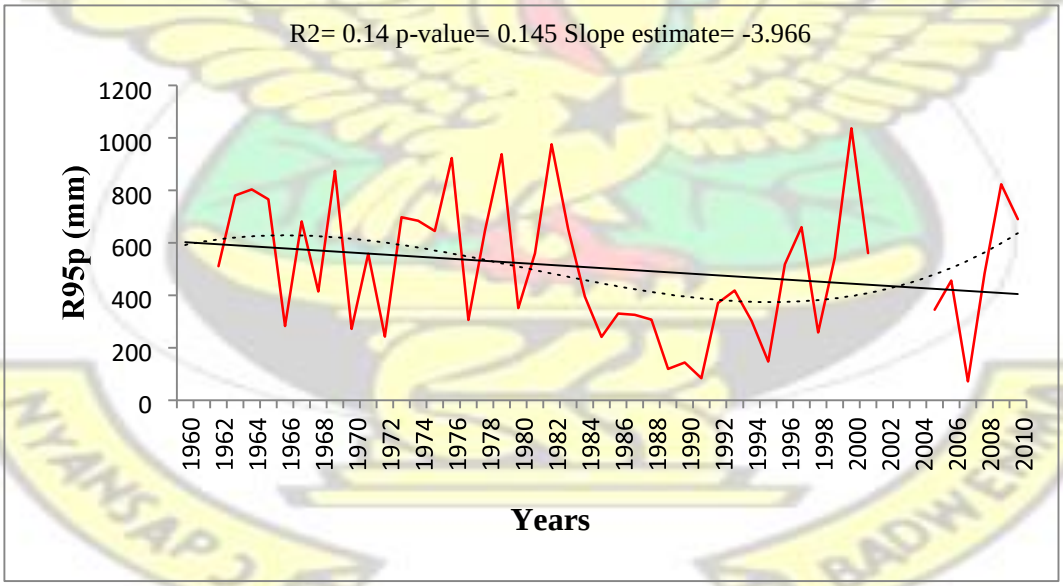


Figure 4.18a: Very wet days (*R95p*) from 1960 to 2010

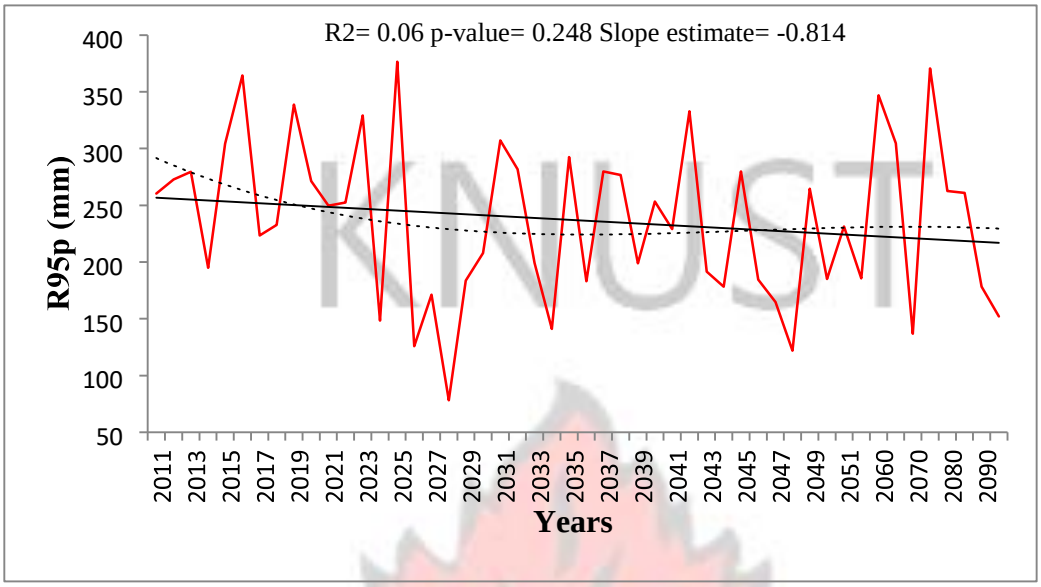


Figure 4.18b: Very wet days (*R95p*) from 2011 to 2100

4.7.7. Extremely wet days (*R99p*)

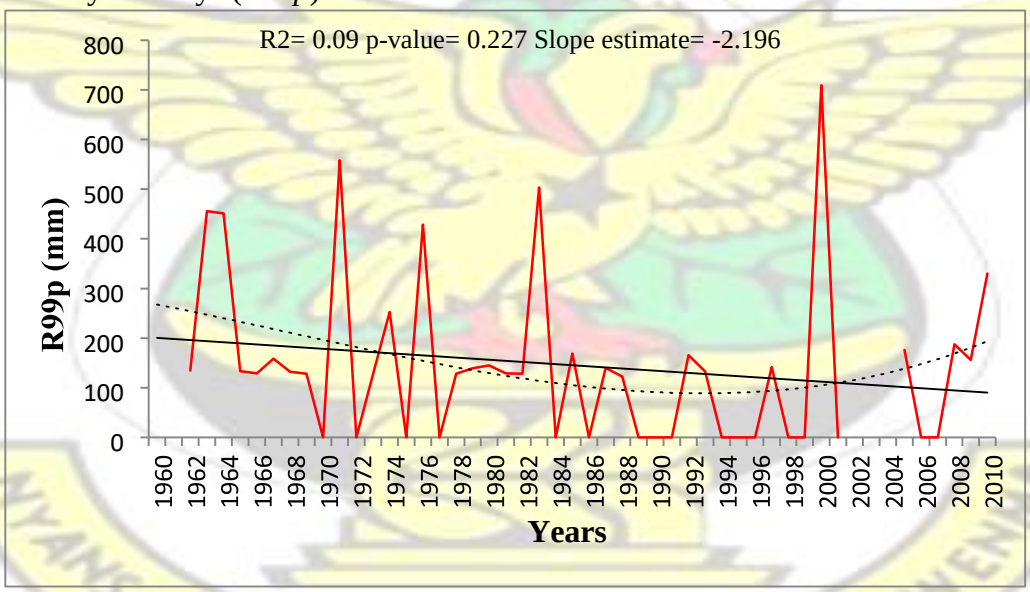


Figure 4.19a: Extremely wet days (*R99p*) from 1960 to 2010

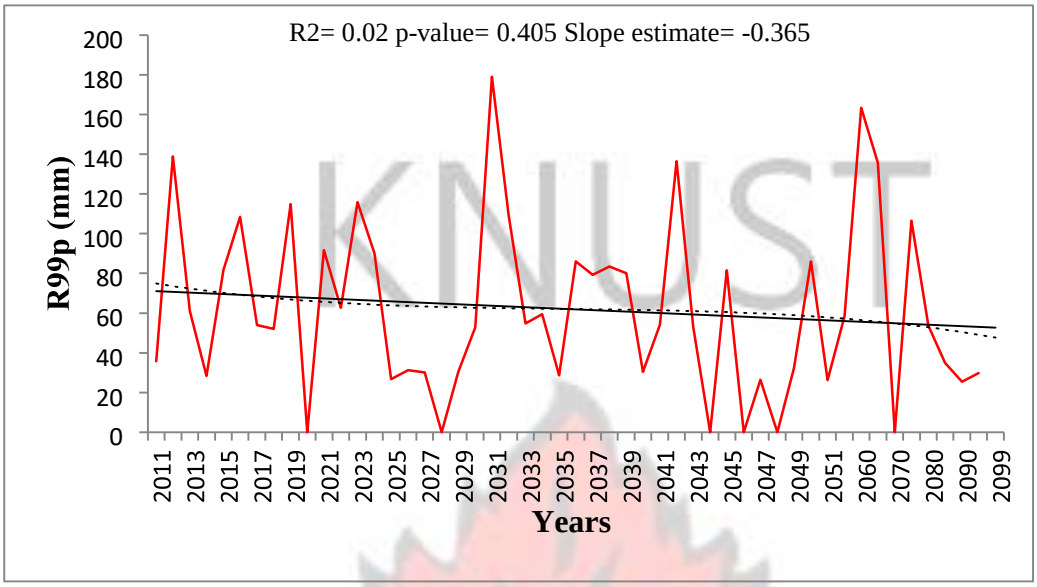


Figure 4.19b: Extremely wet days (*R99p*) from 2011 to 2100

In Figure 4.19a, the amount of *R95p* was different compared to extremely wet days (*R99p*) though there was some similarity from 1960 to 2010. Indeed, there was a negative trend of R99p from 1961 to 1995 with fluctuation between 0-560 mm, followed by a positive trend from 0-700 mm during the period 1995-2010. Regarding Figure 4.19b, *R99p* index from 2011 to 2100 present a negative trend and was not so important (0-200 mm) compared to *R99p* (0-700 mm) from 1960 to 2010. Both Figures showed a negative trend of extremely wet days (*R99p*).

4.7.8. Maximum 1-day precipitation amount (*RX1day*)

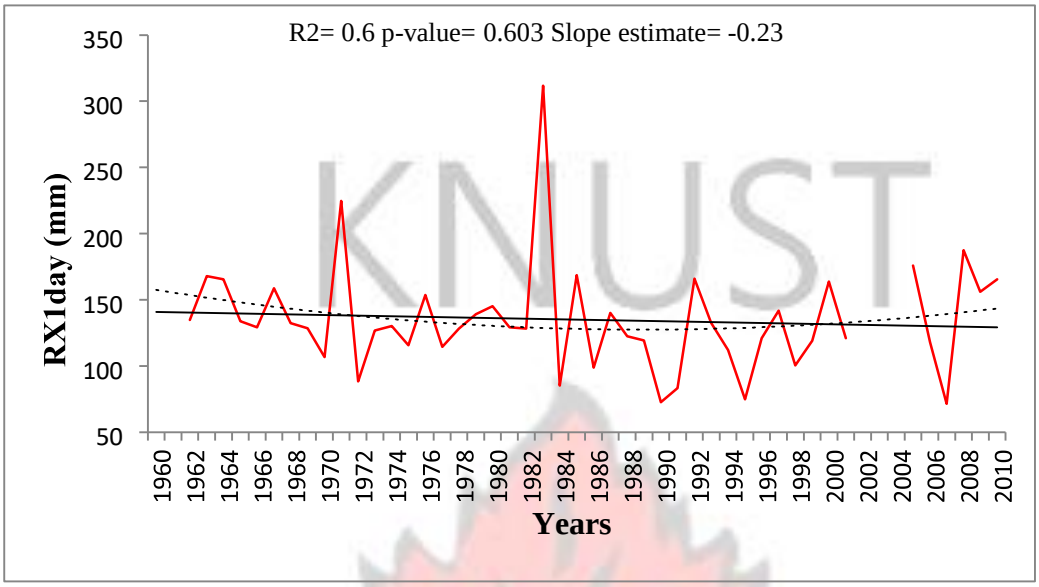


Figure 4.20a: Maximum 1-day precipitation amount (*RX1day*) from 1960 to 2010

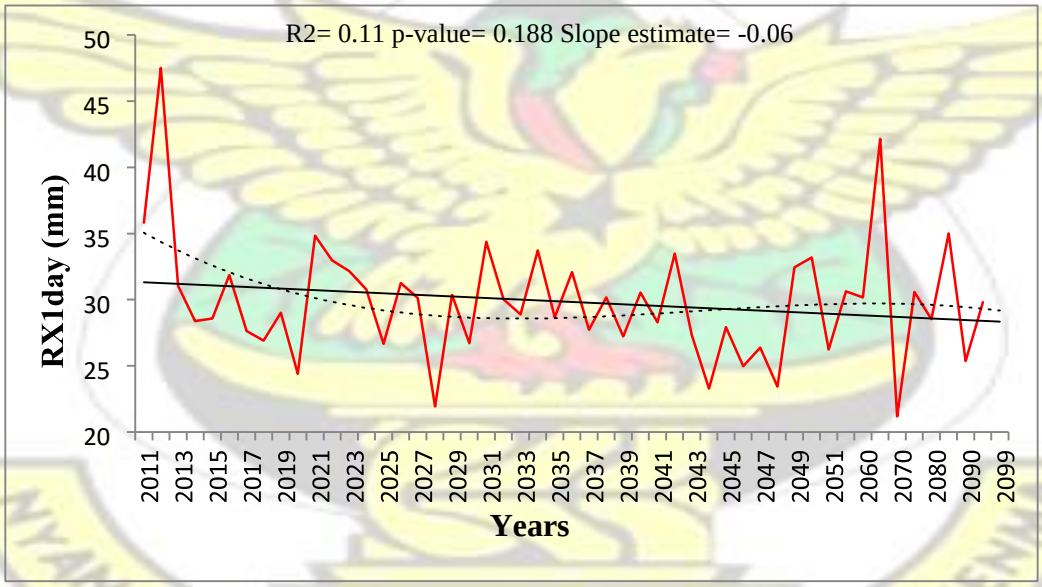


Figure 4.20b: Maximum 1-day precipitation amount (*RX1day*) from 2011 to 2100

Maximum 1-day precipitation amount (*RX1day*) index result showed a general negative trend between 1960-2010 (Figure 4.20a) and 2011-2100 (Figure 4.20b). There was an insignificant decrease of Maximum 1-day precipitation amount (*RX1day*) from 1960 to

1995, following a short rise of *RX1day* from 1995 until 2010 (Figure 4.20a). This slight general decrease trend from 1960 to 2010 fluctuated between 0-200 mm of water/decade with two exceptions made in 1972 and 1983 with the highest *RX1day* peak of 230 mm and 310 mm respectively.

This *RX1day* index result from 2011 to 2100 is shown in Figure 4.20b. There was an overall negative trend with fluctuation between 0-50 mm of water/decade from 2011 to 2100. However, it was observed that during the period of 2011-2100, *RX1day* reached the highest peak in 2014 with 48 mm of water/decade which is an indicator of extreme rainfall occurrence.

4.7.9. Maximum 5-day precipitation amount (*RX5day*)

Maximum 5-day precipitation amount (RX5day) index results showed a general negative trend between 1960-2010 (Figure 4.21a) and 2011-2100 (Figure 4.21b). The plotted result in Figure 4.21a reflects changes of Maximum 5-day precipitation amount from 1960 to 2010. There was a downward trend of RX5 day characterised by a reduction of RX5day from 350 to 100 mm of water/decade excepted in 2000 where it was noted the highest RX5 day rate 460 mm.

RX5 day index from 2011 to 2100 (Figure 4.21b) has a similar decrease trend in Figure 4.21a. However, difference was identified in fluctuation range which was between 50-150 mm of water/decade.

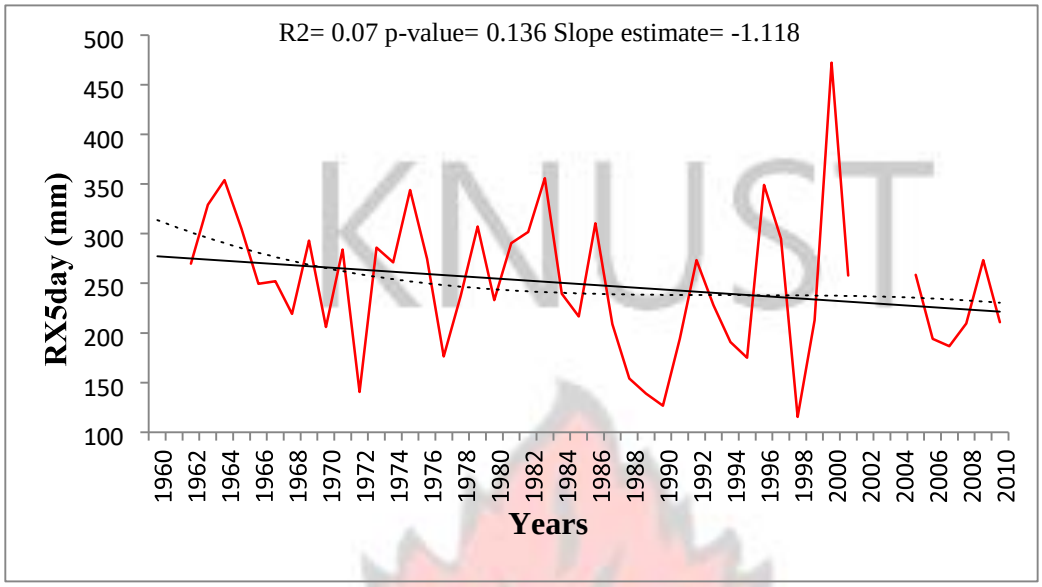


Figure 4.21a: Maximum 5-day precipitation amount (*RX5day*) from 1960 to 2010

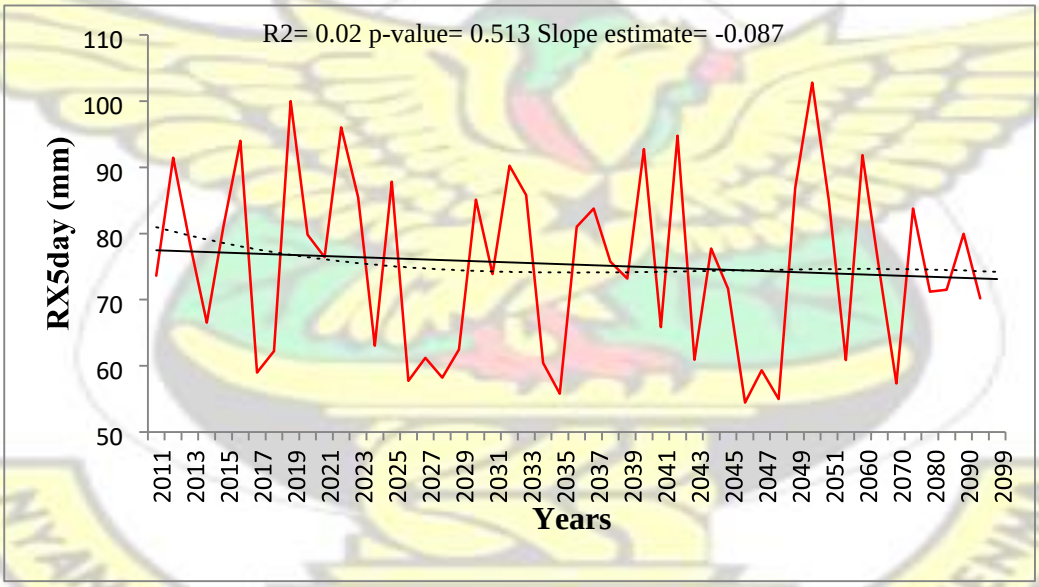


Figure 4.21b: Maximum 5-day precipitation amount (*RX5day*) from 2011 to 2100

4.7.10. Simple daily intensity index (*SDII*)

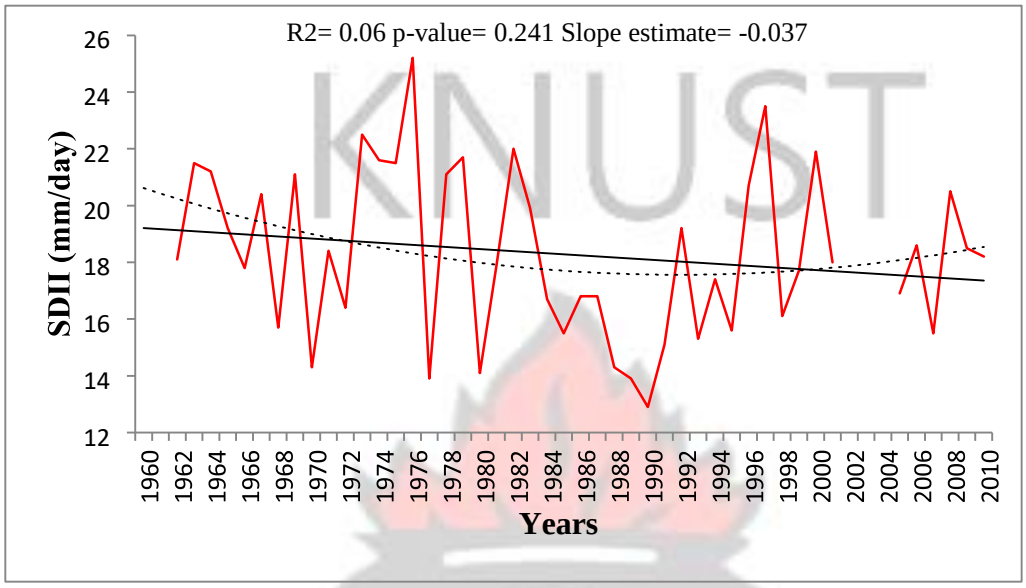


Figure 4.22a: Simple daily intensity index (*SDII*) from 1960 to 2010

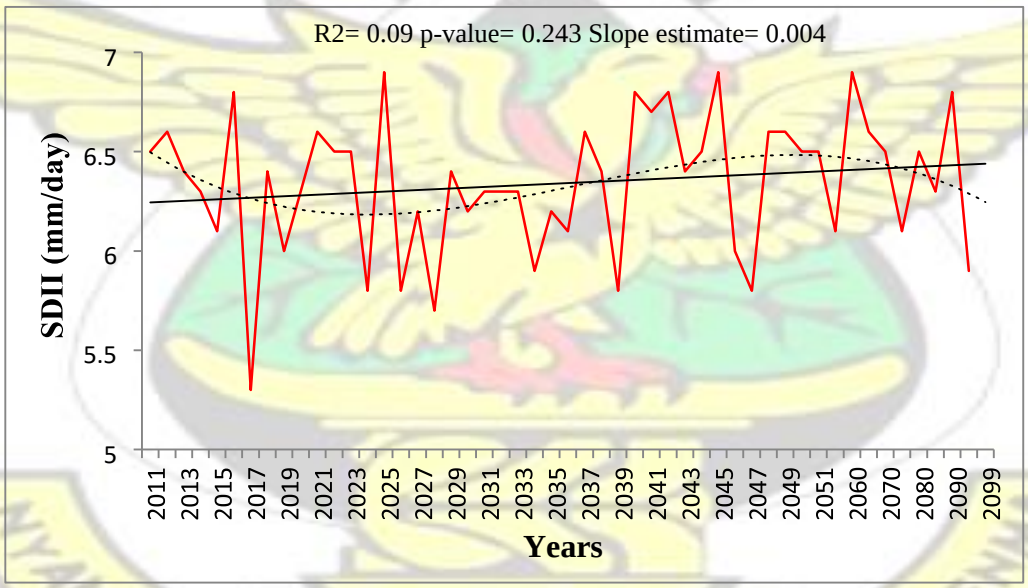


Figure 4.22b: Simple daily intensity index (*SDII*) from 2011 to 2100

Simple daily rainfall intensity (*SDII*) index result showed inverse general trend between 19602010 (Figure 4.22a) and 2011-2100 (Figure 4.22b). Simple daily rainfall intensity (SDII) index decreased

from 1960 to 1990 with an exception of 1975 which recorded the highest intensity index 25 mm/day of that period and after that, there was an increase of *SDII* from 1990 to 2010 and the range was between 18-24 mm/day. Afterwards, *SDII* index present in Figure 4.22b an increase based on general trend from 2011 to 2100. Both Figures 4.22 (a and b) of *SDII* index started by a decrease of intensity and later there was a rise of *SDII* from 1990 to 2010 (Figure 4.22a) and 2030 to 2100 (Figure 4.22b).

In all, ten rainfall indices (10) ((*PRCPTOT, CWD, R10, R20, Rnn, R95p, R99p, RX1day, RX-5day* and *SDII*) were calculated and compared with observed (1960-2010) and future (20112100) data. These rainfall indices showed a general decreased trend of most rainfall indices in present and in future. However, there was an increase trend of *CWD, SDII* and *R10* indices from 2011 to 2100. All indices as negative or positive trends were no significant because P-value was greater than 0.05 excepted *PRCPTOT, R20* and *Rnn* indices from 1960 to 2010 due to their very significant trends (p-value<0.05).

4.8. Analytic Hierarchic Process (AHP) Flood Risk

4.8.1. AHP Hazard map

4.8.1.1. Drainage density map

The drainage density map (Figure 4.23) includes five (5) classes (Table 4.10) to characterise the state of the drainage of surface water in Abidjan. It was observed that very low and low classes represent 21.60 % and 23.51 %, respectively. Then medium class covers 21.36 % followed by high and very high classes which were estimated to be 21.99 % and 11.53 %, respectively. It was noted that, the drainage density was generally low throughout the study area (around 67 %), which implies a low permeability and infiltration of the study area.

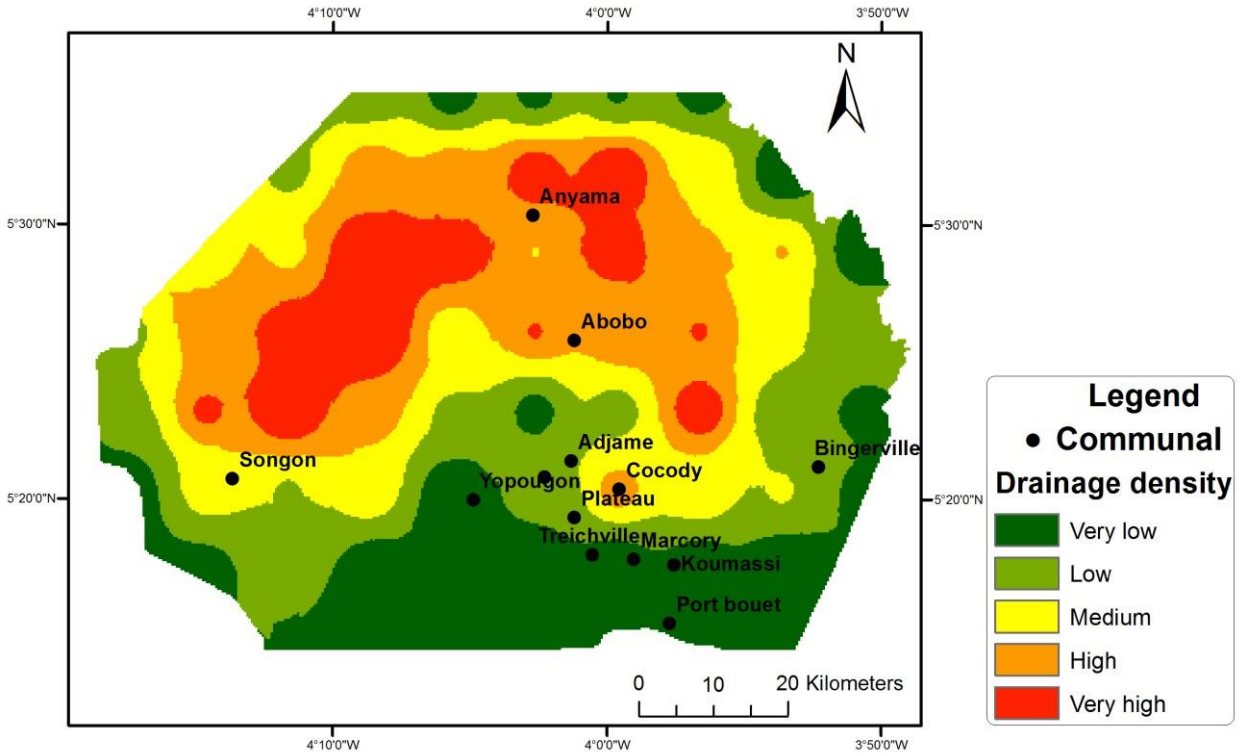


Figure 4.23: Drainage density map

Table 4. 10: Weight assigned to "drainage density" classes

Classes (km^2)	Weight
0.42 – 4.95	9
4.95 – 8.45	8
8.45 – 11.65	5
11.65 – 14.50	3
≥ 14.50	1

4.8.1.2. Slope map

The slope map extract from Aster DEM of the study area is shown in Figure 4.24. It is composed of five (5) classes (Table 4.11) which allow a clear understanding of the topography of the study area. After accomplishment, it was observed that very low and low classes covered 36.76 % and 30.19

% of the study area, respectively. Then, medium class covered 20.22 % followed by high and very high classes which were estimated to cover 9.85 % and 2.98 %, respectively. On the whole, Abidjan is covered by low slopes (87.17 % of the study area), which implies a favourable area as bed for extreme events such as flood.

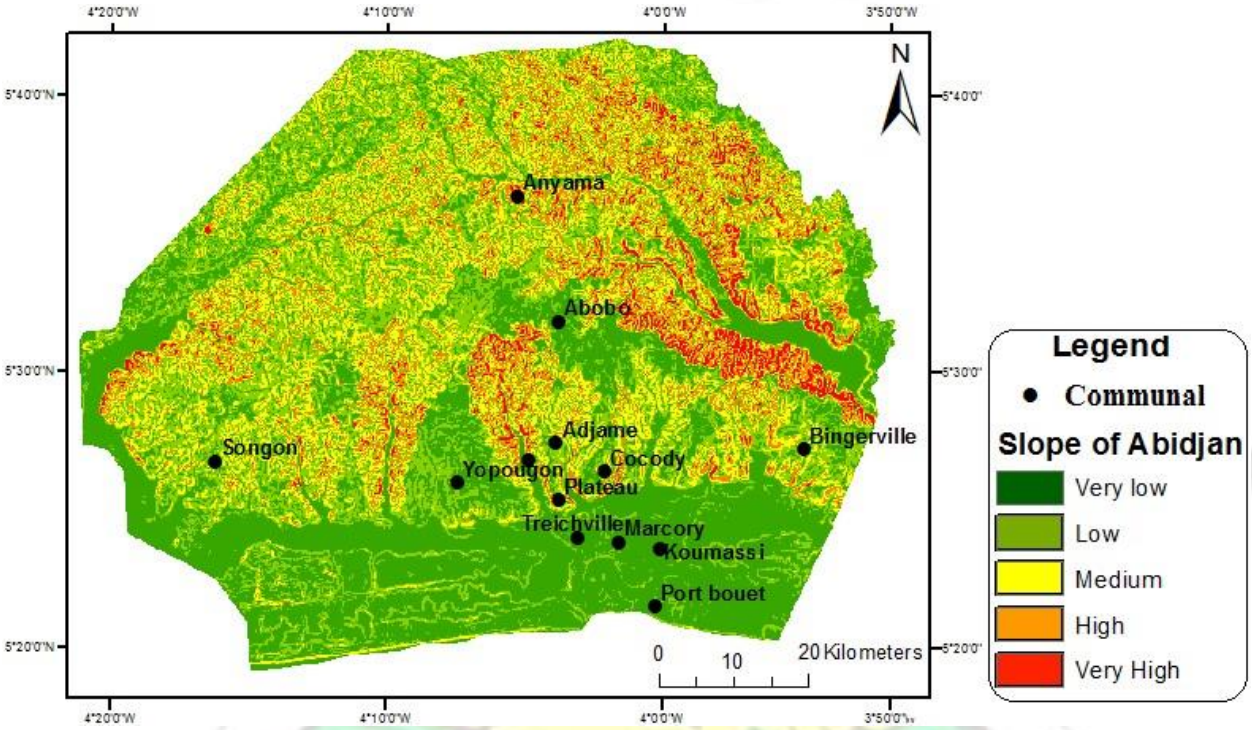


Figure 4.24: Slope map of Abidjan

Table 4. 11: Weight assigned to "Slope" classes

Classes (%)	Weight
0 _ 2	10
2 – 6	8
6 – 10	6
10 – 16	3
≥ 16	1

4.8.1.3. Soil type map

The soil type map extracted from national soil map and validated by soil profile and analysis during a field work within the study area is shown in Figure 4.25. Seven (7) classes were identified (Table 4.12) and used to describe the soil type in the study area: hydromorph organic soil (6.64 %), hydromorph mineral soil (2.7 %), ferralitic soil depleted modal strongly desaturated (57.30 %), ferralitic soil reshuffles depleted shale's highly desaturated (15.23 %), tertiary sand (9.66 %) and lagoon (8.47 %), respectively. Analysis showed that, eight (8) municipalities of Abidjan District were part of ferralitic soil depleted modal strongly desaturated class and four (4) municipalities were recovered by tertiary sand class. Both type of soil indicated and implies a low permeability and infiltration of the study area.

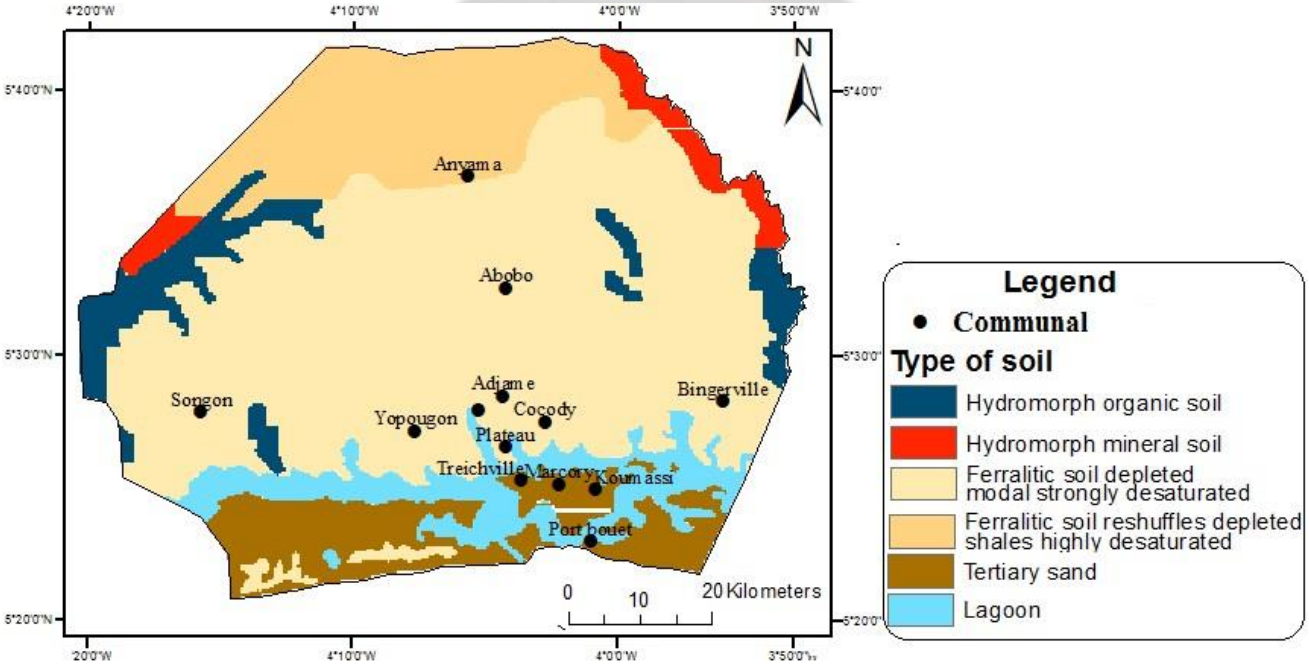


Figure 4.25: Soil type map of Abidjan

Table 4. 12: Weight assigned to "Soil type" classes

Classes	weight
Hydromorph organic soil	8
Hydromorph mineral soil	6
Ferralitic soil depleted modal strongly desaturated	3
Ferralitic soil reshuffles depleted shale's highly desaturated	1
Tertiary sand	2
Lagoon	0

4.8.1.4. Isohyet map

The rainfall variability over the years 1961-1970, 1971-1980, 1981-1990, 1991-2000 and 20002012 was strongly influenced by the overall rainfall decline recorded since 1970 in Côte d'Ivoire (Figure 4.26). This reflects the great heterogeneity in the spatio-temporal distribution of the annual rainfall during these periods.

Rainfall ranged from:

• 1850 mm and 2800 mm during the period of 1961-1970;

• 1500 mm and 2450 mm during the period of 1971-1980;

• 1000 mm and 2300 mm during the period of 1981-1990,

• 1100 mm and 2100 mm during the period of 1991-2000

• 1250 mm and 2150 mm in the period of 2000 - 2012

-From 1961 to 1970, it was noticed that, Abidjan received a total rainfall between 1850-2800 mm and the rainfall increased from west to east (Figure 4.26a).

-From 1971 to 1980, Abidjan received a total amount of rainfall between 1500-2450 mm and still increased from west to east (Figure 4.26b).

-During the period 1981-1990, there was a decrease in total rainfall between 1000 mm and 2300 mm. It was noticed that, rainfall increases from west to east (Figure 4.26c).

-From 1991 to 2000, there was a slight reduction in rainfall amount compared to the previous period. This reduction occurred more in the Western part of Abidjan with rainfall between 11001400 mm. The north and south of the District were covered by 1800-2100 mm of rainfall and that was substantially lower as compared to the previous period (Figure 4.26d).

-From 2001 to 2012, there was also a significant recovery of the total rainfall 1250 mm-2100 mm and was more pronounced in the northern part of the District. However, there was a resumption of total rainfall from the Centre to South of Abidjan (1250-1900 mm). This period was nearly similar to the previous period (Figure 4.26e).

The entire District of Abidjan was characterised by a slightly homogeneous total rainfall distribution. This was due to the presence of the sea which influences the hydrological behaviour but also, Abidjan is a highly urbanised area and therefore has low vegetation cover.

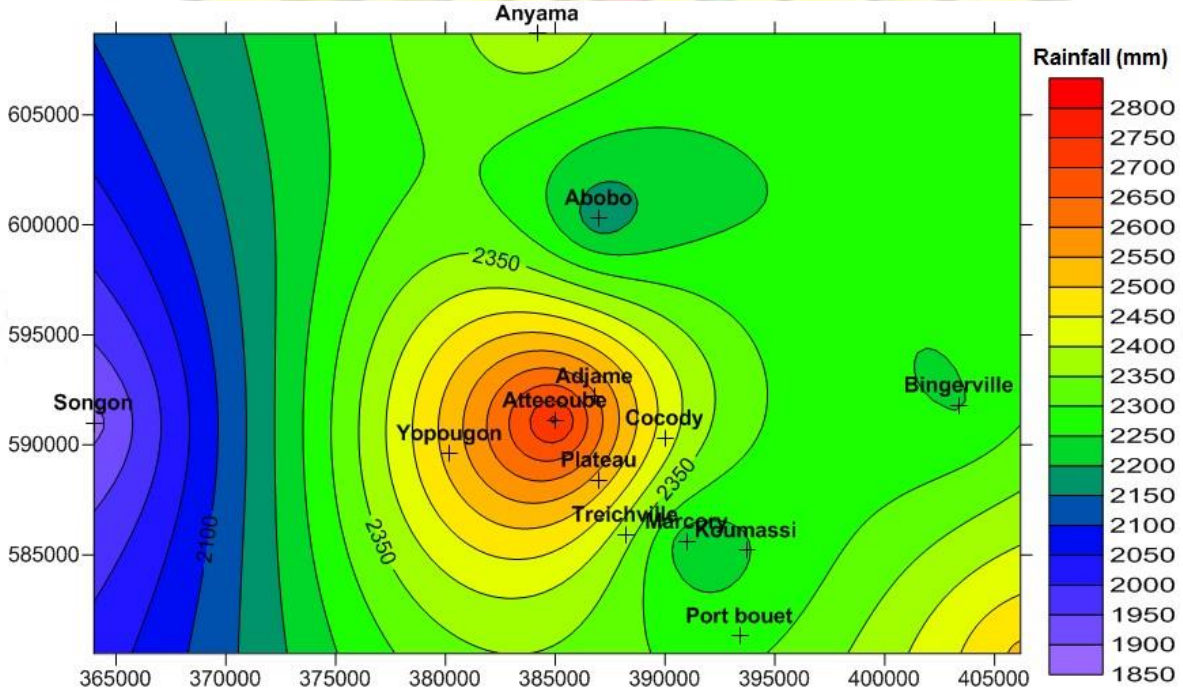


Figure 4.26a: Rainfall variability in Abidjan from 1961-1970

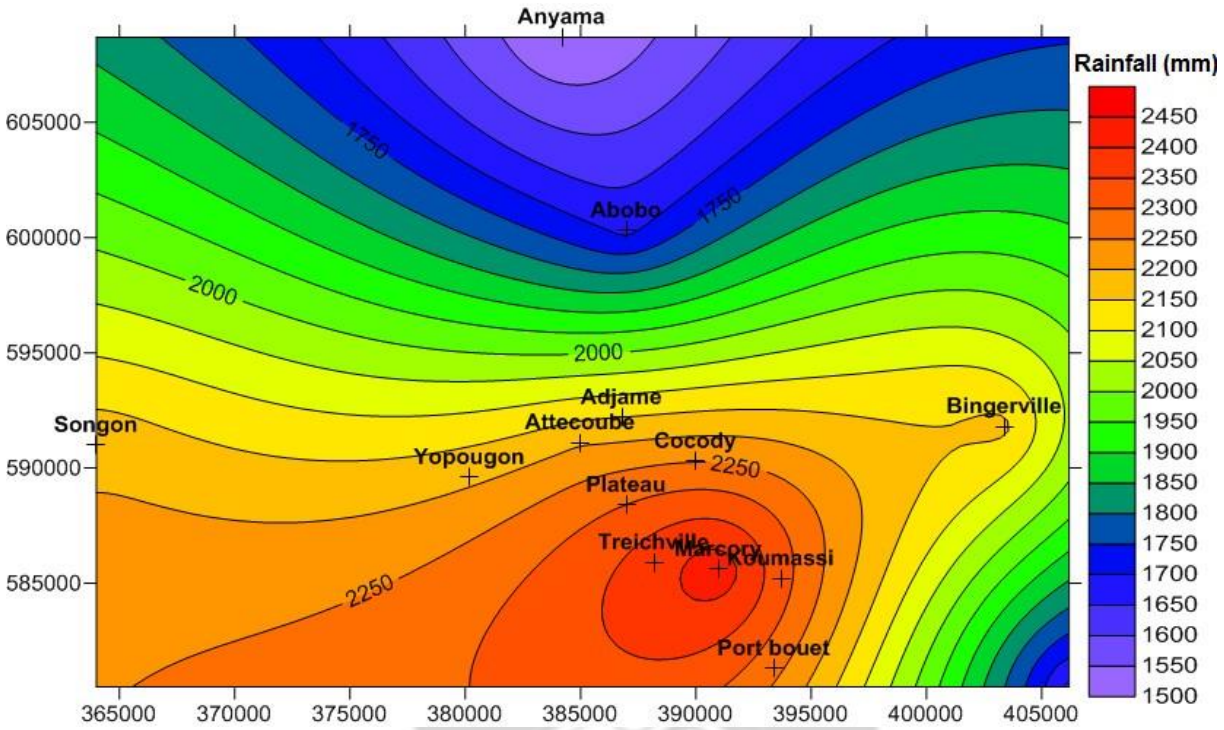


Figure 4.26b: Rainfall variability in Abidjan from 1971-1980

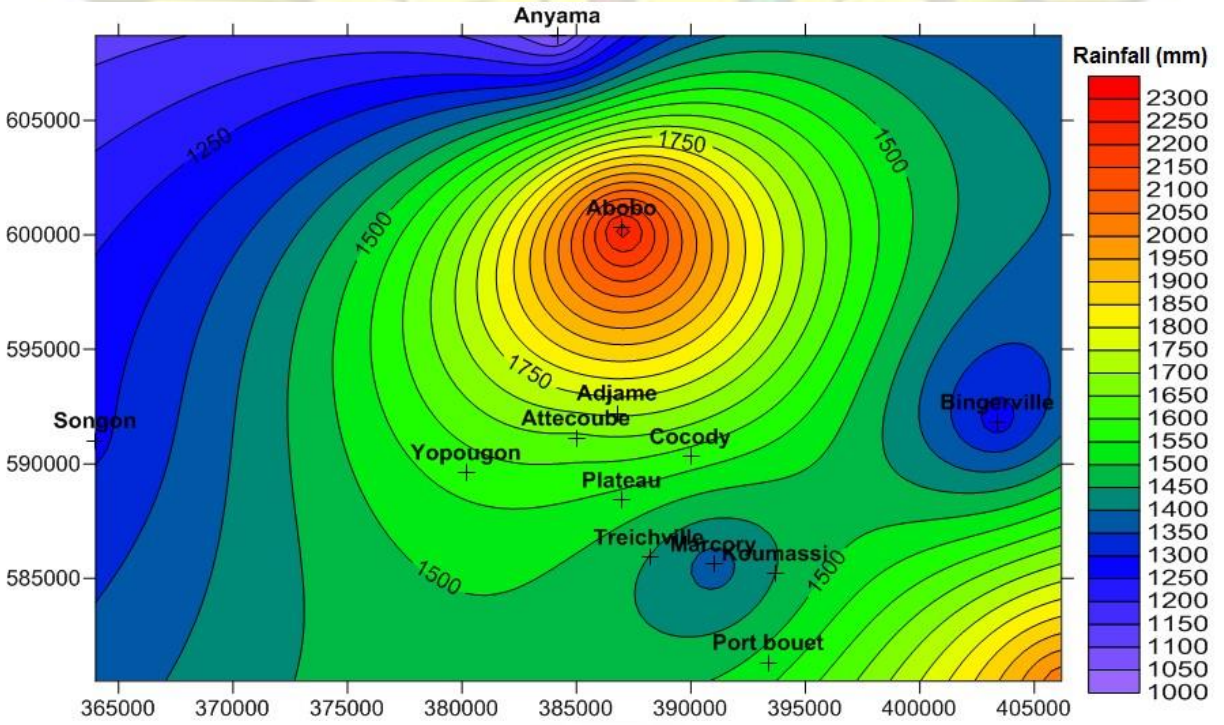


Figure 4.26c: Rainfall variability in Abidjan from 1981-1990

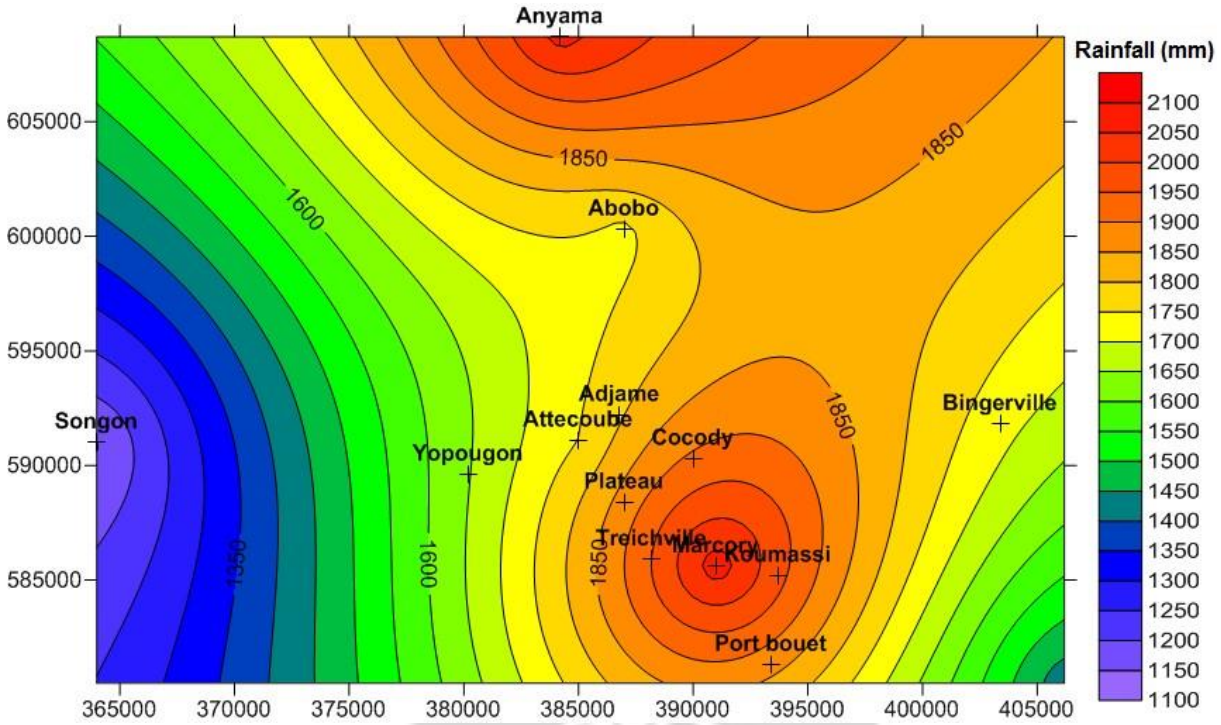


Figure 4.26d: Rainfall variability in Abidjan from 1991-2000

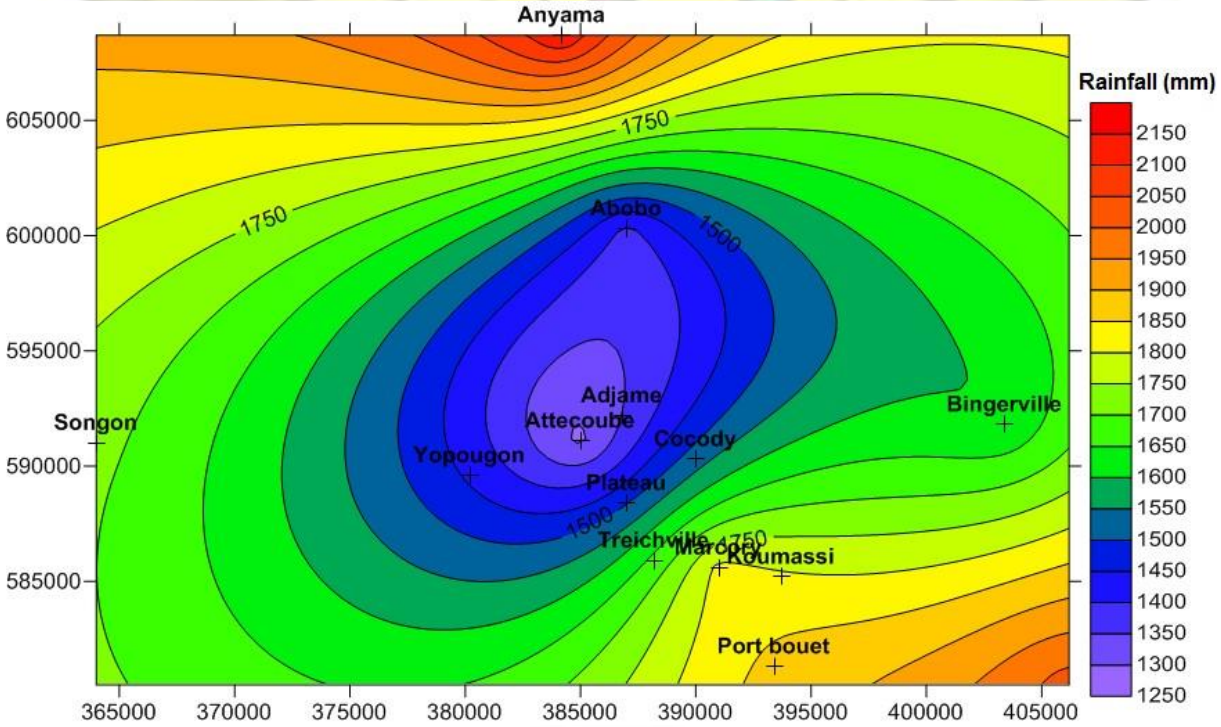


Figure 4.26e: Rainfall variability in Abidjan from 2001-2012

In Figure 4.27 and Table 4.13, the generated Isohyet map described five (5) classes which characterise annual amount and occurrence of precipitation in Abidjan. Very low and low classes were covered by 48.55 % and 17.97 %, respectively. Then, medium class were also covered by 13.4% while high and very high classes were estimated to cover 15.43 % and 4.64 %, respectively. Annual rainfall spatio-temporal distribution density is generally moderate throughout the study area (around 34 %). However, nine out of thirteen (9/13) municipalities of the District were covered by medium to very high amount of precipitation.

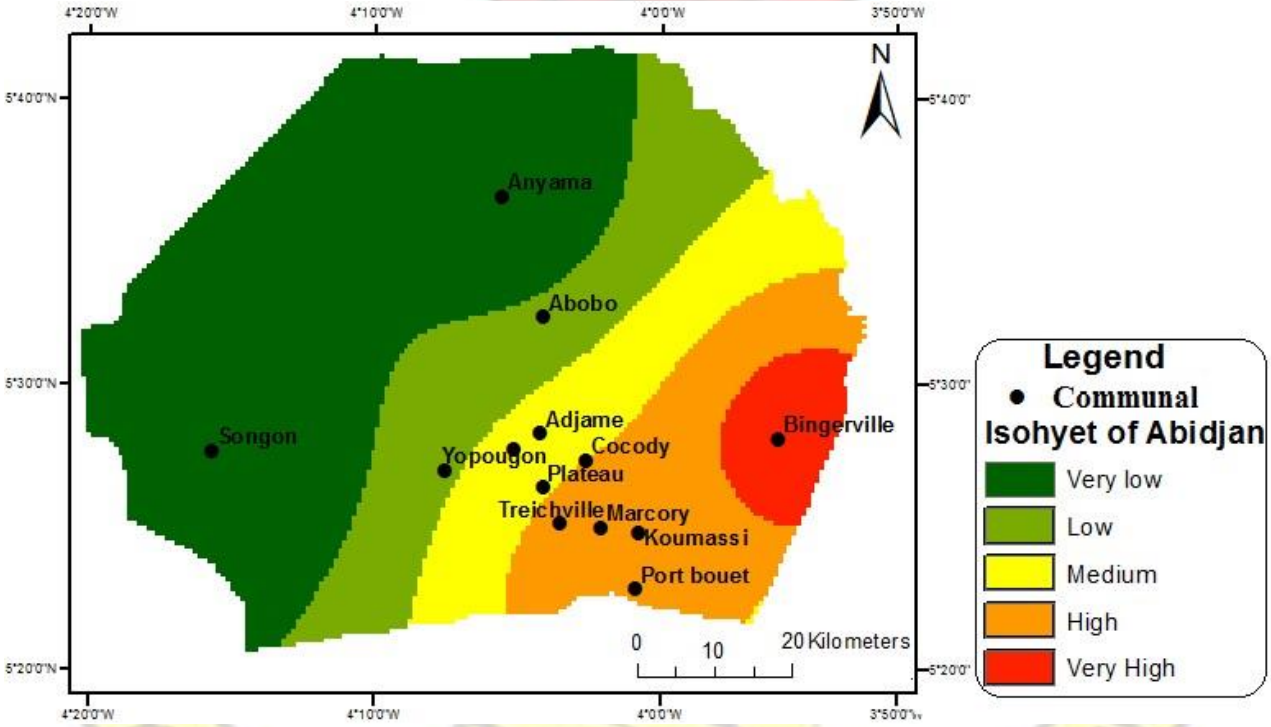


Figure 4.27: Isohyet map of Abidjan

Table 4. 13: Weight assigned to "Isohyet" classes

Classes(mm)	weight
1590 - 1640	1
1640 - 1690	3
1690 - 1750	7
1750 - 1790	9
$\geq$ 1790	10

4.8.1.5. Hazard map

The hazard map (Figure 4.28) is obtained by the combination of parameter maps drainage density (Dd), type of soil (TS), rainfall (I) and slope (S). The calculation process was done using "raster calculator" in spatial analyst tool within ArcGIS and it is defined by the following equation 4.1:

$$Hazard = 0.26S + 0.13Dd + 0.53I + 0.08TS \quad (4.1)$$

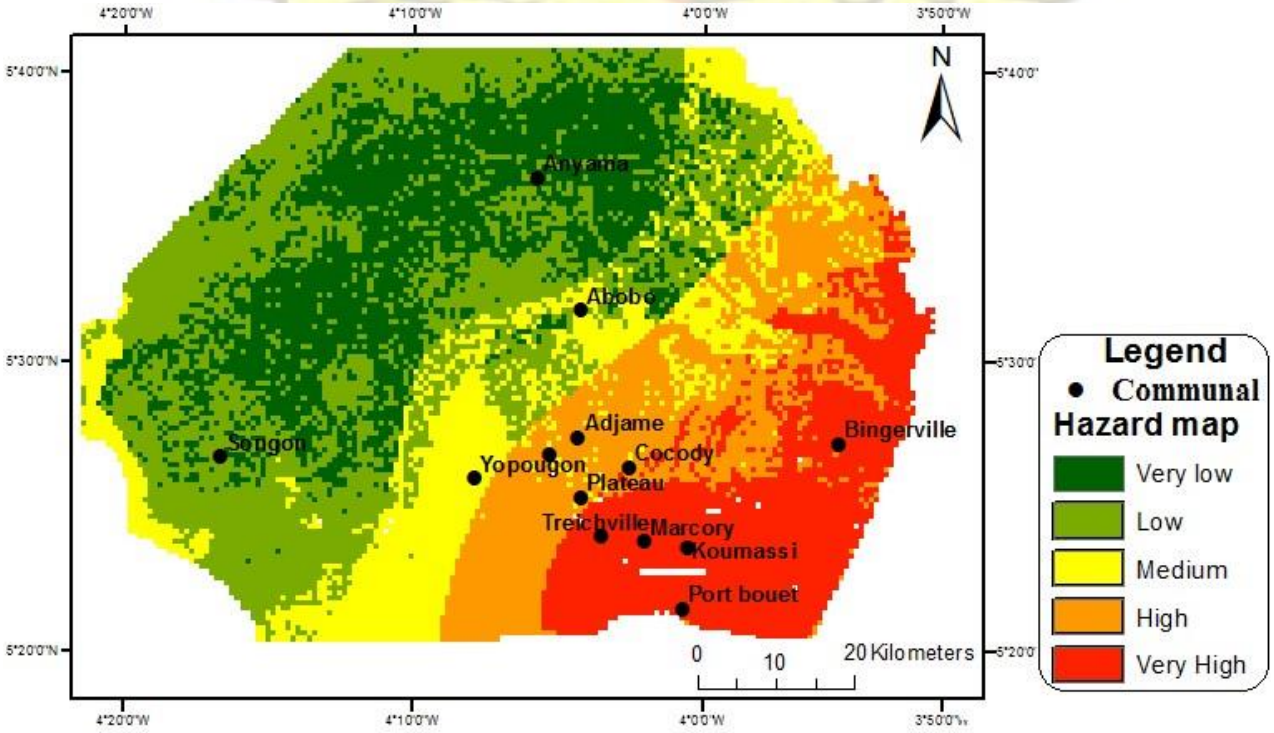


Figure 4.28: Hazard map of Abidjan

The hazard map obtained highlights five (5) areas as shown in Figure 4.28. Very low and low classes covered 22.42 % and 30.67 % respectively of Abidjan. It is essentially over areas with high slope, high drainage density and low precipitation amount. The medium class represents 15.41 % and includes the Yopougon and Abobo municipalities which are classified under high and very high hazard areas. The classes of high and very high hazard are estimated to be 15.34 % and 16.16 % respectively and they cover most of Abidjan municipalities (Adjame, Plateau, Cocody, Treichville, Koumassi, Port-Bouet, marcory, Attecoube and Bingerville) numbering nine out of thirteen (9/13) municipalities. All these areas are within high and very high hazard zones and are dominated by low slope, significant occurrence of rainfall, tertiary sand, ferralitic soil strongly desaturated and low drainage within the Abidjan District.

4.8.2. AHP vulnerability map

4.8.2.1. Population density

In Figure 4.29, population density map shows spatial distribution of the population within Abidjan District. The population density map was classified into five (5) classes (Table 4.14) from very low to very high population density. Areas of very low, low and medium classes cover 15.80 %, 38.64 % and 30.67 %, respectively. While the high and very high classes were estimated to be 11.34 % and 3.5 7%, respectively. Municipalities with more than 400,000 people such as Yopougon, Abobo and Koumassi were classified as areas with very dense population.

KNUST

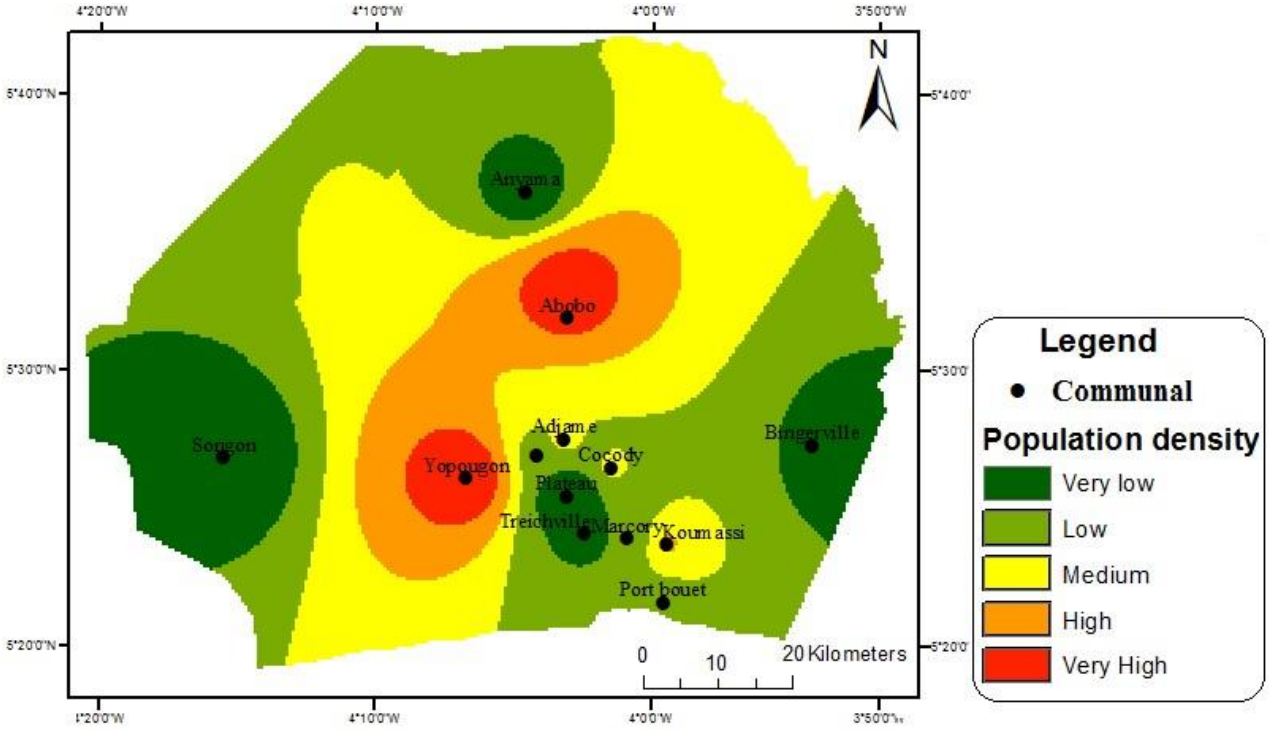


Figure 4.29: Population density of Abidjan

Table 4. 14: Weight assigned to "population density" classes

Classes (Thousand)	Weight
14400 - 220000	1
220000 - 320000	3
320000 - 410000	7
410000 - 573000	9
≥ 573000	10

4.8.2.2. Result of Drainage system

The map in Figure 4.30 provides information on an important parameter of the advent of floods. Presence or absence of drainage system and its dysfunction may be the basis of severe flooding. The different classes obtained from the drainage system density map are five (5) classes (Table

4.15) from very low to very high as follows: very low and low classes 12.32 % and 39.21 %, respectively, medium class 31.40 %. Then, high and very high classes are 14.49 % and 2.57 %, respectively. Areas covered by very low and low drainage system represents more than half of the area with 51 % of the total study area and this shows that, the study area presents a deficit of sewer system network.

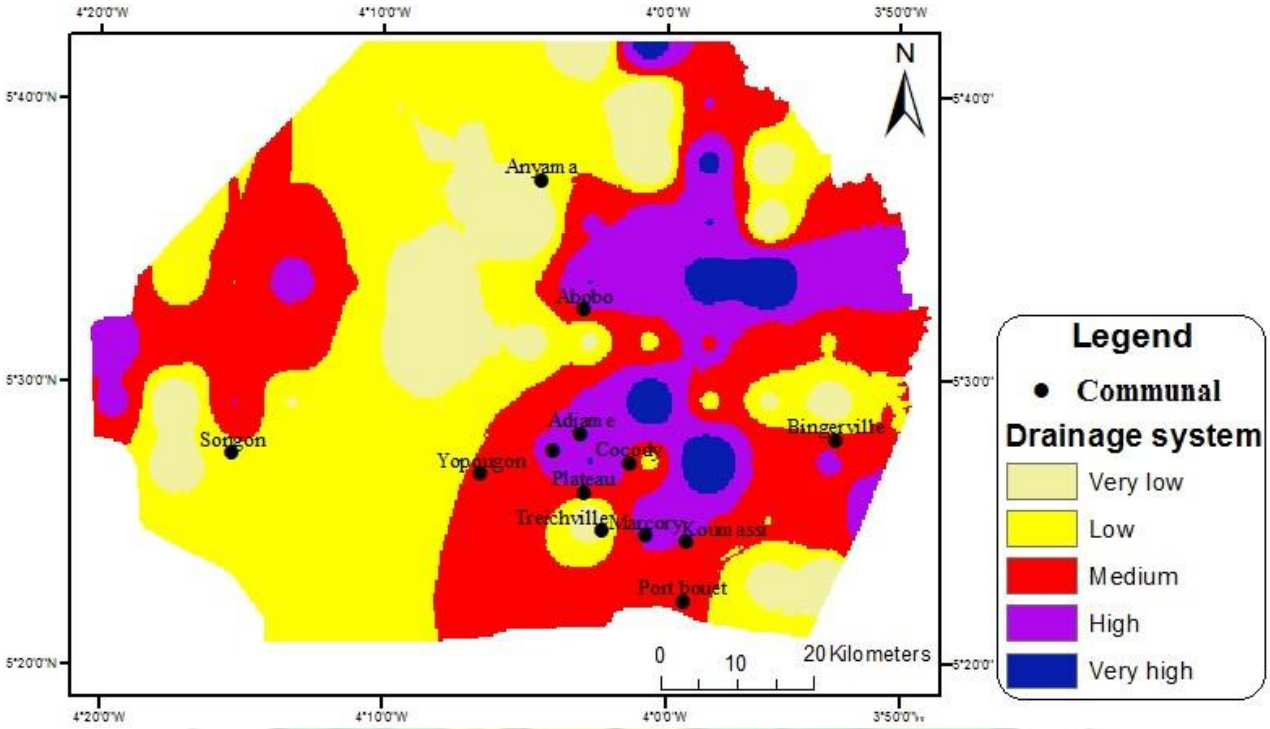


Figure 4.30: Drainage system density of Abidjan

Table 4. 15: Weight assigned to "Drainage system density" classes

Classes (km^2)	Weight
0.05 – 2.30	9
2.30 – 3.20	8
3.20 – 4.20	5
4.20 – 5.80	3
≥ 5.80	1

4.8.2.3. Urban Structure Types (UST)

Land use is an important factor to better understand the physical vulnerability patterns induced by human activities and the map in Figure 4.31 provides information on urban structure types (UST) of Abidjan. Based on the infrastructure types, it is possible to find out areas that can be and not vulnerable to flood. The different classes obtained from the UST classification through oriented based image analysis (OBIA) are eight (8) classes including: bare soil (2.03 %), high residence (3.20 %), Industrial area (2.97 %), informal residence (0.28 %), publics' services (3.21 %), medium residence (7.83 %), water (10.13 %), and vegetation (70.35 %), respectively (Table 4.16).

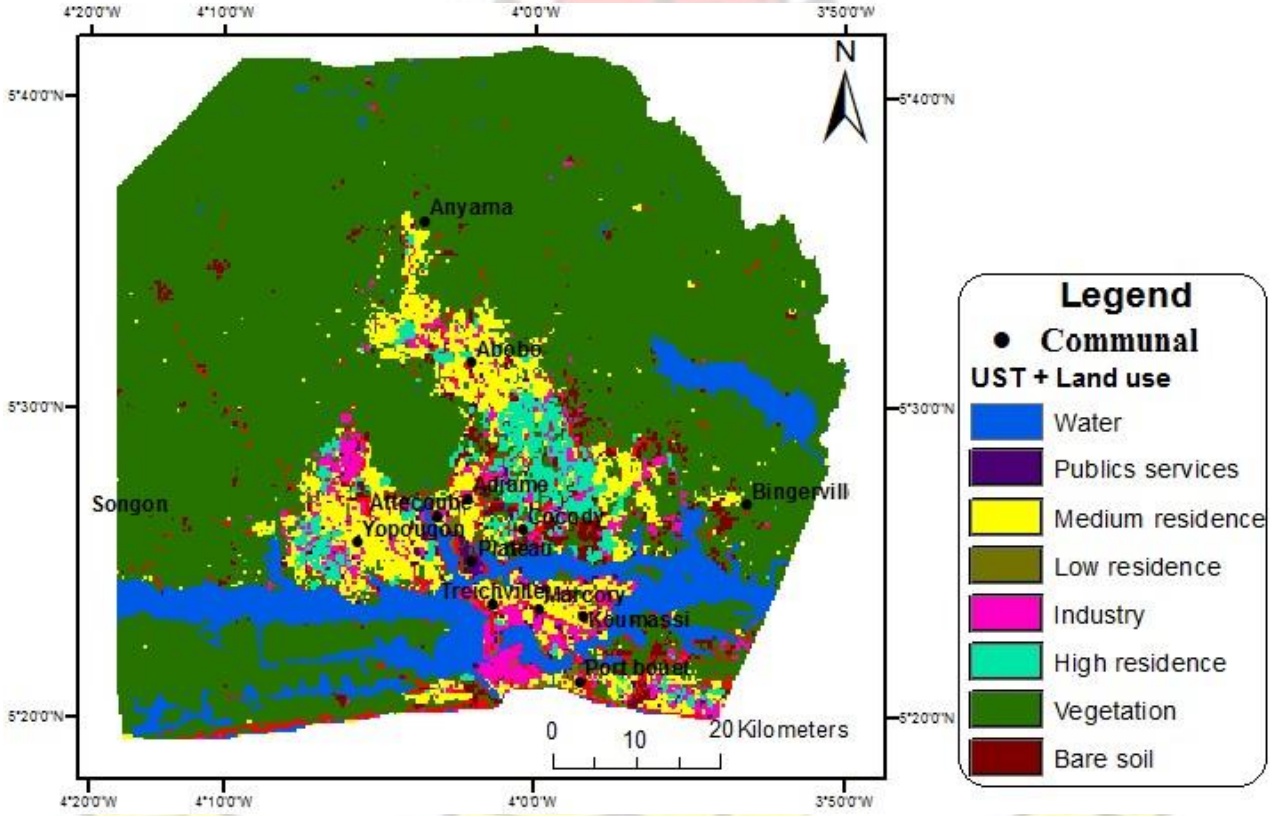


Figure 4.31: Urban structure types of Abidjan

Table 4. 16: Weight assigned to parameter "UST" classes

Classes	Weight

Water body	10
Vegetation	1
Industrial and public service	3
High residence	4
Medium residence	5
Low residence	8
Bare soil	9

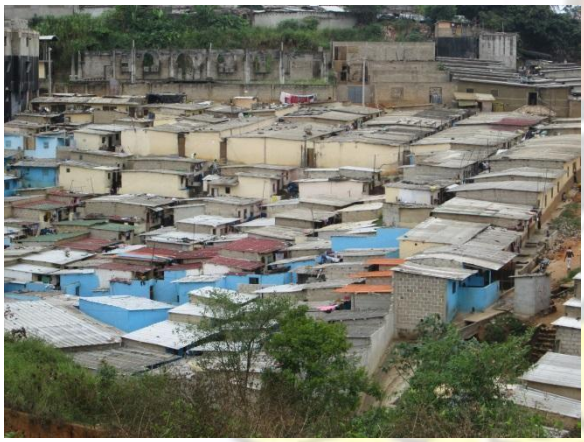


Plate 4.1: Informal settlement



Plate 4.2: Public services

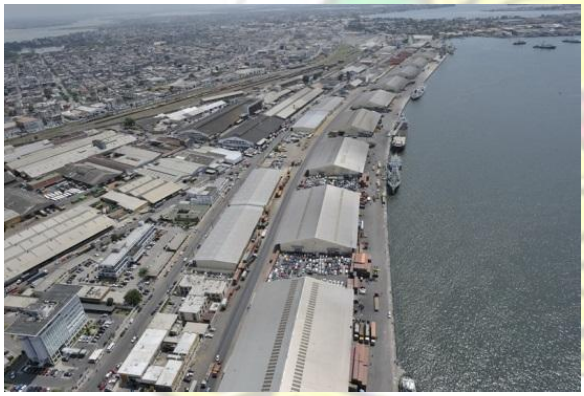


Plate 4.3: Industrial area



Plate 4.4: Medium and high residence

4.8.2.4. AHP vulnerability map

The AHP vulnerability map (Figure 4.32) was obtained by combination of parameter including drainage system density (DS), urban structure types (UST) and population density (PD). The raster calculation process was carried out using the equation 4.2 defined as:

$$\text{Vulnerability} = 0.64 \times PD + 0.26 \times UST + 0.1 \times DS \quad (4.2)$$

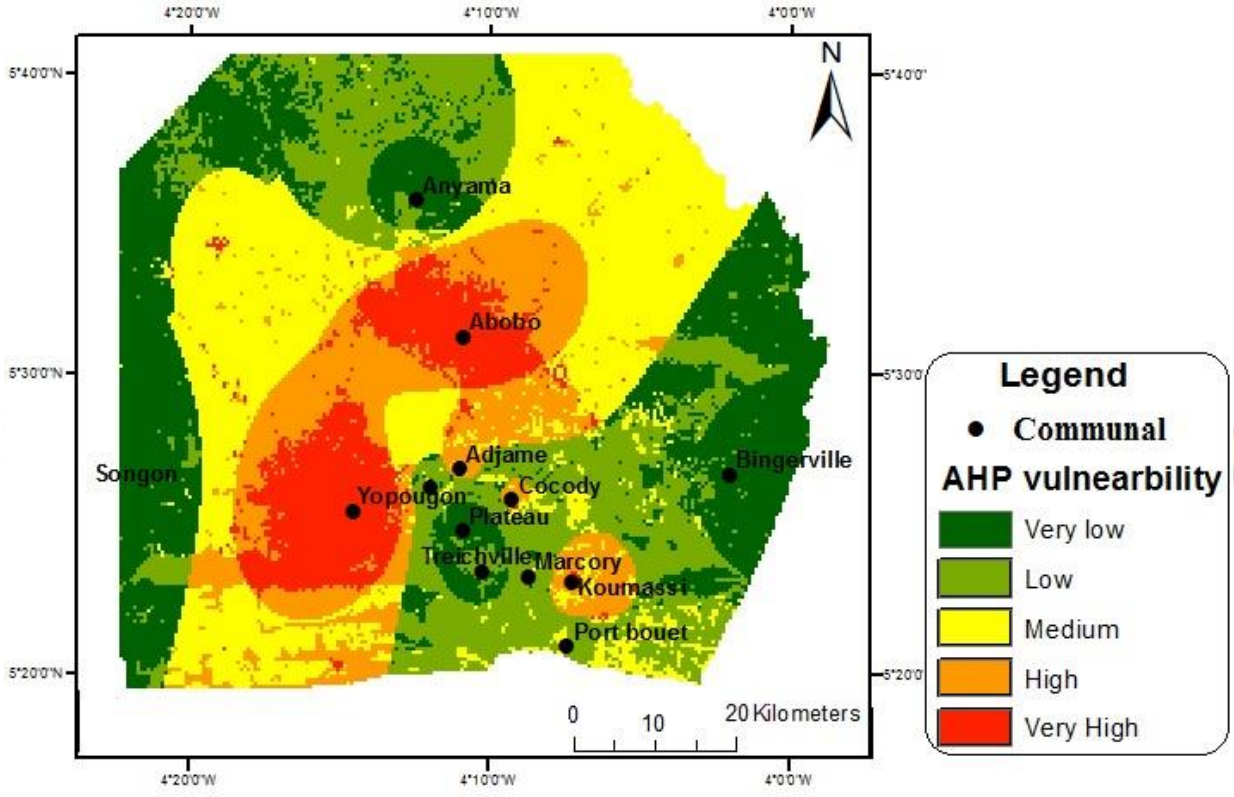


Figure 4.32: Vulnerability map of Abidjan

The vulnerability map obtained by combining UST, population density and sewer system highlights five areas (very low to very high) as shown in Figure 4.32. Very low and low classes cover 24.34 % and 21.63 % respectively of Abidjan. It is essentially areas with vegetation, cropland, less population density, good drainage system, industrial area and high residence area.

Medium class represents 29.89 % and covers most of Abidjan municipalities (Anyama, Plateau, Treichville, Port-Bouet, Marcory, and Bingerville) around six out of thirteen (6/13) municipalities. Areas covered by high and very high classes of vulnerability are 14.59 % and 09.55 %, respectively. Analysis showed that all these areas covered by high and very high vulnerability are dominated by weak drainage systems, high population density and impervious area (Abobo, Yopougon, Attecoube, Koumassi and some area in Cocody) within the Abidjan District.

4.8.3. AHP flood risk map of Abidjan

The AHP flood risk map in Figure 4.33 is a result of vulnerability and hazard maps combination. The calculation process developed from the formula using "raster calculator" within spatial analyst tools in ArcGIS is defined as following:

$$\text{AHPflood risk} = 0.5 \times \text{AHPVulnerability} + 0.5 \times \text{AHPHazard} \quad (4.3)$$

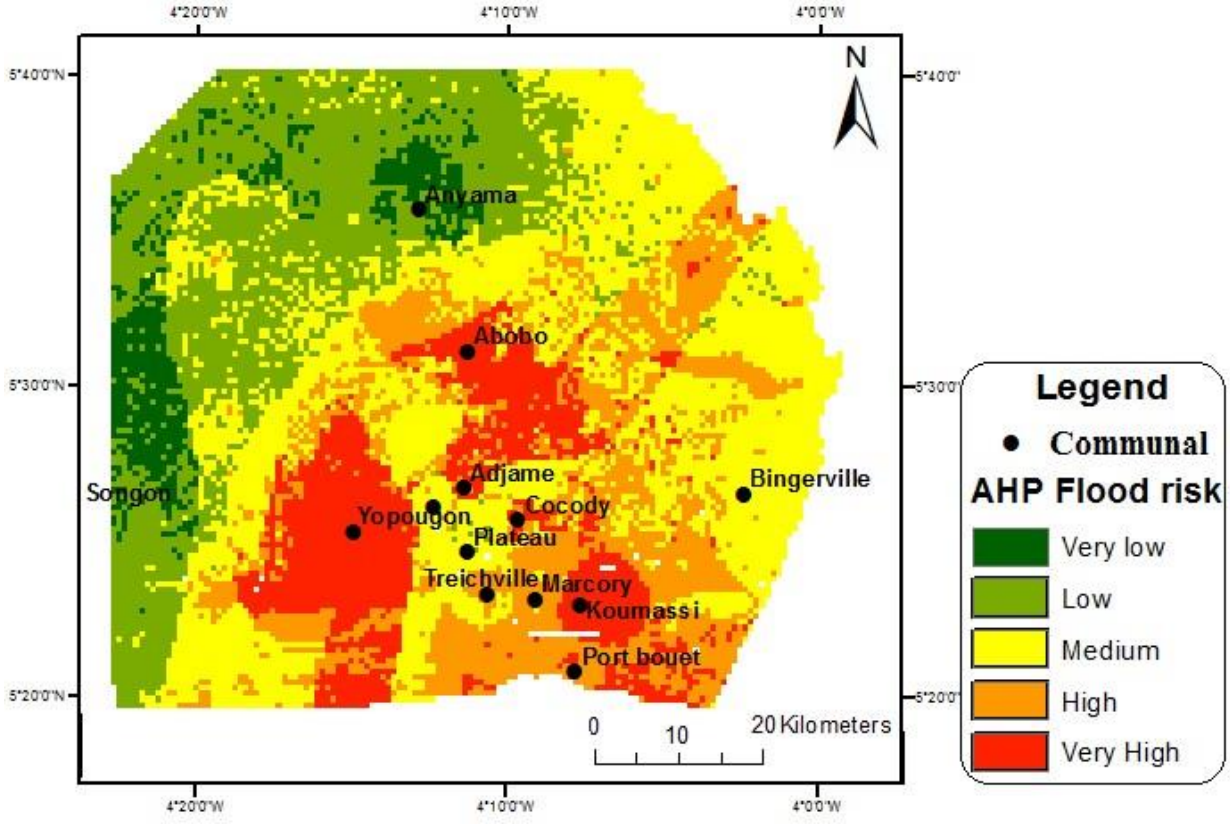


Figure 4.33: AHP flood risk map of Abidjan

The risk of flooding resulting map in Figure 4.33 defines five (5) levels of risk, ranging from very low to very high. Areas with very low, low and medium risk of flooding cover 5.42 %, 24.37 % and 36.31 %, respectively of Abidjan. They are unevenly distributed and characterized by high slope, vegetation areas and low population density. Areas with high and very high risks cover 19.97 % and 13.93 %, respectively. An overall area of high and very high risk of flooding covers 33.9 % of the study area. Municipalities identified to be at high and very high risk of flooding within the Abidjan District are Abobo, Yopougon, Adjame, Attecoube, Koumassi, Port-bouet, Marcory, Treichville and some area of Cocody. The analysis of this map also show that, the urban structure types play a key role in addition to population density, flat slope and heavy rainfall into the risk of flooding in Abidjan; as well as other anthropogenic factors (urban structure type) showing morphology level play an aggravating role in the risk of flooding. The resulting map shows that 34% the study area representing high risk of flooding. Thus, this resulting map can serve as a guideline to decision makers for potential anticipatory measures and mitigation.

4.8.4. Validation of AHP flood risk map of Abidjan

The resulting AHP flood risk was subjected to validation procedures to assess how the results of a multi-criteria flood mapping approach conforms to reality of flood hazard occurrence in Abidjan. The present result relies on flooded area recorded during field work and added by historical record of flood events in Abidjan from the ministry in charge of urbanisation. In the validation process, recorded flooded areas were plotted and then overlaid on the AHP flood risk map as shown in Figure 4.34.

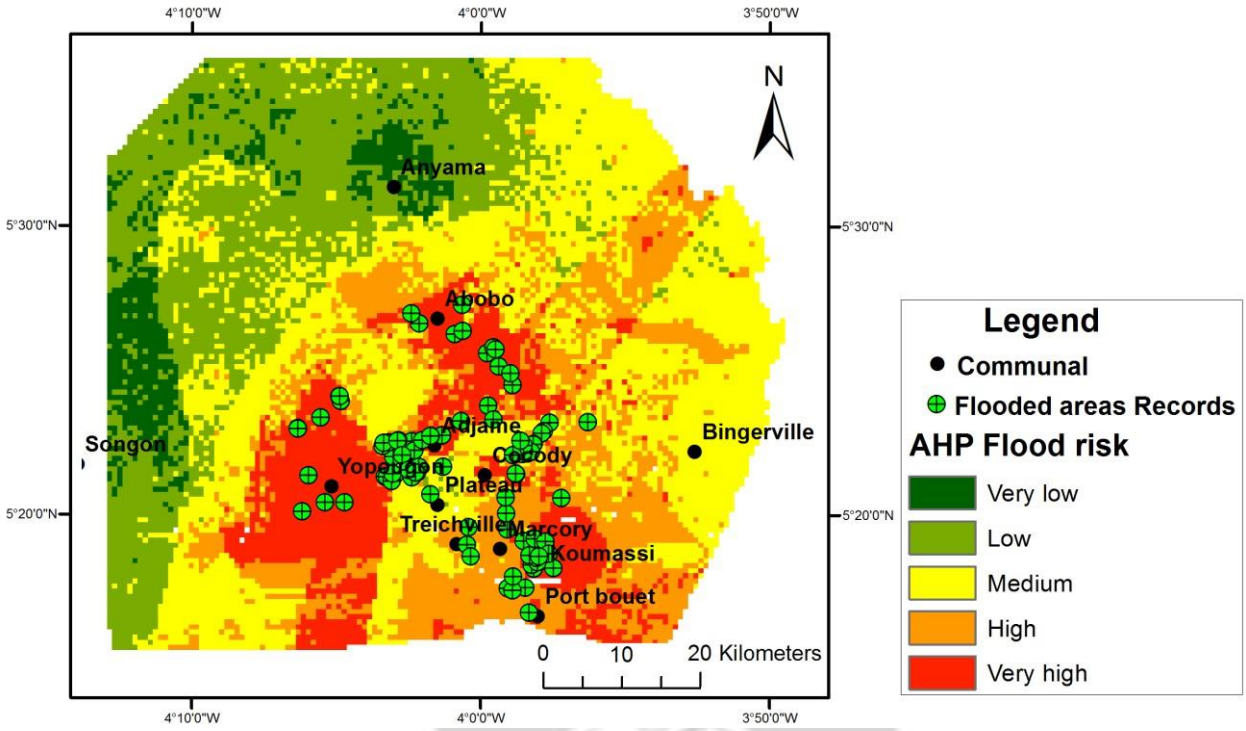


Figure 4.34: Validation of AHP flood risk map with flooded areas records

The results show that from flooded areas record in Figure 4.34, a total of 79 % were all correctly classified by AHP flood risk procedures used in this study under high and very high areas of risk. Of this, 45.65 % fall in the very high risk area whilst 32.61 % fall in the high risk zone. The remaining 21.74 % fall in the medium flood risk zone. This means that the developed flood risk map accurately predicts areas at risk of being flooded in the Abidjan District.

4.9. Flood Hazard Index (FHI) model

4.9.1. Peak of runoff estimation

4.9.1.1. Runoff coefficient estimation

The runoff coefficient map resulting from the intersection of slope, land use and soil type was classified from low to high (0.08-0.9) mainly dominated by low runoff (Figure 4.35). However, most of the thirteen (13) municipalities with a rate of 9/13 municipalities were covered by moderate

to high runoff coefficient except Songon, Bingerville and Anyama. Also within these municipalities high runoff areas are scattered and divers from one area to another. Areas covered by high runoff coefficient were unequally represented and scattered within the study area.

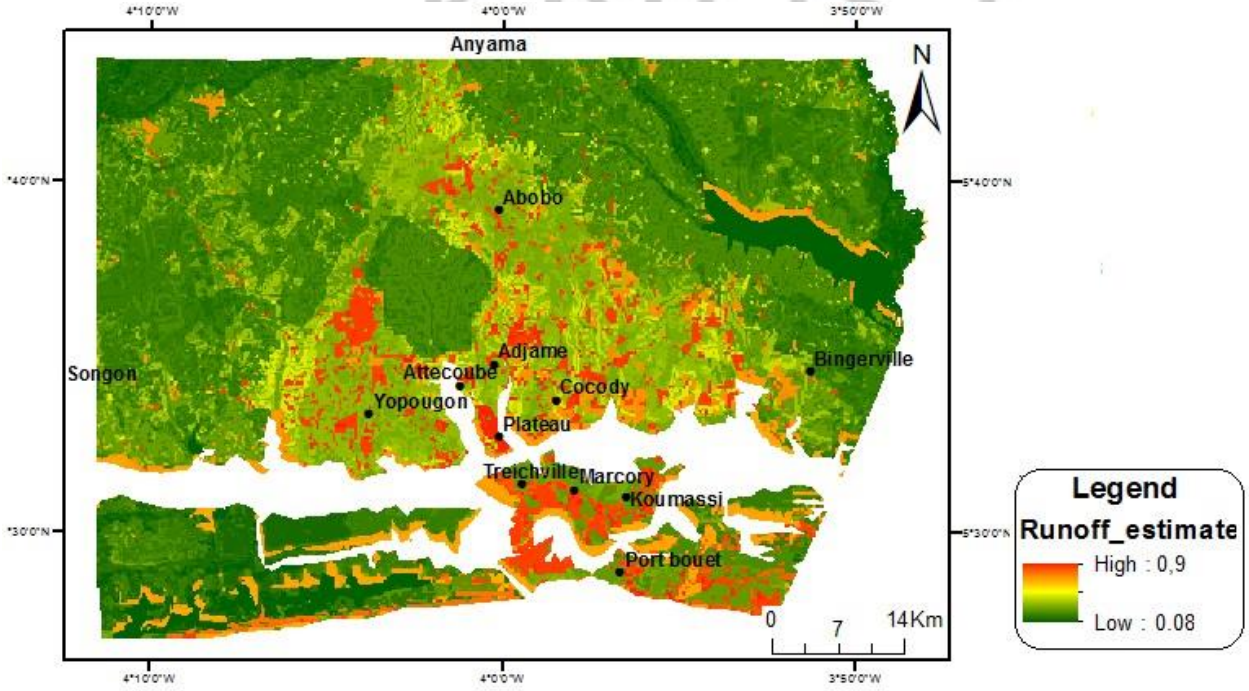


Figure 4.35: Runoff coefficient map of Abidjan

4.9.1.2. Drainage Area

The drainage area vector layer of the study area, covering the area of each LULC types in Figure 4.36, was rasterized and resampled to 30m resolution. Over 70 % of the area is characterised by forest and Farmland and less than 18% was covered by impervious surface. This predominance of vegetated areas leads to low drainage in Abidjan District.

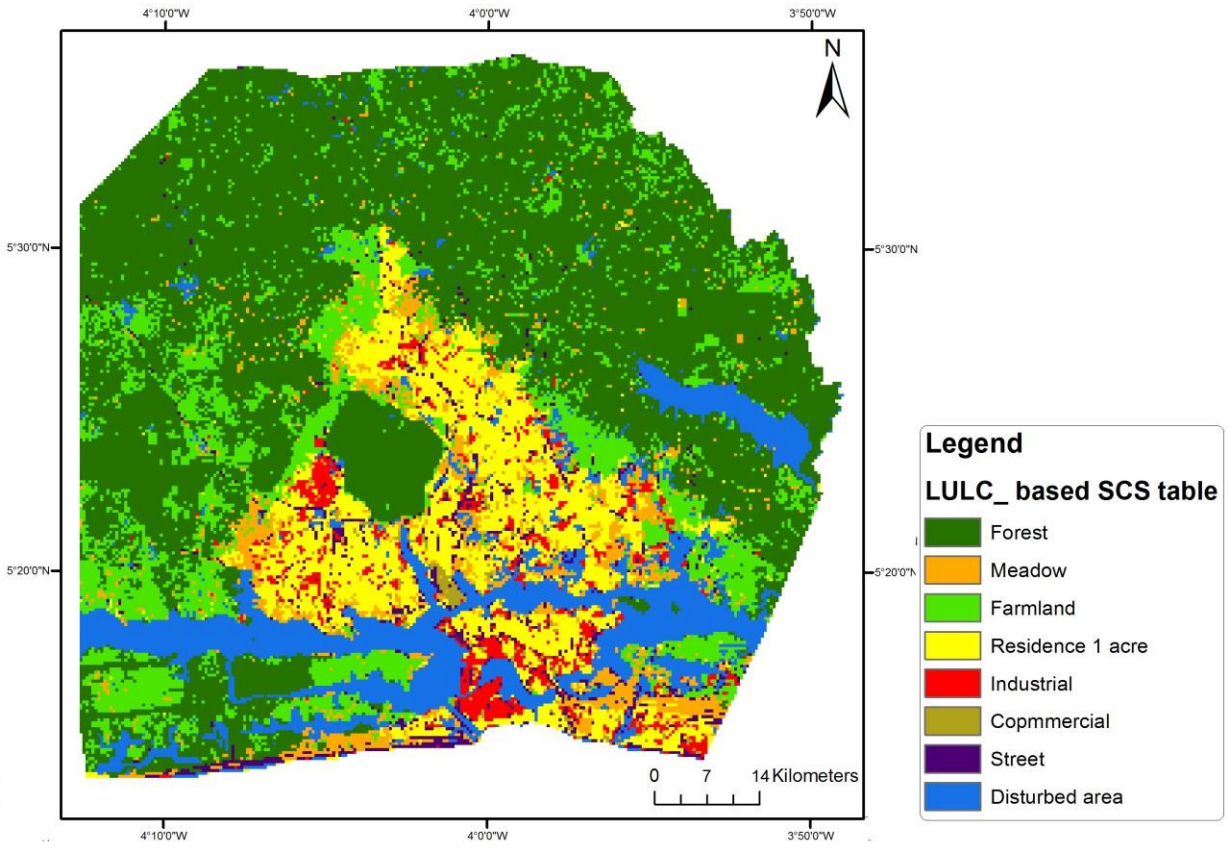


Figure 4.36: LULC based on SCS table

4.9.1.3. Annual Rainfall

Rainfall distribution map in Figure 4.37 have five classes: very low and low classes represent 48.55 % and 17.97 %, respectively, medium class cover 13.4 % followed by high and very high classes which are estimated to 15.43 % and 4.64 % respectively. However, except Songon and Anyama communal. Others were covered by medium to very high amount of precipitation.

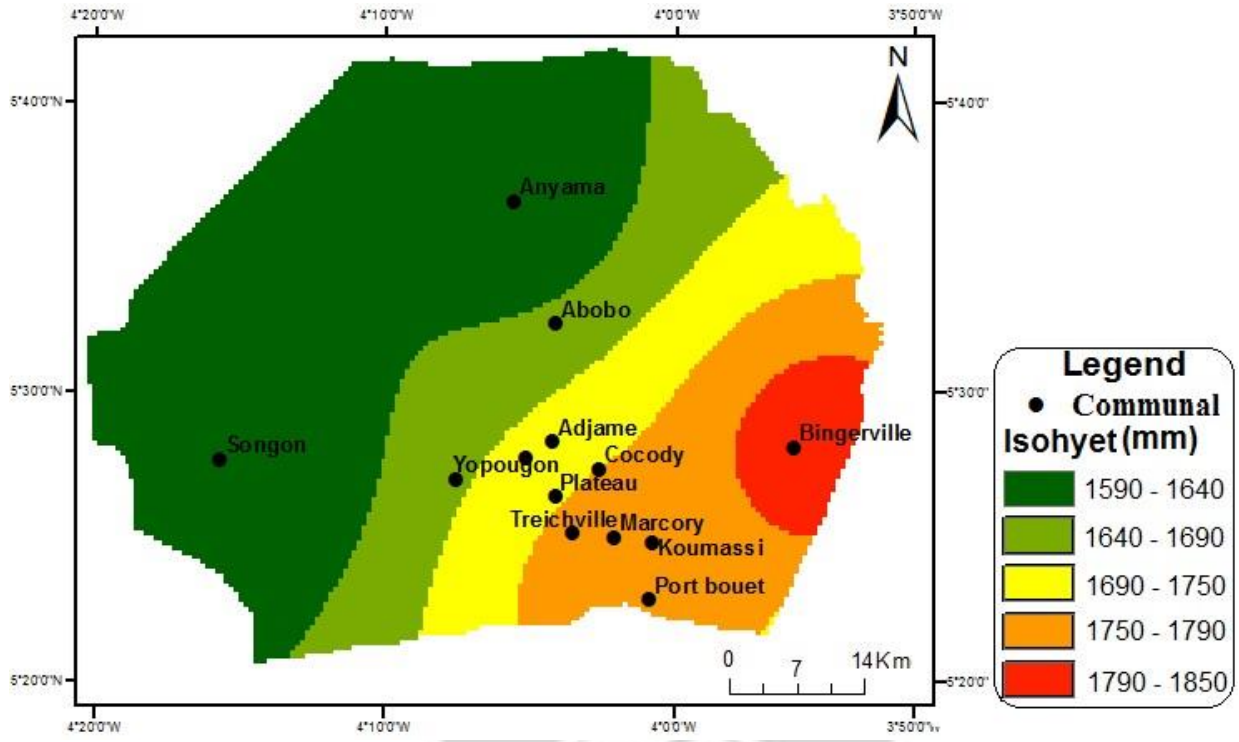


Figure 4.37: Rainfall intensity map of Abidjan

4.9.1.4. Peak of Runoff

At the end of the calculation with the rational method, the peak runoff map was generated (Figure 4.38). Peak runoff map was mainly dominated by low area of peak surface runoff. After standardization and reclassification, five (5) classes were identified. Areas covered by very low and low classes represented 32.97 % and 63.82 %, respectively, medium area 1.97 % while high and very high area of peak runoff were 1.23 % and 0 %, respectively. The peak runoff map indicates that the study area is mostly covered by low level of peak runoff, which means that infiltration in these areas are good. Areas with high peak runoff level cover mainly less than half of the District municipalities, which are characterised by impervious areas in addition to areas close to river and lagoon

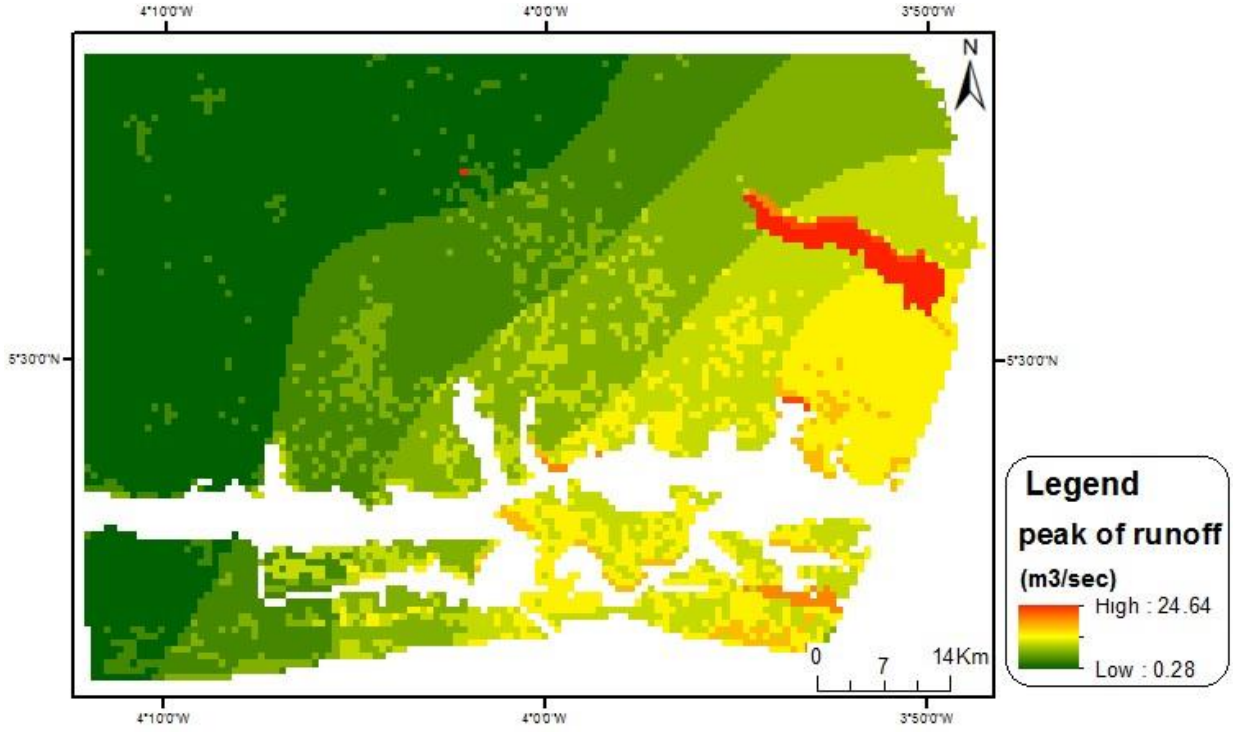


Figure 4.38: Peak runoff map of Abidjan

4.9.2. Digital Elevation Model (DEM)

DEM map in Figure 4.39 showed that in most of Abidjan District (Adjame, Plateau, Treichville, Port-Bouet, Marcory, Songon, Yopougon, Attecoube, Koumassi, Cocody and Bingerville), a rate of eleven out of thirteen (11/13) municipalities is covered by low to moderate elevation region except Anyama and Abobo. This implies a favourable area as bed for extreme events such as flood. After standardization and reclassification five (5) classes were also identified. Areas covered by very low and low classes represented 31.90 % and 18.47 %, respectively, medium area covered 20.58 % while high and very high area of elevation covered 18.66 % and 10.39 %, respectively.

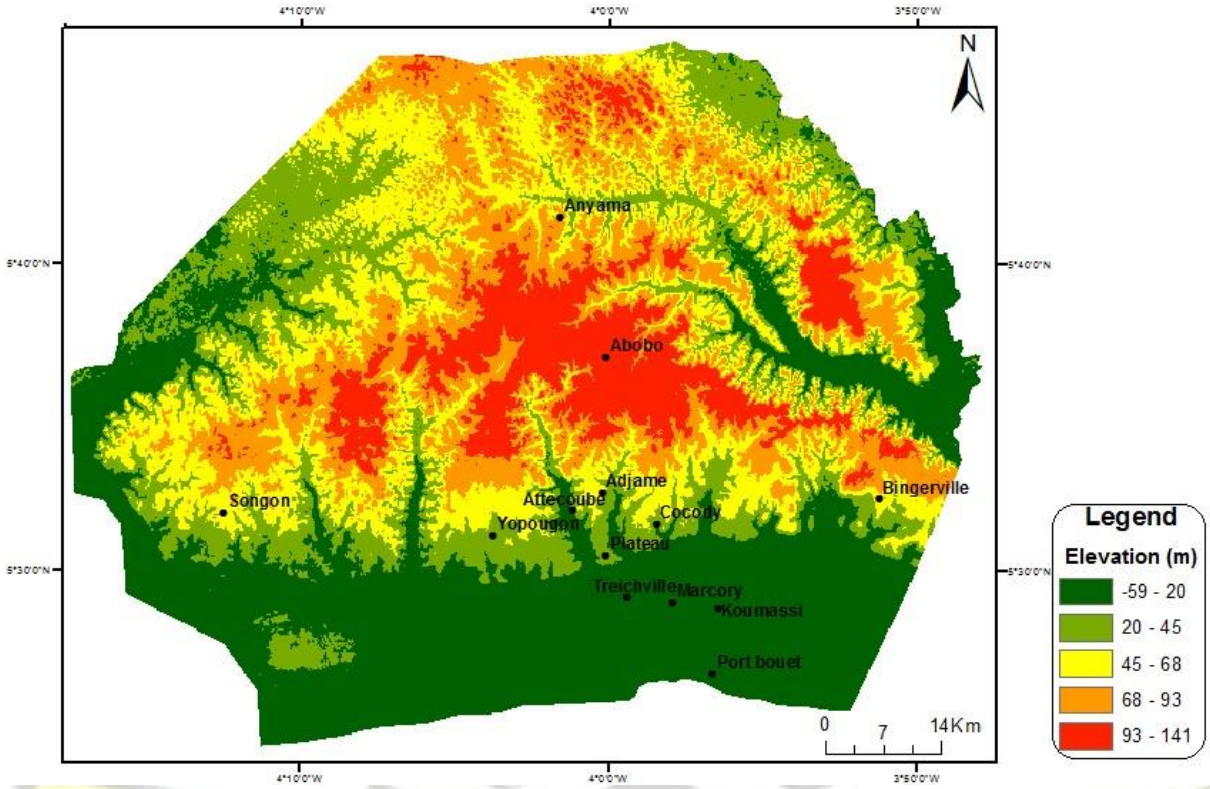


Figure 4.39: Digital Elevation Model (DEM) map of Abidjan

4.9.3. Flood hazard index map

The flood hazard index resulting map is a combination of hydrological and statistical model using Peak of runoff and DEM in final step. This map defines five classes of hazard risk including very low, low, moderate, high and very high areas at risk of flooding in Abidjan (Figure 4.40). Areas covered by Very low and low areas of flood hazard covered 24.46 % and 17.68 %, respectively, medium and high area of flood hazard were covered by 32.77 % and 22.12 %, respectively while very high area of represented 2.97 %.

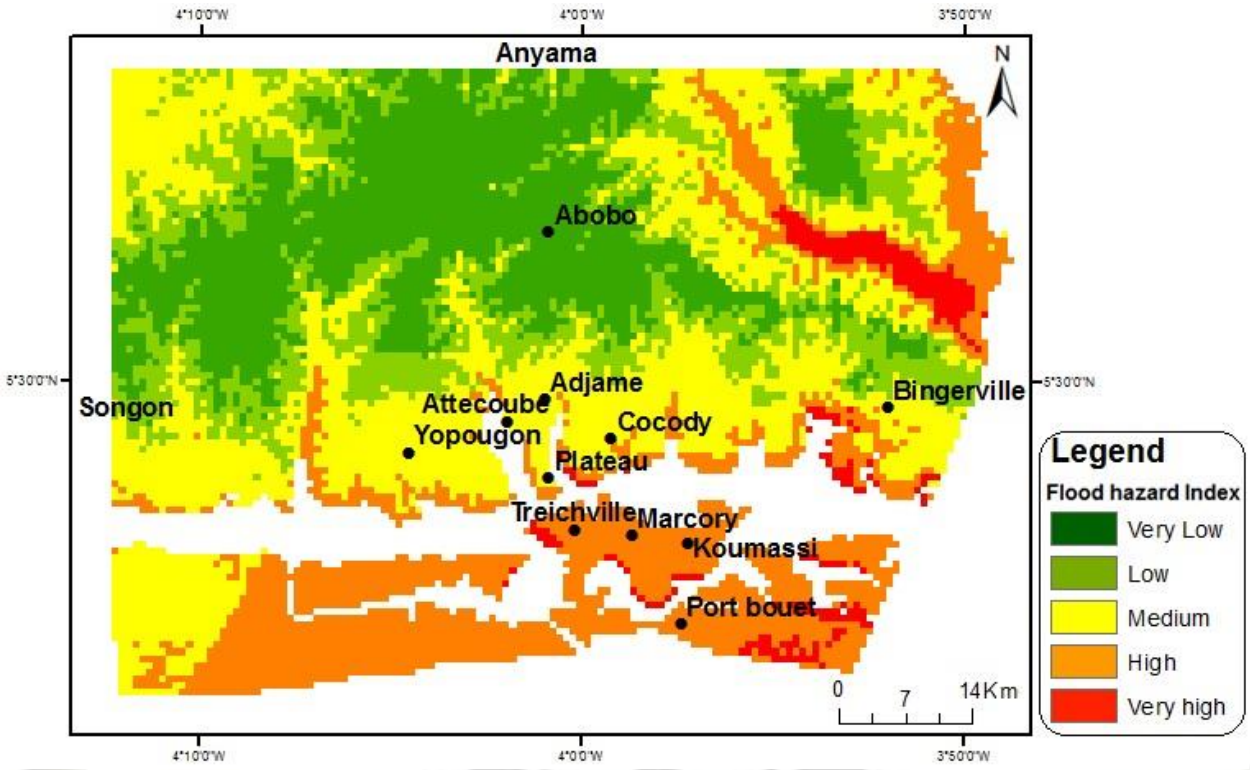


Figure 4.40: Flood hazard index map of Abidjan

Deep analysis of this map showed that flat DEM and moderate to very high peak of runoff play a really key role in flood hazard occurrence and Flood Hazard Index (FHI) mainly depend on the elevation. On the whole, area at high flood hazard index within Abidjan District were Portbouet, Koumassi, Marcory, Treichville and some areas of Cocody, Attecoube, Adjame and Yopougon.

CHAPTER 5: DISCUSSIONS

5.1. Land use/land cover dynamics of Abidjan

In this study, a spatial temporal dynamics of land uses/land cover in Abidjan was assessed based on image classification and change detection method. The method applied was to highlight urban area dynamics within Abidjan District and get a deeper comprehension. The results show change in the three classes: vegetation, water and settlement from one place to another. The increase in

settlement area was identified as major land use change compared to vegetation and water areas. The reliability of this study is based on the accuracy assessment results. An increase in settlement area over 14.95 % from 1990 to 2014 was highlighted by the dynamic results. Regarding urban land use change, the increase in settlement areas has been documented extensively (Yan *et al*., 2015; Megahed *et al*., 2015; Yao *et al*., 2015 and Goertz *et al.*, 2003). This urbanisation sprawl explained the consequence of population growth and demand for goods and is supported by Yao *et al*., (2015), who indicated that, urban sprawl in Abidjan District from 2002 to 2014 is mainly due to population growth during the crisis (2002-2011) and its demand for development.

The NDBI map highlighted urban area increase from 1990 to 2014 and confirmed land use results. However, increase in settlement area was most important between 2002 and 2014, compared to 1990 and 2002. Indeed due to the country's crisis which started in 2001, there was a lot of population migration (rapid uncontrolled urbanization) from the north to the southern part of the country mainly to Abidjan. Moreover, due to Landsat image resolution and reflectance it was difficult to differentiate between bare soil and build- up during the processing and analysis which can be factors of some bias.

5.2. LARS-WG model

The methodology for analysing the trend of weather data under present and future condition to predict future climate change in Abidjan using HAdCM3 model in LARS-WG to achieve it, was supported by Goodarzi *et al*., 2014. The results consistency is linked to the strength of input parameters. The observed daily data (temperature, rainfall, solar radiation) for 50 years were used without the need to generate data as baseline data. The significant results of the different statistical test through the Q-test showed that the availability of large observed data reduced the range of uncertainty. This result confirms the assertion of Sobhany and Fateminiya, 2014, who said

LARSWG gave high accuracy results of climate modelling and they were supported by many researchers using LARS-WG (Semenov, 2008; Goodarzi *et al*., 2014; Molanejad *et al*., 2014). The HadCM3 model used in this study is from GCMs which is already part of LARS-WG model and subjectivity is also noted in the choice and range of data as input. This subjectivity is reduced by checking the consistency of observed data as baseline by doing calibration and validation of the data before generating the future scenarios which increases our confidence in the models' predictions and reduces the level of uncertainty. The choice of HadCM3 model as used in the present study was based on comparison between HadCM3 and MPEH5 models output and also supported by literature. Then, Potential evapotranspiration (PET) scenario data was generated by the model itself using the solar radiation data as input through algorithm.

However, GCMs and impact models are undergoing continuous development and improvement because some research have showed some uncertainty and limitations by applying Global Climate model at local scale due to methodical model calibration. Also, the availability data from others stations within the District could increase accuracy level of the results and help for comparison between several stations.

5.3. rclimdex processing

Weather and extreme events analysis mainly floods were investigated through rainfall indices calculation of Abidjan in present and future condition using rclimdex model. The results based on the 10 rainfall indices calculated revealed variation between negative and positive trends from one index to another. Regarding the decreasing trend of these rainfall indices: Annual total wet-day precipitation (*PRCPTOT*), Number of heavy precipitation days (*R10*), Number of very heavy precipitation days (*R20*), Number of days above 25 mm (*Rnn*), Very wet days (*R95p*) and Extremely wet days (*R99p*) from 1960 to 2010 summarized a reduction of rainfall in Abidjan

following observation made by L'Hote *et al*., (2002) and Ali, (2011) which revealed a decrease in annual total rainfall in West Africa mainly in the sahelian zone. However, the same results shows positive trend for consecutive wet days (*CWD*) index from 1960 to 2010 which is in accordance with Sarr, (2011) who found an increasing trend of consecutive wet days from the late1980s in sahelian region. Hence, consecutive wet days (*CWD*), Simple daily intensity index (*SDII*) and Number of heavy precipitation days (*R10*) indices show an increasing trend in the future (20112100) with no significance (P-value> 0.05). From 1960 to 2010 and 2011 to 2100 most of the rainfall (10) indices were not significant except *PRCPTOT, R20* and *Rnn* indices trends from 1960 to 2010, which were significant with a P-value < 0.05. However, according to Ly *et al*., (2013), the occurrence of extremes is usually the result of different factors at different time scales. Then, very few studies had been undertaken concerning extreme indices calculation in humid zone of West Africa to compare with results of this study. But availability of daily data from other stations within the study area could improve the results consistency by comparison between rainfall indices from various stations.

5.4. AHP flood risk map

The Abidjan District flood risk was evaluated using the multi-criteria analysis approach specifically AHP, combining vulnerability and hazard assessment. The flood risk was around 70 % when the summation of moderate, high and very high classes was done. The analysis showed that 34 % of the study area is flood risk zone whiles a study by (OCHA, 2014) found that 26% of Abidjan District area was at risk of flooding. Per the findings of OCHA (2014), this study results highlighted that, flooded areas increased from 26% to 34% between 2013 and 2015, in Abidjan. The analysis shows that most of the municipalities' are within high and very high flood risk areas. Eight out of thirteen (8/13) municipalities of the Abidjan District areas are at a high risk of flooding and therefore need optimal design of technical solutions from the society. The reliability of the

resulting flood risk map which gives acceptable results is based on input parameters, historical and recorded flood data used for validation. However, input factors under hazard and vulnerability are not standard and depend on the study area, focus and available data as observed in various studies (Yahaya *et al*., 2010; Yalcin *et al*., 2004; Bapalu and Sinha, 2005; Saley *et al*., 2013). Regarding flood risk map and modelling research undertaken, West Africa, has been documented extensively (Saley *et al*., 2013; Saley *et al*., 2005; Mbow *et al*., 2008; Forkuo, 2011). Results from the hazard map shows 32 % of the area as high hazard risk with rainfall and slope being the most significant causative factors in flood occurrence. The vulnerability map also showed 24 % of the area as highly vulnerable to flood with population density and land use through urban structure types as relevant factors in flood risk.

Multi-criteria analysis (AHP) adopted for this study within Abidjan District enabled multi-source data combinations, which constituted a real advantage. The method was based on physical, hydrogeological and anthropogenic parameters. The parameters used in the flood risk map required interpolations to allow their crossing. The results indicated that, AHP can be used as an efficient method to assess and map flood risk ((Wang *et al*., 2011; Sowmya *et al*., 2015; Orencio, and Fujii, 2013; Cozannet *et al.* 2013; Pourghasemi *et al.* 2014 Papaioannou *et al*., 2015; Nejad *et al*., 2015; Saley *et al*., 2005). AHP methodology allowed for a better understanding of all the elements or indicators contributions in flood process based on weight given to each of them. However, using data from different sources, interpolating and reclassifying data in GIS to the same resolution are factors of some bias during the processing and analysis. Normalization and weighted steps of these parameters are important to reduce bias and uncertainty in the final result. Also, AHP method shows some failure due to the subjectivity in choosing the value of the weighting for indicators from arbitrary judgments of experts (Papaioannou *et al*., 2015). This weakness is reduced by the

consistency ratio test of judgments. Saaty, (1980) provides a constancy ratio threshold which must be less than 10% to make a coherent judgment. The value of consistency ratio as part of this study is 3% and concludes that the judgments can be considered coherent. This study was inspired by previous studies (Mbow *et al*., 2008; Saley *et al*., 2013; Forkuo, 2011, Savane *et al*., 2003) in West Africa. However, it is clear that the risk of flooding is linked to combined action of many different factors under two criteria: hazard and vulnerability. However, the result can be improved by the development of urban structure types (UST) through oriented based image analysis (OBIA) method using high-resolution images (Ikonos, RapidEye, QuickBird) to raise classification details on urban morphology with good accuracy. Other parameters such as flow accumulation, and flow velocity could be investigated as indicators of one of the criteria. Hydrologic modelling in 2D or 3D for efficient processing and management of floods (Santiago *et al*., 2015) can be added.

5.5. Flood hazard index model

In this model, a combination of hydrology (Rational method) and statistic models were assessed in case of flood occurrence. Both methods were applied to join their strengths for reliable flood hazard index map (FHI) in Abidjan. The benefit of combining hydrology and statistic models in FHI assessment was supported by Asare-Kyei *et al*., (2015). The results show that, very high and high areas of flood hazard were covered by 25.09 % while medium area was covered by 32.77 %. Regarding the results, Abidjan is less vulnerable to flood hazard. However, the same results shows that areas with very low and low elevation were areas detected as high areas of flood hazard which means FHI is more dependent on elevation than peak runoff. In the study area, most of the high areas of flood occurrence were found across lagoon, river and sea. Indeed, four out of thirteen (4/13) municipalities were totally covered by areas of high and medium flood hazard. Also, five out of thirteen (5/13) municipalities areas near to the lagoon were also covered by areas of high and medium flood hazard. In total, nine out of thirteen (9/13) municipalities can be considered as

areas covered by medium and high flood hazard which was also found by the AHP flood risk map. It means rational method can be applied at District levels and it gives acceptable results. A hydrological model normally relies on measured runoff coefficient to determine peak runoff values. In this study, estimation of runoff coefficient cannot be exactly the same as those measured. In addition, DEM of the study area, which is almost flat did not help to improve the model output.

CHAPTER 6: CONCLUSIONS AND RECOMMENDATIONS

6.1. CONCLUSIONS

i) The results of this thesis show the prominence of remote sensing and GIS in flood risk assessment. The investigation of the spatio-temporal dynamics of land use/ cover change between 1990, 2002 and 2014 using the Maximum likelihood algorithm and in addition Normalized Difference Build-up Index (NDBI) within Abidjan District revealed a considerable change in the landscape. Rapid expansion of urban area and forest degradation were the major land use change observed from 1990-2014. Vegetation change was the most important with a rate of 9.64 % of the total change that occurred during the 24-year period. Also, water change showed a rate of 5.31 %. Both changes involved total conversion of 14.95 % abstraction of landscape to urban zone.

ii) LARS-WG model was used to generate specific climate change scenarios (weather data) for prediction of weather events at Abidjan site using HAdCM3 Model and the optimistic emission scenario SRA1B. Analysis after comparison between baseline and the generation of future weather data from 2011-2030, 2046-2065 and 2065-2099 shows that, for the next 90 years, there will be short term and long term increase in temperature and precipitation and a decrease in solar radiation in Abidjan. LARS_WG was able to generate future scenarios and gave better understanding and view concerning weather data variability in the future, more specifically rainfall in case of flood risk event.

iii) rclimdex model was used to calculate ten (10) rainfall indices to assess flood occurrence as an extreme event from 1960-2010 and 2011-2100 after quality control and homogenisation of the data. Results through ten (10) rainfall indices (*PRCPTOT, CWD, R10, R20, Rnn, R95p, R99p, RX1day, RX-5day* and *SDII*) and comparison between observed and future indices revealed a decreasing trend observed in rainfall from 1960-2010 and 2011-2100. However, general observation made indicates an increasing trend from 1995-2010 for all rainfall indices and in addition *CWD, SDII* and R10 indices show an increase from 2011 to 2100. This observation or positive trend could explain that extreme rainfall events are more frequent nowadays in Abidjan and some indices including *PRCPTOT, R20* and *Rnn* results were very significant (p-value <0.05). Then, increase of *CWD*, *SDII* and *R10* indices from 2011 to 2100 clearly indicate that heavy rainfall will occur in the future in Abidjan District. Moreover, these indices with positive trends were no significant because P-value was greater than 0.05.

iv) The Multi-Criteria Analysis approach used in mapping areas at risk of flooding required a combination of hazard map (slope, drainage, soil type and isohyet) and vulnerability map (population, sewer system density and land use). These two complementary criteria highlight the use of geo-information techniques in natural disaster assessment. The AHP method used allowed the identification of areas at risk of flooding in Abidjan. The analysis of the risk of flooding map shows five risk classes:

- 5.23 % of mapped zones have a very low risk. These areas are characterized by a high slope which promotes runoff, low population and good drainage system.
- 24.37 % of the mapped zone presents low risk. In these areas the characteristics are identical to those of low-risk areas.

- 36.31 % of Abidjan area counted as moderate risk. These areas were mainly covered by moderate slope, acceptable runoff, and drainage systems.
- 19.97 % of the study area has a high risk. This level of risk is explained by the presence of intense anthropogenic activity, heavy rainfall and low slopes.
- 13.92 % of the mapped areas had a very high risk.

The resulting map shows that 34 % of the study area presents high and very high risk of flooding. The District of Abidjan exposed area at risk is important. Eight out of thirteen (8/13) municipalities (Abobo, Yopougon, Adjame, Attecoube, Koumassi, Port-bouet, Marcory and some area of Cocody) are covered by high and very high areas at risk of flood. Thus, the generated map can serve as a guide for decision makers to come out with mitigation measures, better land use planning and flood risk management under climate change.

v) The resulting Flood hazard index map was a combination of two separate models which were coupled in this study and has proved the feasibility to model flood. Combination of both models shows the strength of these to develop a Flood Hazard Index with acceptable accuracy level. The flood hazard index shows that, 25.09 % of Abidjan is covered by very high and high flood zones and the remaining 32.77 % were classified into medium risk zone. On the whole, the areas at high and very high flood hazard within Abidjan District were Port-bouet, Koumassi, Marcory Treichville, some areas of Cocody, Attecoube, Adjame and Yopougon. These are mainly low land areas across the lagoon. However, flood hazard index is mainly dependent on the elevation of the study area and the resulting map could serve as a useful reference for decision makers and proposing possible solutions and mitigation strategies.

6.2. RECOMMENDATIONS

Based on the results of this research, strict measures need to be taken concerning flood risk mitigation.

vi) Policy makers should strengthen urbanization legislation, land use planning and enforcement to regulate and control urbanization. In order to prevent more significant damage. vii) Special attention should be paid in monitoring areas under very high and high flood risk. And also an effective preparedness strategies should be developed to manage future extreme rainfall or floods occurrence within Abidjan District.

viii) The use of high-resolution images: Ikonos, RapidEye, QuickBird to develop urban structure type (UST) classification gives more details and high accuracy for land use /land cover classification and change detection.

ix) Monitoring and maintenance of the weather station stations in Abidjan District should be improved and other data recorded. This will contribute to solve or reduce data gaps, and help to obtain more reliable results regarding the spatio-temporal variations and distribution of weather data for further analysis and extremes events evaluation.

x) Areas identified as a high risks require more detailed mapping studies that can improve and refine the finding results.

xi) This study can still be improved by investigating the contribution of flood statistics (flood depth and velocity) and flow accumulation, Digital Water Model which could also influence the magnitude and the occurrence of flooding.

xii) Finally effective preparedness strategies ought to be developed to manage future extreme rainfall or floods occurrence within Abidjan District.

REFERENCES

Aaron, C. and Venkatesh, M., 2009. Effect of topographic data, geometric configuration and modeling approach on flood inundation mapping, *Journal of Hydrology*, 377:131–142.

Adel, S. and Gang-Jun, L., 2006. Flood induced land cover change detection using multi temporal ETM+ imagery. Proceedings of the 2nd Workshop of the EARSeL SIG on Land Use and Land Cover, Center for Remote Sensing of Land Surfaces, Bonn, 28-30 September 2006, 8.

Aghui, N. and Biemi, J., 1984. Géologie et hydrogéologie des nappes de la région d'Abidjan et risques de contamination. An. Univ. Nat. Côte d'Ivoire, sér. c, t. 20: 331-347. (*In French*)

Ahoussi, K. E., Loko, S., Koffi, Y. B., Soro, G., Oga, Y. M. S., Soro, N., 2013. Evolution spatio-Temporelle Des Teneurs en Nitrates Des Eaux Souterraines De La Ville d'Abidjan (COTE D'IVOIRE). *International Journal of Pure & Applied Bioscience*, 1(3): 45-60. (*In French*)

Ajin, R. S., Krishnamurthy, R. R., Jayaprakash, M. and Vinod, P. G., 2013. Flood hazard assessment of Vamanapuram River Basin, Kerala, India: An approach using Remote Sensing & GIS techniques. *Advances in Applied Science Research*, 4(3): 263-274.

Alexakis, D. D., Grillakis, M. G., Koutroulis, A. G., Agapiou, A., Themistocleous, K., Tsanis, I. K., and Hadjimitsis, D.G., 2014. GIS and remote sensing techniques for the assessment of land use change impact on flood hydrology: the case study of Yialias basin in Cyprus. *Natural Hazards and Earth System Science*, 14(2): 413-426.

Alexander, L. V., Zhang, X., Peterson, T. C., Caesar, J., Gleason, B., Klein Tank, A., Haylock,

M., Collins, D., Trevin, B., Rahimdah, F., et al., 2006. Global Observed Changes in Daily Climate Extremes of Temperature and Precipitation. *Journal of Geophysical Research*, III D05109. http://dx.doi.org/10.1029/2005JD006290

Algahtani, O. S., Salama, A. S., Iliyasu, A. M., Selim, B. A. and Kheder, K., 2015. Monitoring Urban and Land Use Changes in Al-Kharj Saudi Arabia using Remote Sensing Techniques. *Progress in Systems Engineering*, 515-523.

Ali, A., 2011. Climate variability and change in the Sahel. Understanding the current situation by observing Climate change in the Sahel. A challenge for sustainable development. AGRHYMET Monthly Bulletin (Special Issue), 17-20. http:// www.agrhymet.ne/PDF/Bulletin%20mensuel/specialChCang.pdf

Ali, S., Saeed, S., Reza, M., 2012. Probabilistic flood inundation mapping of ungauged rivers: Linking GIS techniques and frequency analysis, *Journal of Hydrology* (458–459): 68-86.

Al-Rawas, G., Koch, M., and El-Baz, F., 2001. Using GIS for flash flood hazard mapping in Oman. *Earth Observation Magazine*, 10(8): 18-20.

AlSarmi, S. H. and Washington R., 2014. Changes in climate extremes in the Arabian Peninsula: analysis of daily data. *International Journal of Climatology*, 34(5): 1329-1345.

Andre, D. et Damienne, P., 2007. La résilience: un concept pour la gestion des risques. Armand Colin, Annales de géographie, 654: 115-125. (*In French*)

Anonymous, 1990. Analyse multicritère: Optimisation et analyse de faisabilité, 24. (*In French*)

Apel, H., Thieken, A. H., Bruno, Merz. and Gunter, Bloschl., 2006. A Probabilistic Modelling

System for Assessing Flood Risks. *Natural Hazards*, 38: 79-100. DOI 10.1007/s11069005-8603-7, Springer 2006, 22.

Asare-Kyei, D., Forkuor, G. and Venus, V., 2015. Modelling flood hazard zones at the sub-District level with the rational model integrated with GIS and Remote Sensing approaches. *Water*, 7(7): 3531-3564.

Asgar, S. H., Alireza, P., Majid, R., 2013. Flood Zoning in Rural Watersheds by GIS and HECGEO-RAS (Case study: North western Iran). *Greener Journal of Science, Engineering and Technology Research*, 3(3): 076-081.

Babatolu, J., Akinnubi, R., Folagimi, A. and Bukola, O., 2014. Variability and Trends of Daily Heavy Rainfall Events over Niger River Basin Development Authority Area in Nigeria. *American Journal of Climate Change*, 3: 1-7. doi: 10.4236/ajcc.2014.31001.

Bachaoui, B., Bachaoui, E. M., El Harti, A., Bannari, A. et El Ghmari, A., 2007. Cartographie des zones à risque d'érosion hydrique : exemple du haut atlas marocain. *Revue Télédétection*, 7 (1-2-3-4): 393-404.

Bapalu, G. V. and Sinha, R., 2005. GIS in flood hazard mapping: a case study of Kosi River Basin. Retrieved September 9, 2014. from http://www.gisdevelopment.net/application/natural_hazards/floods/floods001pf.htm

Benediktsson, J. A., Palmason, J. A. and Sveinsson J. R., 2005. Classification of hyperspectral data from urban areas based on extended morphological profiles. *Geoscience and Remote Sensing, IEEE Transactions on*, 43 (3): 480-491.

Benediktsson, J. A., Pesaresi, M. and Amason, K., 2003. Classification and feature extraction for remote sensing images from urban areas based on morphological transformations. *Geoscience and Remote Sensing, IEEE Transactions on*, 41(9): 1940-1949.

Bengtson, H., 2010. Hydraulic Design of Storm Sewers, Including the Use of Excel, an online, continuing education course for PDH credit. Retrieved from http://www.onlinepdh.com/engcourses/course/view.php?id=64

Bhatt, G. D., Sinha, K., Deka, P. K. and Kumar, A., 2014. Flood Hazard and Risk Assessment in Chamoli District, Uttarakhand Using Satellite Remote Sensing and GIS Techniques. *International Journal of Innovative Research in Science, Engineering and Technology*, 3(8): 9.

Billi, P., Alemu, Y. T. and Ciampalini, R., 2015. Increased frequency of flash floods in Dire Dawa, Ethiopia: Change in rainfall intensity or human impact? *Natural Hazards*, 76: 1373-1394. doi: 10.1007/s11069-014-1554-0 1-22.

Birkmann, J., 2007. Risk and vulnerability indicators at different scales: Applicability, usefulness and policy implications. *In Environmental Hazards* 7: 20-31.

Blaschke, T., 2010. Object based image analysis for remote sensing. *ISPRS Journal of Photogrammetry and Remote Sensing*, 65(1): 2-16.

Bremner, J., Lopez-Carr, D., Suter, L., and Davis, J., 2010. Population, poverty, environment, and climate dynamics in the developing world. *Interdisciplinary Environmental Review*, 11(2): 112-126.

Brou, Y. T., 2005. Climat, mutations socio-économiques et paysages en Côte d'Ivoire. Mém. HDR, Univ. Sci. Techn. Lille, France, 212. (*In French*)

Brou, Y. T., 1997. Analyse et dynamique de la pluviométrie dans le Sud forestier ivoirien : recherche de corrélations entre les variables climatiques et les variables liées aux activités anthropiques. Thèse 3ème cycle, Univ. Cocody, Côte d'Ivoire, 211. (*In French*)

Brou, Y. T., 2005. Climat, mutations socio - économiques et paysages en Côte d'Ivoire, Rapport d'activités scientifique, pédagogique, administrative et publications. Memoire HDR, 106. (*In French*)

Carlo, G., Silvio, G., and Valentina G., 2013. A dynamic assessment tool for exploring and communicating vulnerability to floods and climate change. *Environmental Modelling & Software*, 44: 136-147. Contents lists available at SciVerse ScienceDirect, journal homepage: www.elsevier.com/locate/envsoft.

Chakraborty, A. and Joshi, P K., 2014. Mapping disaster vulnerability in India using analytical hierarchy process. *Geomatics, Natural Hazards and Risk*, 20. doi: 10.1080/19475705.2014.897656

Charlchai, T., Chao, Y., Abdollah, B. and Omthip, D., 2004. Assessment of flood risk in Hat Yai Municipality, Southern Thailand, using GIS. *Journal of Natural Disaster Science*, 26(1): 1-14.

Cheikh, M., Aminata, D., Amadou, T. D. and Cheikh, I. N., 2008. Urban sprawl development and flooding at Yeumbeul suburb (Dakar-Senegal). *African Journal of Environmental Science and Technology*, 2(4): 075-088. Available online at http://www.academicjournals.org/AJest.

Chen, J., Hill, A. A. and Urbano, L. D., 2009. A GIS-based model for urban flood inundation. *Journal of Hydrology*, 373: 184-192.

Cinco, T. A., de Guzman, R. G., Hilario, F. D. and Wilson, D. M., 2014. Long-term trends and extremes in observed daily precipitation and near surface air temperature in the Philippines for the period 1951–2010. *Atmospheric Research*, 145-146: 12-26. doi: http://dx.doi.org/10.1016/j.atmosres.2014.03.025

Cloke, H. L., Wetterhall, F., He, Y., Freer, J. E. and Pappenberger, F., 2013. Modelling climate impact on floods with ensemble climate projections. *Quarterly Journal of the Royal Meteorological Society*, 139(671): 282-297.

Cristobal, J., 2011. Combining remote sensing and GIS climate modelling to estimate daily forest evapotranspiration in a Mediterranean mountain area. *Hydrology and Earth System Sciences*, 13.

Dabara, I. D., 2012. Analysis of the relationships of urbanization dynamics and incidences of urban flood disaster in gombe metropolis, Nigeria. *Journal of Sustainable Development in Africa*, 14(2), 14.

Dauphine, A., 2001. Risques et catastrophe, Observer Spatialiser Comprendre Gérer, Armand Colin, Paris, 288. (*In French*)

Drăguţ, L., Csillik, O., Eisank, C., Tiede, D., 2014. Automated parameterisation for multi-scale image segmentation on multiple layers. *ISPRS Journal of Photogrammetry and Remote Sensing*, 88: 119–127.

Drăguţ, L., Tiede, D., and Levick, S.R., 2010. ESP: a tool to estimate scale parameter for multiresolution image segmentation of remotely sensed data. *International Journal of Geographical Information Science*, 24(6): 859-871.

Dronova, I., Gong, P., Wang, L., and Zhong, L., 2015. Mapping dynamic cover types in a large seasonally flooded wetland using extended principal component analysis and object-based classification. *Remote Sensing of Environment*, 158: 193-206.

Duan, W., He, B., Takara, K., Luo, P., Nover, D., Yamashiki, Y., Huang, W., 2014. Anomalous atmospheric events leading to Kyushu's flash floods, July 11-14, 2012. *Natural Hazards*, 73: 1255-1267.

Efstratiadis, A., Koussis, A. D., Koutsoyiannis, D., and Mamassis, N., 2014. Flood design recipes vs. reality: can predictions for ungauged basins be trusted. *Natural Hazards Earth System Sciences*, 14: 1417-1428.

Elmoustafa, A. and Mohamed, M., 2013. Flash Flood Risk Assessment Using Morphological Parameters in Sinai Peninsula. *Open Journal of Modern Hydrology*, 3(3): 122-129. doi: 10.4236/ojmh.2013.33016

Forkuo, E. K., 2011. Flood Hazard Mapping using Aster Image data with GIS. *International Journal of Geomatics and Geosciences*, 1(4): 19.

Forkuo, E. K., 2013. The use of digital elevation models for water-shed and flood hazard mapping. *International Journal of Remote Sensing and Geosciences*, 2(2): 10.

Fossou, R. M. N., Soro, N., Traore,V. B., Lasm, T., Sambou, S., Soro, T., Orou, R. O., Cisse, M. T. et Kane, A., 2014. Variabilité climatique et son incidence sur les ressources en eaux de surface: cas des stations de Bocanda et de Dimbokro, Centre-Est de la Côte d'Ivoire en Afrique de l'Ouest. *Afrique SCIENCE*, 10(4): 118-134. (*In French*)

Francesca, F., Emanuele, M. and Gabriele, B., 2014. Remote sensing analysis for flood risk management in urban sprawl contexts. *Geomatics, Natural Hazards and Risk*, 19. doi: 10.1080/19475705.2014.913695.

Gbode, I. E., Akinsanola, A. A. and Ajayi, V.O., 2015. Recent Changes of Some Observed Climate Extreme Events in Kano. *International Journal of Atmospheric Sciences*, Article ID 298046, 6. http://dx.doi.org/10.1155/2015/298046

Gerl, T., Bochow, M. and Kreibich, H., 2014. Flood Damage Modelling on the Basis of Urban Structure Mapping Using High-Resolution Remote Sensing Data. *Water*, 6: 2367-2393. doi:10.3390/w6082367.

GIEC, 2007. Bilan 2007 des changements climatiques. Contribution des Groupes de travail I, II et III au quatrième Rapport d'évaluation du Groupe d'experts intergouvernemental sur l'évolution du climat [Équipe de rédaction principale, Pachauri, R.K. et Reisinger, A. (publié sous la direction de~)]. GIEC, Genève, Suisse, 103. (*In French*)

Goetz, S. J., Smith, A. J., Jantz, C., Wright, R. K., Prince, S. D., Mazzacato, M. E., and Melchior, B., 2003. Monitoring and predicting urban land use change. In Proc. *IEEE International, Geoscience and Remote Sensing Symposium, IGARSS*, 3: 1567-1569.

Goneri, L. C., Manuel, G., Thomas, B., Carola, M., Marissa, Y., 2013. An AHP-derived method for mapping the physical vulnerability of coastal areas at regional scales. *Natural Hazards*

and Earth System Sciences, European Geosciences Union (EGU), 13: 1209-1227. doi: 10.5194/nhess-13-1209-2013.

Gong, P. and HOWARTH, P., 1990. The use of structural information for improving land-cover classification accuracies at the rural-urban fringe. *Photogrammetric Engineering and Remote Sensing*, 56(1): 67-73.

Goodarzi, E., Bavani M.A., Dastorani, M.T. and Talebi, A., 2014. Evaluating effect of downscaling methods; change-factor and LARS-WG on surface runoff (A case study of Azam-Harat River basin, Iran). *Desert*, 19 (2): 99-109.

Goula, B. T. A., Kouassi, V. J. and Savane, I., 2006. Impacts du changement climatique sur les ressources en eau en zone tropicale humide : cas du bassin versant du Bandama en Côte d'Ivoire. *Agron. Afr.*, 18(1) 1-11. (*In French*)

Hallegatte, S., Fanny, H., Anand, P., Narayanan, K., Subimal, G., Subhankar, K., Unmesh, P., Abhijat, A., Sanjib, P., Jan, C-M., Celine, H., Nicola, R., Sumana, B., Bachu, M., Priya, S., Dhore, K., Rafique, F., Mathur, P., Naville, N., 2010. Flood Risks, Climate Change Impacts and Adaptation Benefits in Mumbai: An Initial Assessment of Socio-Economic Consequences of Present and Climate Change Induced Flood Risks and of Possible Adaptation Options", OECD Environment Working Papers, No. 27, OECD Publishing. 62.

Halwatura, D. and Najim, M. M. M., 2013. Application of the HEC-HMS model for runoff simulation in a tropical catchment. *Environmental Modelling & Software*, 46: 155-162.

Hamid, R. P., Masood, B. and Biswajeet, P., 2014. A comparative assessment of prediction capabilities of modified analytical hierarchy process (M-AHP) and Mamdani fuzzy logic

models using Netcad-GIS for forest fire susceptibility mapping. *Geomatics, Natural Hazards and Risk*, 27. doi: 10.1080/19475705.2014.984247.

Hamlet, A. F., 2011. Assessing water resources adaptive capacity to climate change impacts in the Pacific Northwest Region of North America. *Hydrology and Earth System Sciences*, 44374471.

Hapuarachchi, H. A. P., Wang, Q. J. and Pagano, T. C., 2011. A review of advances in flash flood forecasting. *Hydrological Processes*, 25: 2771-2784.

Hauhouot, C., 2008. Analysis of the rainfall risks in the precarious Districts of Abidjan: Survey of cases in Attécoubé, *Geo-Eco-Trop*, 32: 75-82.

Haylock, M. R., Peterson, T. C., Alves, L. M., Ambrizzi, T., Anunciação, Y. M. T., Baez,J., Barros, V. R., Berlato, M. A, Bidegain, M., Coronel, G., Corradi, V., Garcia, V. J., Grimm, A .M., Karoly, D., Marengo, J.A., Marino, M.B., Moncunill, D. F., Nechet, D., Quintana, J., Rebello, E., Rusticucci, M., Santos, J. L., Trebejo, I., Vincent, L. A., 2006. Trends in to taland extreme South American rainfall in 1960-2000 and links with sea surface temperature. *Journal of Climate*, 19: 1490-1512.

Hellmers, S., Manojlovic, N., Palmaricciotti, G., Kurzbach S. and Fröhle, P., 2015. Multiple linked sustainable drainage systems in hydrological modelling for urban drainage and flood risk management. *Journal of Flood Risk Management*, 12. doi: 10.1111/jfr3.12146

Herold, M., Scepan, J. and Clarke, K. C., 2002. The use of remote sensing and landscape metrics to describe structures and changes in urban land uses. *Environment and Planning A*, 34(8): 1443-1458.

Herold, M., Scepan, J., Müller, A. and Günther, S., 2002. Object-oriented mapping and analysis of urban land use/cover using IKONOS data. In 22nd Earsel Symposium Geoinformation for European-Wide Integration, 4-6.

Hubert, P., Carbonel, J P., Chaouche, A., 1989. Segmentation des séries hydrométéorologiques. Application à des séries de précipitations et de debits de l'Afrique de l'Ouest, *Journal de l'Hydrologie*, 110: 349-367. (*In French*)

Huck, A., Hese, S., and Banzhaf, E., 2011. Delineating parameters for object-based urban structure mapping in Santiago de Chile using QuickBird data.*The International Archives of the Photogrammetry, Remote Sensing and Spatial Information Sciences*, 38(4/W19): 6.

Huong, H. T. L., and Pathirana, A., 2013. Urbanization and climate change impacts on future urban flooding in Can Tho city, Vietnam. *Hydrol. Earth Syst. Sci*., 17: 379-394. www.hydrolearth-syst-sci.net/17/379/2013/doi:10.5194/hess-17-379-2013.

ICSU Regional Office for Africa, 2007. Natural and Human-induced Hazards and Disasters in sub-Saharan Africa, 32.

Intergovernmental Panel on Climate Change (IPCC), 2007. Climate Change 2007: Impacts, Adaptation and Vulnerability. Contribution of Working Group II to the Fourth Assessment Report of the Intergovernmental Panel on Climate Change. ML PARRY, OF CANZIANI, JP PALUTIKOF, PJ VAN DER LINDEN & CE HANSON (Eds.). Cambridge University Press, Cambridge, UK, 976.

Intergovernmental Panel on Climate Change (IPCC), 2007. Climate Change 2007: Synthesis Report. Contribution of Working Groups I, II and III to the Fourth Assessment Report of

the Intergovernmental Panel on Climate Change [Core Writing Team, Pachauri, R.K and Reisinger, A. (eds.)]. IPCC, Geneva, Switzerland, 104.

Jansen, L. J. and Di Gregorio, A., 2002. Parametric land cover and land-use classifications as tools for environmental change detection. *Agriculture, Ecosystems & Environment*, 91(1): 89100.

Jeyaseelan, A. T., 2003. Droughts and floods assessment and monitoring using remote sensing and GIS. *Satellite remote sensing and GIS applications in agricultural meteorology*, 291-313.

Johann, G. and Leismann, M., 2013. How to realise flood risk management plans efficiently in an urban area – the Seseke project. *Journal of Flood Risk Management*, 9. doi: 10.1111/jfr3.12075.

Jourda, J. P., Kouame, K. J., Saley, M. B., Kouamé, K. F., Kouadio, B. H. and Kouame, K., 2006. A new cartographic approach to determine the groundwater vulnerability of the Abidjan aquifer. *Groundwater Pollution in Africa*, 103-114.

Jourda, J. P., Kouame, K. F., Soro, N., Kouame, K. J.; Kouadio, B. H., Saley, M. B., Kouame, k. et Ahoussi, E., 2003. Gestion et protection des eaux souterraines urbaines: apports d'un système d'information géographique à la réalisation de la carte de vulnérabilité de la nappe du continental terminal au niveau de l'agglomération d'Abidjan. 7ème édition de la Conférence Francophone ESRI France. (*In French*)

Kebede, B., 2012. Application of GIS and Remote Sensing Techniques for Flood Hazard and Risk Assessment: The Case of Dugeda Bora Woreda of Oromiya Regional State, Ethiopia. Paper

for the 2012 Berlin Conference on the Human Dimensions of Global Environmental Change, 17.

Keggenhoff, I., Elizbarashvili, M., Amiri-Farahani, A., and King, L., 2014. Trends in daily temperature and precipitation extremes over Georgia, 1971–2010. *Weather and Climate Extremes*, 4: 75-85. doi: http://dx.doi.org/10.1016/j.wace.2014.05.001

Kendall, M.G., 1975. Rank correlation methods, Charles Griffin, London Lettenmaier d.p. (1988). Multivariate Nonparametric Tests for Trend in Water Quality. *Water Resources Bulletin*, 24: 505-512.

Kevin, M., Siddique, M., Julian, S., 2012. Using Multi-criteria Evaluation and GIS for Flood Risk Analysis in Informal Settlements of Cape Town: The Case of Graveyard Pond. *South African Journal of Geomatics*, 1(1): 15.

Kim, B-S. and Kim, H-S., 2014. Evaluation of flash flood severity in Korea using the modified flash flood index (MFFI). *Journal of Flood Risk Management*, 13. doi: 10.1111/jfr3.12057

Knebl, M. R., Yang, Z. L., Hutchison, K., Maidment, D. R., 2005. Regional scale flood modelling using NEXRAD rainfall, GIS, and HEC-HMS/RAS: a case study for the San Antonio River Basin Summer 2002 storm event. *Journal of Environmental Management*, (75): 325-336.

Kouame, K. J., Jourda, J. P., Saley, M. B., Deh, S. K., Anani, A. T. and Biemi, J., 2013. Mapping of groundwater vulnerability zones to pollution in various hydrogeological environments of Côte d'Ivoire by drastic method. *International Journal of Scientific & Engineering Research*, 4(5): 9.

Kouassi, A. M., Kouame, K. F., Goula, B. T. A., Lasm, T., Paturel, J. E. & Biemi, J., 2008. Influence de la variabilité climatique et de la modification de l'occupation du sol sur la relation pluie-débit a partir d'une modélisation globale du bassin versant du N'zi (Bandama) en Côte d'Ivoire. *Rev Ivoir. Sci. Technol*., 11: 207-229. (*In French*)

L'Hote, Y., Mahé, G., Some, B., Triboulet, J.P., 2002. Analysis of a Sahelian annual rainfall indexfrom1896to2000; the drought continues. *Hydrological Sciences Journal*, 47(4): 563572.

Lambin, E. F., Rounsevell, M. D. A. and Geist, H. J., 2000. Are agricultural land-use models able to predict changes in land-use intensity? *Agriculture, Ecosystems & Environment*, 82(1): 321-331.

Lambin, E. F., Turner, B. L., Geist, H. J., Agbola, S. B., Angelsen, A., Bruce, J. W., ... and Xu, J., 2001. The causes of land-use and land-cover change: moving beyond the myths. *Global Environmental Change*, 11(4): 261-269.

Loroux, B. F. E., 1978. Contribution à l'étude hydrogéologique du bassin sédimentaire côtier de Côte d'Ivoire. Thèse Université de Bordeaux I, France, 93.

Lubes-Niel, H., Masson, J. M., Paturel, J. E., Servat, E., 1998.Variabilité climatique et statistiques. Etude par simulation de la puissance et de la robustesse de quelques tests utilisés pour vérifier l'homogénéité de chroniques. *Revue des Sciences de l'Eau*, 3: 383-408. (*In French*)

Lv, Q., Dou, Y., Niu, X., Xu, J., Xu, J., and Xia, F., 2015. Urban Land Use and Land Cover Classification Using Remotely Sensed SAR Data through Deep Belief Networks. *Journal of Sensors*, 501: 538063.

Marzocchi, W., Mastellone, M. L., Di, R. A., Novelli, P., Romeo, E. and Gasparini, P., 2009. Principles of multi-risk assessment: Interaction amongst natural and man-induced risks. EUROPEAN COMMISSION, Directorate-General for Research, Environment Directorate: Research performed in the frame of Na.R.As (NATURAL RISKS ASSESSMENT), 76. doi: 10.2777/30886

Masaru, M. and Hiroyuki, Y., 2010. Quantification of increased flood risk caused by global climate change for urban river management Planning, Selected for publication in "Water Science & Technology". Reproduced with the permission of IWA Publishing. *NOVATECH*, 12.

McSharry, P. E., Max, A. L., Harvey, J., Rodda, E. and Rodda, J., 2013. Quantifying flood risk of extreme events using density forecasts based on a new digital archive and weather ensemble predictions, *Quarterly Journal of the Royal Meteorological Society*, 139: 328333.

Megahed, Y., Cabral, P., Silva, J. and Caetano, M., 2015. Land Cover Mapping Analysis and Urban Growth Modelling Using Remote Sensing Techniques in Greater Cairo Region-Egypt. *ISPRS International Journal of Geo-Information*, 4(3): 1750-1769.

Meraj, G., Romshoo, S. A., Yousuf, A. R., Altaf, S. and Altaf, F., 2015. Assessing the influence of watershed characteristics on the flood vulnerability of Jhelum basin in Kashmir Himalaya. *Natural Hazards*, 77: 153-175. doi 10.1007/s11069-015-1605-1.

Ministere de l'Amenagement du Territoire et de l'Environnement (MATE), 2001. Textes relatifs à la prévention des risques naturels majeurs, Recueil des textes fondateurs, 1ére édition, DPPR-SDPRM, 155. (*In French*)

Mohammed, S., Mohammad, S. H. S., Shamim, M. H., 2013. Disaster risk index: How far should it take account of local attributes? *International Journal of Disaster Risk Reduction*, 3: 76-87.

Molanejad, M., Soltani, M. and Saadat, A. R. A., 2014. Simulation of extreme temperature and precipitation events using LARS-WG stochastic weather generator. *International Journal of Scholarly Research Gate*, 2 (3): 121-129.

Morjani, Z. E. A. E., 2011. Methodology document for the WHO e-atlas of disaster risk.Volume 1. Exposure to natural hazards Version 2.0 Flood hazard modelling, 1: 35. Taroudant polydisciplinary faculty of the Ibn Zohr University of Agadir, Morocco.

Morjani, Z. E. A. E., 2011. Methodology document for the WHO e-atlas of disaster risk.Volume 1. Exposure to natural hazards Version 2.0 preparation of the datasets, 122. Taroudant polydisciplinary faculty of the Ibn Zohr University of Agadir, Morocco.

Mouhamed, L., Traore, S. B., Alhassane, A. and Sarr, B., 2013. Evolution of some observed climate extremes in the West African Sahel. *Weather and Climate Extremes*, 1: 19-25.

Mulders, M. A., 2001. Advances in the application of remote sensing and GIS for surveying mountainous land. *International Journal of Applied Earth Observation and Geoinformation*, 3(1): 3-10.

Musungu, K., Motala, S. and Smit, J., 2012. Using multi-criteria evaluation and GIS for flood risk analysis in informal settlements of Cape Town: the case of Graveyard Pond. *South African Journal of Geomatics*, 1(1): 92-108.

Nejad, A. R. V., Esmaeili, S. and Aghamohammadi, H., 2015. Earthquake Risk Modeling using GIS for urban buildings, Case study: Tehran Municipality, District 3. *Advances in Natural and Applied Sciences*, 9(1): 36-43.

New, M., Hewitson, B., Stephenson, D.A., Tsiga, A., Kruger, A., Manhique, A., Gomez, B., Coelho, C.A.S., Masisi, D.N., Kululanga, E., Mbambalala, E., Adesina, F., Saleh, H., Kanyanga, J., Adosi, J., Bulane, L., Fortunata, L., Mdoka, M.L., Lajoie, R., 2006. Evidence of trends in daily climate extremes over Southern and West Africa. *J. Geophys. Res*., 111, D14102. http://dx.doi.org/10.1029/2005JD006289.

Nicholson, S. E., Kim, J., Hoopingarner, J., 1988. Atlas of African rainfall and its variability. Tallahassee: Florida State University.

Noori, M., Sharifi, M. B., Zarghami, M. and Heydari, M., 2013. Utilization of LARS Model for Modelling of Meteorological Parameters in Golestan, Province of Iran. *Journal of River Engineering*, 1(1).

Norton, B. A., Coutts, A. M., Livesley, S. J., Harris, R. J., Hunter, A. M., and Williams, N. S., 2015. Planning for cooler cities: A framework to prioritise green infrastructure to mitigate high temperatures in urban landscapes. *Landscape and Urban Planning*, 134: 127-138.

Novack, T. and Stilla, U., 2014. Classification of Urban Settlements Types based on space-borne SAR datasets. *In ISPRS Annals of Photogrammetry, Remote Sensing and Spatial Information Sciences*, II-7(1): 55-60.

Nuri, A. Z., Farzaneh, M. and Espanayi, K., 2014. Assessment of climatic parameters uncertainty under effect of different downscaling techniques. *International Research Journal of Applied and Basic Sciences*, 8(9): 1316-1320.

Nyarko, B. K., 2002. Application of a Rational Model in GIS for Flood Risk Assessment in Accra, Ghana. *Journal of Spatial Hydrology*, 2(1): 14.

Osman, Y., Al-Ansari, N., Abdellatif, M., Aljawad, S. B. and Knutsson, S., 2013. Expected Future Precipitation in Central Iraq Using LARS-WG Stochastic Weather Generator. *Engineering*, 6: 948-959. http://dx.doi.org/10.4236/eng.2014.613086

Papaioannou, G., Vasiliades, L. and Loukas, A., 2015. Multi-Criteria Analysis Framework for Potential Flood Prone Areas Mapping. *Water Resource Management*, 29: 399-418. doi 10.1007/s11269-014-0817-6.

Papon, A. and Lemarchand, R., 1973. Géologie et minéralisation du Sud- Ouest de la Cote d'Ivoire : Synthèse des travaux de l'opération SASCA, SODEMI-Abidjan, 285. (*In French*)

Pasche, E., Manojlovic, N. and Behzadnia, N., 2008. Floods in Small Urban Catchments: Hydrological Sensitivity, Risk Assessment and Efficient Integrative Strategies of Mitigation. 11th International Conference on Urban Drainage, Edinburgh, Scotland, UK, 2008, 11.

Paturel, J. E., Servat, E., Kouame, B., Lubes-Niel, H., Ouedraogo, M., Masson, J. M., 1997. Climatic variability in humid Africa along the Gulf of Guinea Part II: an integrated regional approach. *Journal of Hydrology*, 191: 16-36.

Pedcris, M. O. and Masahiko, F., 2013. A localized disaster-resilience index to assess coastal communities based on an analytic hierarchy process (AHP). *International Journal of Disaster Risk Reduction*, 3: 62–75.

Pedersen, A. N., Mikkelsen, P. S. and Arnbjerg-Nielsen, K., 2012. Climate change-induced impacts on urban flood risk influenced by concurrent hazards. *Journal of Flood Risk Management*, 5: 203-214.

Pettitt, A. N., 1979. A non-parametric approach to the change–point problem, *Appl. Statist.*, 28(2): 126-135.

Rao, C. N., 2014. Climate change analysis in southern Telangana region, Andhra Pradesh using LARS-WG model. *CURRENT SCIENCE*, 107(1), 54.

Rau, J-Y., Jhan, J. P. and Hsu, Y. C., 2015. Analysis of Oblique Aerial Images for Land Cover and Point Cloud Classification in an Urban Environment.

Raza, S. F., Ahsan, M. S. and Ahmad, S. R., 2014. Rapid assessment of a flood-affected population through a spatial data model. *Journal of Flood Risk Management*, 7. doi: 10.1111/jfr3.12134.

Revadekar, J. V., Patwardhan, S. K. and Rupa, Kumar, K., 2011. Characteristic Features of Precipitation Extremes over India in the Warming Scenarios. *Advances in Meteorology*, Volume 2011, Article ID 138425, 11. doi:10.1155/2011/138425.

Saadat, H., Adamowski, J., Bonnell, R., Sharifi, F., Namdar, M., and Ale-Ebrahim S., 2011. Land use and land cover classification over a large area in Iran based on single date analysis of satellite imagery. *ISPRS Journal of Photogrammetry and Remote Sensing*, 66(5): 608-619.

Saadat, H., Adamowski, J., Tayefi, V., Namdar, M., Sharifi, F. and Ale-Ebrahim, S., 2014. A new approach for regional scale interrill and rill erosion intensity mapping using brightness index assessments from medium resolution satellite images. *Catena*, 113: 306-313.

Saaty, T. L., 1980. The Analytic Hierarchy Process: Planning, Priority setting, Resource allocation, Mc Graw-Hill, New York, 19.

Saaty, T. L., 1990. The Analytic Hierarchy Process: Planning, Priority setting, Resource allocation, Mc Graw-Hill, New York, 19.

Salajegheh, A., Bakhshaei, M., Chavoshi, S., Keshtkar, A. R., Najafi, Hajivar, M., 2009. Floodplain mapping using HEC-RAS and GIS in semi-arid regions of Iran. *DESERT*, 14: 83-93.

Saley, M. B., Danumah, J. H., Sorokoby, V. M., Kanohin, F. O., Atcheremi, D., Denean, S. P., Kouame, F. K. and Djagoua, V. E., 2013. Méthodologie pour la cartographie des zones vulnerables a l'inondation par systeme d'information géographique et analyse multicritère: application au bassin versant de la Davo a Sassandra (sud-ouest de la Cote d'Ivoire). *Africa Geoscience Review*, 20(1): 21-33. (*In French*)

Saley, M. B., Kouame, K. F., Penven, M. J., Biémi, J. and Kouadio, B. H., 2005. Cartographie des zones à risque d'inondation dans la région semi-montagneuse à l'Ouest de la Côte d'Ivoire: Apports des MNA et de l'imagerie satellitaire. *Télédétection* 5(1-2-3): 53-67. (*In French*)

Sanyal, J., and Xi, L. X., 2003. Application of GIS in flood hazard mapping: a case study of Gangetic West Bengal, India. Paper presented at the Poster session of Map Asia 2003, 8. http://www.gisdevelopment.net/application/natural_hazards/floods/pdf/ma03138.pdf

Sarr, B., 2011. Return of heavy downpours and floods in a context of changing climate. Climate change in the Sahel. A challenge for sustainable development. AGRHYMET Monthly Bulletin (Special Issue), 9-11. http://www.agrhymet.ne/PDF/Bulletin%20mensuel/specialChCang.pdf〉.

Savane, I., Coulibaly, N. and Soro, N., 2003. Analyse multicritère spatiale pour l'identification de la vulnérabilité aux risques naturels d'Abobo (banlieue de la ville d'Abidjan, Côte d'Ivoire). *Rev. Ivoir. Sci. Technol*, 4: 94-107. (*In French*)

Savane, I., Coulibaly, K.M. and Gioan, P., 2003. Variabilité climatique et ressources en eaux souterraines dans la région semi-montagneuse de Man. *Secheresse*, 12(4): 231-237. (*In French*)

Schnebele, E. and Cervone, G., 2013. Improving remote sensing flood assessment using volunteered geographical data. *Nat. Hazards Earth Syst. Sci.*, 13: 669-677. doi:10.5194/nhess-13-669-2013.

Sekac, T. and Jana, S. K., 2014. Change detection of busu river course in Papua New Guineaimpact on local settlements using Remote Sensing and GIS Technology. *International Journal of Scientific & Engineering Research*, 5(8): 891.

Semenov, M. A. and Brooks, R. J., 1999. Spatial interpolation of the LARS-WG stochastic weather generator in Great Britain. *Climate Research*, 11: 137-148.

Semenov, M. A. and Barrow, E. M., 1997. Use of a stochastic weather generator in the development of climate change scenarios. *Climatic Change*, 35: 397-414.

Semenov, M. A. and Barrow, E. M., 2002. LARS-WG: A Stochastic Weather Generator for Use in Climate Impact Studies, 28.

Semenov, M. A. and Stratonovitch, P., 2010. Use of multi-model ensembles from global climate models for assessment of climate change impacts. *Climate Research*, 41: 1-14.

Semenov, M. A., Brooks, R. J., Barrow, E. M., Richardson, and Clarence, W., 1998. Comparison of the WGEN and LARS-WG stochastic weather generators for diverse climates. *Climate Research*, 10: 95-107.

Semenov, M., 2014. Delivering CMIP5-based climate scenarios for impact assessments in Europe. EGU General Assembly Conference Abstracts, 1.

Servat, E., Paturel, J. E., Kouame, B., Travalglio, M., Ouedraogo, M., Lubes-Niel, H., Fristch, J. M., Masson, J. M. et Marieu, B., 1998. Identification, caractérisation et conséquence d'une variabilité hydrologique en Afrique de l'Ouest et Centrale. *In Water Ressources Variability in Africa during the XXth Century, IAHS Publication*, 252: 323-337. (*In French*)

Singh, K. K., Nigam, M. J. and Pal, K., 2014. Detection of 2011 Tohoku Tsunami Inundated Areas in Ishinomaki City Using Generalized Improved Fuzzy Kohonen Clustering Network. *European Journal of Remote Sensing*, 47, 461-475.

Sobhany, B. and Fateminiya, F. S., 2014. Modelling of Climatic Parameters in Province of Southern Khorasan. *Physical Geography*, 46(3): 9.

Song, X., Zhang, J., Zhan, C., Xuan, Y., Ye, M. and Xu, C., 2015. Global sensitivity analysis in hydrological modeling: Review of concepts, methods, theoretical framework, and applications. *Journal of Hydrology*, 523: 739-757.

Sowmya, K., John, C M. and Shrivasthava, N K., 2015. Urban flood vulnerability zoning of Cochin City, southwest coast of India, using remote sensing and GIS. *Natural Hazards,* 75: 12711286.

Stephenne, N. and Lambin, F. E., 2001. A dynamic simulation model of land-use changes in Sudano-sahelian countries of Africa (SALU). *Agriculture, Ecosystems and Environment*, 85: 145-161.

Stephenson, T. S., Vincent, L. A., Allen, T., Van Meerbeeck, C. J., McLean, N., Peterson, T. C. ... and Trotman, A. R., 2014. Changes in extreme temperature and precipitation in the Caribbean region, 1961–2010. *International Journal of Climatology*, 34 (9): 2957-2971.

Stoll, S., Hendricks, Franssen, H. J., Butts, M. and Kinzelbach, W., 2011. Analysis of the impact of climate change on groundwater related hydrological fluxes: a multi-model approach including different downscaling methods. *Hydrology and Earth System Sciences. Sci*., 15: 21-38.

Strobl, R. O., Forte, F. and. Lonigro, T., 2012. Comparison of the feasibility of three flood-risk extent delineation techniques using Geographic Information System: case study in Tavoliere delle Puglie, Italy. *Journal of Flood Risk Management,* 5: 245-257.

Sudha, Y., 2012. A Hybrid Approach of Integrating HEC-RAS and GIS Towards the Identification and Assessment of Flood Risk Vulnerability in the City of Jackson, MS. *American Journal of Geographic Information System*, 1(1): 7-16. doi: 10.5923/j.ajgis.20120101.02.

Tang, J., 2015. Modelling Urban Land Use Change: Integrating Remote Sensing with Socioeconomic Data. *Computational Approaches for Urban Environments, Springer,* 293310.

Tanoh, K. R., 2007. Analyse spatio-temporelle de la relation pluie-nappe du continental terminal dans le District d'Abidjan (Sud de la Côte d'Ivoire), mémoire de DEA, Université de Cocody, 63.

Tastet, J. P., 1979. Environnements sédimentaires et structuraux quaternaires du littoral du golfe de Guinée (Côte d'Ivoire, Togo, Bénin). Thèse de Doctorat d'Etat ès Sciences Naturelles. Université de Bordeaux I. Bordeaux (France), 212.

Tehrany, M. S., Pradhan, B., Mansor, S., Ahmad, N., 2015. Flood susceptibility assessment using GIS-based support vector machine model with different kernel types. *Catena*, 125: 91-101.

Thieken, A., Bruno, M., Heidi, K., Heiko, A., 2006. Methods for flood risk analysis: Concepts and challenges: International Workshop on Flash Floods in Urban Areas, Muscat – Sultanate of Oman, 4-6 September 2006, 12.

Todini, F., De Filippis, T., De Chiara, G., Maracchi, G., Martina, M. L. V., and Todini, E., 2004. Using a GIS approach to asses flood hazard at national scale. Paper presented at the European Geosciences Union, 1st General Assembly, Nice, France, 2004.

Trnka, M., Rötter, R. P., Ruiz-Ramos, M., Kersebaum, K. C., Olesen, J. E., Žalud, Z. and Semenov, M. A., 2014. Adverse weather conditions for European wheat production will become more frequent with climate change. *Nature Climate Change*, 4: 7. doi: 10.1038/NCLIMATE2242.

Tsakiris, G., 2014. Flood risk assessment: concepts, modelling, applications. *Natural Hazards Earth System Sciences*, 14: 1361-1369. doi:10.5194/nhess-14-1361-2014.

Txomin, H. L., Ruiz, A., José, Gil-Yepes, L., Jorge, A. R., Josep, E.P-P., 2013. Multi-level object-based urban mapping from remote sensing and GIS data. GIS Ostrava 2013 - Geoinformatics for City Transformation, 10.

UICN-BRAO, GWP-WAWP, CILSS, 2003. Eau, changement climatique et désertification en Afrique de l'ouest : Stratégie régionale de préparation et d'adaptation, 59.

UNISDR, (UNITED NATIONS INTERNATIONAL STRATEGY FOR DISASTER REDUCTION), 2009. Global Assessment Report on Disaster Risk Reduction. Risk and Poverty in a Changing Climate –Invest today for a safer tomorrow United Nations, Geneva, Switzerland.

Van Dijk, A. I. J. M. and Renzullo, L. J., 2011. Water resource monitoring systems and the role of satellite observations, *Hydrology and Earth System Sciences*, 17.

Wang, X. L., 2008. Penalized maximal F test for detecting undocumented mean shift without trend change. *Journal of Atmospheric and Oceanic Technology*, 25(3): 368-384.

Wang, X. L., Chen, H., Wu, Y., Feng, Y. and Pu, Q., 2010. New techniques for the detection and adjustment of shifts in daily precipitation data series. *Journal of Applied Meteorology and Climatology*, 49(12): 2416-2436.

Wang, X. L. and Feng, Y., 2010. RHtestsV3 User Manual. Available online at http://cccma. seos. uvic. ca/ETCCDMI/RHtest/RHtestsV3 UserManual. doc. Climate Research Division, Science and Technology Branch, Environment Canada, Toronto, Ontario, Canada.

Wang, Y., Li, Z., Tang, Z. and Zeng, G., 2011. A GIS-Based Spatial Multi-Criteria Approach for Flood Risk Assessment in the Dongting Lake Region, Hunan, Central China. *Water Resour Manage*, (25): 3465–3484. doi: 10.1007/s11269-011-9866-2.

Wu, W., Zhao, S., Zhu, C. and Jiang, J., 2015. A comparative study of urban expansion in Beijing, Tianjin and Shijiazhuang over the past three decades. *Landscape and Urban Planning*, 134: 93-106.

Wurm, M., Taubenböck, H. and Dech, S., 2010. Quantification of urban structure on building block level utilizing multisensoral remote sensing data. *Remote Sensing*, 78310H-78310H.

Wurm, M., Taubenbock, H., Roth, A. and Dech, S., 2009. Urban structuring using multisensoral remote sensing data: By the example of the German cities Cologne and Dresden. Urban *Remote Sensing Event*, 1-8.

Yahaya, S., Ahmad, N., Abdalla, R. F., 2010. Multi-criteria analysis for flood vulnerable areas in Hadejia-Jama'are River basin, Nigeria. *European Journal of Scientific Research*, 42(1): 71-83.

Yalcin, A., 2008. GIS-based landslide susceptibility mapping using analytical hierarchy process and bivariate statistics in Ardesen (Turkey): comparisons of results and confirmations. *Catena*, 72(1): 1-12.

Yalcin, G., Akyurek, Z., 2004. Analyzing flood vulnerable areas with multicriteria evaluation, 6.

Yan, G., Qi, F., Wei, L., Aigang, L., Yu, W., Jing, Y., ... and Qianqian, M., 2014. Changes of daily climate extremes in Loess Plateau during 1960-2013. *Quaternary International*, 1-17. http://dx.doi.org/10.1016/j.quaint.2014.08.052.

Yan, W. Y., Shaker, A., and El-Ashmawy, N., 2015. Urban land cover classification using airborne LiDAR data: A review. *Remote Sensing of Environment*, 158: 295-310.

Yao, K., Idrees, M. O., Pradhan, B. and Nabeel, S. M., 2015. Detecting Land Use Land Cover Change Impacted by Civil Crisis in Ivory Coast using Remote Sensing and GIS. *Asian Journal of Applied Sciences*, 3(05): 550-558.

Yao, X., Wang, Z. and Wang, H., 2015. Impact of urbanization and land-use change on surface climate in middle and lower reaches of the Yangtze River, 1988–2008. *Advances in Meteorology*, 11.

Yu, D. and Coulthard T. J., 2015. Evaluating the importance of catchment hydrological parameters for urban surface water flood modelling using a simple hydro-inundation model, *Journal of Hydrology*. doi: http://dx.doi.org/10.1016/j.jhydrol.2015.02.040.

Zhao, C., Wang, W. and Xing, W., 2012. Regional Analysis of Extreme Temperature Indices for the Haihe River Basin from 1960 to 2009. *Procedia Engineering*, 28(0): 604-607. doi: http://dx.doi.org/10.1016/j.proeng.2012.01.776

Zazo, S, Molina, J-L. and Rodríguez-G, P., 2015. Analysis of flood modelling through innovative geomatic methods. *Journal of Hydrology*, 524: 522-537.

APPENDICES

Appendix 1: Rational Method Runoff Coefficient Table from U.S. Soil Conservation Service (SCS)

	Runoff Coefficient, C					
	Soil Group A			Soil Group B		
Slope :	< 2%	2-6%	> 6%	< 2%	2-6%	> 6%
Forest	0.08	0.11	0.14	0.10	0.14	0.18
Meadow	0.14	0.22	0.30	0.20	0.28	0.37
Pasture	0.15	0.25	0.37	0.23	0.34	0.45
Farmland	0.14	0.18	0.22	0.16	0.21	0.28
Res. 1 acre	0.22	0.26	0.29	0.24	0.28	0.34
Res. 1/2 acre	0.25	0.29	0.32	0.28	0.32	0.36
Res. 1/3 acre	0.28	0.32	0.35	0.30	0.35	0.39
Res. 1/4 acre	0.30	0.34	0.37	0.33	0.37	0.42
Res. 1/8 acre	0.33	0.37	0.40	0.35	0.39	0.44
Industrial	0.85	0.85	0.86	0.85	0.86	0.86
Commercial	0.88	0.88	0.89	0.89	0.89	0.89
Streets: ROW	0.76	0.77	0.79	0.80	0.82	0.84
Parking	0.95	0.96	0.97	0.95	0.96	0.97
Disturbed Area	0.65	0.67	0.69	0.66	0.68	0.70

Rational Method Runoff Coefficients - Part I

	Runoff Coefficient, C					
	Soil Group C			Soil Group D		
Slope :	< 2%	2-6%	> 6%	< 2%	2-6%	> 6%
Forest	0.12	0.16	0.20	0.15	0.20	0.25
Meadow	0.26	0.35	0.44	0.30	0.40	0.50
Pasture	0.30	0.42	0.52	0.37	0.50	0.62
Farmland	0.20	0.25	0.34	0.24	0.29	0.41
Res. 1 acre	0.28	0.32	0.40	0.31	0.35	0.46
Res. 1/2 acre	0.31	0.35	0.42	0.34	0.38	0.46
Res. 1/3 acre	0.33	0.38	0.45	0.36	0.40	0.50
Res. 1/4 acre	0.36	0.40	0.47	0.38	0.42	0.52
Res. 1/8 acre	0.38	0.42	0.49	0.41	0.45	0.54
Industrial	0.86	0.86	0.87	0.86	0.86	0.88
Commercial	0.89	0.89	0.90	0.89	0.89	0.90
Streets: ROW	0.84	0.85	0.89	0.89	0.91	0.95
Parking	0.95	0.96	0.97	0.95	0.96	0.97
Disturbed Area	0.68	0.70	0.72	0.69	0.72	0.75

Rational Method Runoff Coefficients - Part II